

NORWEGIAN UNIVERSITY OF SCIENCE AND  
TECHNOLOGY

DEPARTMENT OF MARINE TECHNOLOGY

MASTER THESIS - MARINE MACHINERY

---

**Fault Detection of Offshore Wind Turbine  
Drivetrain. State-of-the-Art, Development  
Trend and Role of Digital Twin**

---

*Author:*

Elisa Elmies

*Supervisor:*

Dr. Amir Rasekhi Nejad

January 30, 2019



---

## Abstract

This master thesis reviews some of the challenges offshore wind turbines encounter and how a model-based condition monitoring and the use of a digital twin are likely to be beneficial for its profitability. The thesis shows the development of wind turbines from its origin to the state-of-the-art. As the demand for wind energy increases, the turbines move offshore and grow in both size and number. This consequently leads to an increase in costs as well. It is discussed how the expenditure in operation and maintenance challenges the profitability and what the root causes are. Studies are shown confirming the gearbox and drivetrain in particular to be responsible for many failures and the most downtime. Hereof, bearings are the root cause of most of the damage. The thesis examines the most common fault modes of the drivetrain and bearings in specific to showcase the underlying factors of the downtime. Existing and new fault detection methods for the drivetrain and bearings are reviewed. The importance of a comprehensive maintenance method such as condition monitoring is covered. For this, the difference between a data-based and a model-based approach is discussed and the possibilities of multi-body simulation are highlighted. The thesis also discussed why a digital twin is a promising technology for the offshore wind energy sector. With the knowledge the industry has from maintenance strategies for bearings, simulation models to build up a digital twin can be developed. This can contribute greatly to a better understanding and monitoring and thus an optimised offshore wind turbine. The thesis narrows down to review some techniques in the field of vibration analysis, which is the most common OWT fault detection method. This is done by analysing the measurement from a test rig at both free and forced vibrations.

---

## Sammendrag

Denne masteroppgaven gjennomgår noen av utfordringene vindmøller møter på og hvordan en modellbasert tilstandsovervåking og bruk av en digital tvilling vil være gunstig for lønnsomheten. Avhandlingen viser utviklingen av vindturbiner fra opprinnelsen til dagens stand. Etter hvert som etterspørselen for vindkraft øker, flyttes turbinene offshore og vokser i både størrelse og antall. Dette fører følgelig til en økning i kostnadene også. Det diskuteres hvordan utgiftene i drift og vedlikehold utfordrer lønnsomheten og hva årsakene er. Studier er vist som bekrefter at girkassen og drivverket hovedansvarlig for mange feil og mest nedetid. I disse er lagrene hovedårsaken til det meste av skaden. Avhandlingen undersøker de vanligste feilmodusene til drivverket og spesielt lagrene for å vise de underliggende faktorene for nedetiden. Eksisterende og nye feildeteksjonsmetoder for drivverket og lagrene er gjennomgått. Betydningen av en omfattende vedlikeholdsmetode som tilstandsovervåking er dekket. For dette diskuteres forskjellen mellom en databasert og en modellbasert tilnærming, og mulighetene for multibody simulation blir fremhevet. Oppgaven diskuterer også hvorfor en digital tvilling er en lovende teknologi for vindenergisektoren offshore. Med den kunnskapen bransjen allerede har fra vedlikeholdsstrategier for lagrene, kan simuleringer for å bygge opp en digital tvilling utvikles. Dette kan bidra sterkt til en bedre forståelse og overvåking og dermed en optimalisert offshore vindturbin. Avhandlingen smalner ned for å gjennomgå noen teknikker innen vibrasjonsanalyse som er den vanligste feildeteksjonsmetoden for offshore vindturbiner. Dette gjøres ved å analysere målinger fra både frie og tvungne vibrasjoner på et testdrivverk.

---

## Preface

This master thesis was written as the final work of a Master of Science in Technology (NTNU) in Trondheim during the autumn semester of 2018. My field of specialisation is within Marine Machinery and the thesis is part of an ongoing work at the Marine Drivetrain Research Lab the Marine Technology Department at NTNU.

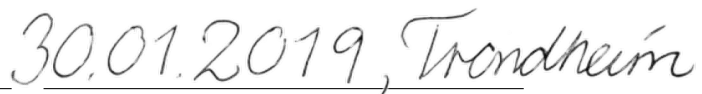
Due to my previous studies in Marine Biology and a tremendous interest in marine resources, I was determined to write about a topic that concerned any of the various areas in which the marine sector could contribute towards a more environmental friendly future. During a course in Machinery and Maintenance, I learned more about the various applications of vibration analysis. The professor in this subject, Dr. Amir R. Nejad, an Associate Professor in Machinery Dynamics and Vibration, educated me about the possibilities of condition monitoring in offshore wind turbines. I chose to study one semester longer in order to change my specialisation in Aquaculture to Marine Machinery to get Dr. Nejad as my supervisor as the field of OWTs had piqued my interest.

The thesis is the result of many hours hard work and several direction changes. The initial intention was to investigate and numerically describe the degradation of bearings. It turned out that this was not beneficial without the appropriate test equipment. Secondly, the goal was to use inverse methods to formulate a solution for a drivetrain system. A couple of weeks literature search and a meeting with employees at the Department of Mathematical Sciences revealed that this would require more prior planning. The reason being this would require a scheduled plan to exchange knowledge on respectively mathematical and mechanical knowledge. The final objective was to dive into the existing methods for failure detection and condition monitoring in offshore wind turbines today with the goal to narrow it down to describing the most challenging subsystems, drivetrain and bearings. Moreover, the motivation for a model-based approach were to be explained by comparing it to a data-based approach. The next main aim was to study the possibilities of a digital twin and what its role in the wind energy industry could be if applied. Finally, a case study was done to investigate how well failure detection applies to revealing known failures and what can be learned about the system. I hope this study contributes somewhat to the understanding of the importance of studying the degradation of bearings, a model-driven approach and the possibilities a digital twin offers with utilising the growing knowledge on CM and simulations.



---

Elisa Elmies



---

Date and Place



---

## Acknowledgement

First and foremost, I would like to thank my supervisor, Dr. Amir Rasekhi Nejad, for sharing his enthusiasm and joy for the subject of wind turbines, fault detection and digital twins. I am very grateful that he provided both time and help to understand the challenges and questions that were met during the work with this master thesis. I also want to thank him for encouraging me to keep working on the topic even though the main objective had to change several times.

Additional appreciations go to my office colleagues, parents and Ola Opkvitne for both valuable and motivational discussions during the past year.

---

## Abbreviations

<i>AE</i>	Acoustic Emission
<i>AGMA</i>	American Gear Manufacturing Association
<i>CAE</i>	Computer-Aided Engineering
<i>CapEx</i>	Capital Expense
<i>CM</i>	Condition Monitoring
<i>DOF</i>	Degree of Freedom
<i>DT</i>	Digital Twin
<i>EWEA</i>	European Wind Energy Association
<i>FE</i>	Force Element
<i>FEM</i>	Finite Element Method
<i>FFT</i>	Fast Fourier Transform
<i>FLS</i>	Fatigue Limit State
<i>FMI</i>	Functional Mock-Up Interface
<i>FMU</i>	Functional Mock-Up Unit
<i>HAWT</i>	Horizontal Axis Wind Turbine
<i>HMS</i>	High-Speed Shaft
<i>IMS</i>	Intermediate-Speed Shaft
<i>IoT</i>	Internet of Things
<i>ISO</i>	International Organisation of Standardisation
<i>MBS</i>	Multi-Body Simulation
<i>MBSE</i>	Model-Based System Engineering
<i>NREL</i>	National Renewable Energy Laboratory
<i>O&amp;M</i>	Operation and Maintenance
<i>OpEx</i>	Operational Expense
<i>OWT</i>	Offshore Wind Turbine
<i>RCF</i>	Rolling Contact Fatigue
<i>RMS</i>	Root Mean Square
<i>RUL</i>	Remaining Useful Life
<i>SCADA</i>	Supervisory Control and Data Acquisition
<i>SPM</i>	Shock Impulse Method
<i>ULS</i>	Ultimate Limit State
<i>VAWT</i>	Vertical Axis Wind Turbine
<i>WEA</i>	White Etching Area
<i>WEC</i>	White Etching Crack
<i>WSF</i>	White Structure Flaking

---

# Contents

<b>Abstract</b>	<b>I</b>
<b>Preface</b>	<b>III</b>
<b>Acknowledgement</b>	<b>IV</b>
<b>Abbreviations</b>	<b>V</b>
<b>List of Figures</b>	<b>VIII</b>
<b>1 Introduction</b>	<b>1</b>
1.1 Motivation . . . . .	1
1.2 Objective . . . . .	3
1.3 Background . . . . .	3
1.3.1 History and Development . . . . .	3
1.3.2 Offshore . . . . .	5
1.3.3 Layout . . . . .	6
1.3.4 Drivetrain . . . . .	7
1.3.5 Failures and Downtime . . . . .	8
1.4 Structure of the Thesis . . . . .	9
1.4.1 Chapter 2 . . . . .	9
1.4.2 Chapter 3 . . . . .	9
1.4.3 Chapter 4 . . . . .	9
1.4.4 Chapter 5 . . . . .	10
<b>2 Failure Modes</b>	<b>12</b>
2.1 General . . . . .	12
2.2 Failure Studies . . . . .	12
2.3 Drivetrain Failure Modes . . . . .	16
2.3.1 Misalignment . . . . .	16
2.3.2 Imbalance . . . . .	17
2.3.3 Bent Shaft . . . . .	18
2.3.4 Rolling Element Bearing Defect . . . . .	18
2.3.5 Mechanical looseness . . . . .	18
2.4 Bearing Degradation . . . . .	18
2.4.1 Axial Cracks and White Structure Flaking . . . . .	20
2.4.2 Spalling . . . . .	20
2.4.3 Pitting . . . . .	21
2.4.4 Bearing Life Computation . . . . .	21
<b>3 Fault Detection and Condition Monitoring</b>	<b>24</b>
3.1 General . . . . .	24
3.2 Data-Driven Fault Detection . . . . .	26
3.2.1 Visual . . . . .	27
3.2.2 Temperature . . . . .	27
3.2.3 Lubrication and Oil Debris . . . . .	27
3.2.4 Acoustic Emission . . . . .	28

---

3.2.5	Electrical Effects . . . . .	30
3.2.6	Shock Pulse . . . . .	30
3.2.7	Vibration Analysis . . . . .	30
3.2.8	Stator Current . . . . .	34
3.2.9	Multivariate Statistical Analysis . . . . .	34
3.2.10	Limitations Data-Driven . . . . .	34
3.3	Model-Based Approach . . . . .	35
3.3.1	Fast Fourier Transform Spectrum Analysis . . . . .	36
3.3.2	Multi-Body Simulation . . . . .	38
3.3.3	Modal Analysis . . . . .	40
3.3.4	Inverse Method . . . . .	44
3.4	Remaining Useful Life . . . . .	51
<b>4</b>	<b>Digital Twin</b>	<b>54</b>
4.1	General . . . . .	54
4.2	Origin and State-of-the-Art . . . . .	54
4.3	Concept Architecture . . . . .	55
4.4	Sensors . . . . .	56
4.5	Big Data and Analytics . . . . .	57
4.6	Software . . . . .	58
4.7	Possibilities . . . . .	58
4.8	Challenges . . . . .	61
<b>5</b>	<b>Case Study</b>	<b>63</b>
5.1	General . . . . .	63
5.1.1	Test Rig . . . . .	63
5.1.2	System Identification . . . . .	64
5.1.3	Fault Detection . . . . .	66
5.1.4	Fault Severeness . . . . .	69
5.1.5	Force calculation . . . . .	70
<b>6</b>	<b>Discussion</b>	<b>73</b>
6.1	Case Study . . . . .	73
6.2	Bearing Modelling . . . . .	74
6.3	Model-Based Approach . . . . .	74
6.4	Digital Twin . . . . .	75
<b>7</b>	<b>Conclusion</b>	<b>77</b>
7.1	Further Work . . . . .	78
<b>Appendix A FFT for all three hammer tests.</b>		<b>II</b>
<b>Appendix B Displacement for all three hammer tests.</b>		<b>IV</b>
<b>Appendix C Orbit plot</b>		<b>VI</b>

---

---

## List of Figures

1.1	Cumulative power capacity in the European Union 2005-2016 [4]. . .	1
1.2	Global cumulative installed wind capacity 2001-2017 [6]. . . . .	2
1.3	First wind mill [9]. . . . .	4
1.4	Poul La Cour first electricity producing wind turbine [9]. . . . .	4
1.5	Horizontal wind turbine [13]. . . . .	5
1.6	Global cumulative offshore capacity in 2017 and annual capacity 2011-2017 [20]. . . . .	6
1.7	Main parts of turbine, showing (1) blades, (2) rotor, (3) gearbox, (4) generator, (5) bearings, (6) yaw system and (7) tower [23]. . . . .	7
1.8	5-MW reference gearbox, schematic layout [25]. . . . .	7
1.9	Past and ongoing initiatives collecting and analysing data regarding performance and reliability of wind turbines [26]. . . . .	8
1.10	Downtime caused by wind turbine subsystems [28]. . . . .	9
2.1	Failure/turbine/year and downtime from two large surveys of land-based European wind turbines over 13 years [30]. . . . .	12
2.2	Failure rates against downtime for all assemblies [31]. . . . .	14
2.3	Vulnerability map for a 5-MW gearbox [33]. . . . .	15
2.4	Vulnerability map for a 750-kW gearbox [34]. . . . .	16
2.5	Angular misalignment [35]. . . . .	16
2.6	Parallel misalignment [35]. . . . .	17
2.7	Rotor or disk with imbalance U [36]. . . . .	17
2.8	Distribution of damage locations in the gearbox [37]. . . . .	18
2.9	Schematic roller bearing set up [42]. . . . .	19
2.10	Distribution of failure modes in the gearbox [37]. . . . .	20
2.11	Axial cracks dominated by high-speed and intermediate-speed stage bearings inner raceway [37]. . . . .	20
2.12	Fatigue spall in (a) ball bearing and (b) ball bearing raceway [48]. . .	21
2.13	Micropitting on an intermediate pinion bearing [50]. . . . .	21
3.1	Condition monitoring concept [58]. . . . .	25
3.2	A plot of the high speed temperatures at different rotor speeds [63]. .	26
3.3	A typical acoustic emission burst signal [96]. . . . .	29
3.4	Typical orbit plots from two proximity probes for respectively normal condition, misalignment, severe misalignment and rubbing [130]. . . .	34
3.5	Model building in general [137]. . . . .	35
3.6	FFT indicating respectively parallel or angular misalignment [138]. .	37
3.7	FFT indicating imbalance [138]. . . . .	37
3.8	FFT indicating bent shaft [138]. . . . .	38
3.9	5-MW gearbox MBS model [33]. . . . .	39
3.10	Motion types for the unforced 1-DoF system [153]. . . . .	41
3.11	Effects of damping on free vibration [154]. . . . .	42
3.12	Damped vibration with $\zeta < 1.0$ . . . . .	43
3.13	Methodology of inverse vibration analysis for RUL calculation. . . . .	44
3.14	Harmonic movement description. . . . .	45
3.15	1DoF mounted rotating machinery with imbalance. . . . .	48

---

3.16	A schematic L-curve plot for TGSVD or Tikhonov regularisation, where the norm of the semi-solution is plotted against the norm of the residual. The optimal level for regularisation is obtained with the parameter value corresponding to the corner of the curve [167]. . . . .	51
3.17	Illustration of RUL [171]. . . . .	52
3.18	RUL estimation steps [171]. . . . .	52
4.1	Digital twin of wind turbine in information video by GE Renewable Energy [188]. . . . .	58
4.2	Different dimensions when using simulation technology throughout the entire life cycle of a system [189]. . . . .	59
5.1	The test rig with indicated sensor placement and order. . . . .	63
5.2	FFT results of amplitude per frequency in sensor 3 by hammer test 1, 2 and 3. . . . .	64
5.3	Campbell diagram. . . . .	65
5.4	Displacement for hammer test 1, 2 and 3 sensor 3. . . . .	66
5.5	Orbit plot at 24 [Hz] at sensor 1, 2 and 3. . . . .	68
5.6	Orbit plot of three sensors measurements at 12 [Hz] and 35 [Hz]. . . . .	69
5.7	The attachment-placement of weights to produce fault cases. . . . .	69
5.8	Plot of the mean force measured at the second sensor at 24[Hz]. . . . .	70
5.9	Plot of the mean velocity measured at the second sensor at 24[Hz]. . . . .	71
5.10	Plot of the mean acceleration measured at the second sensor at 24[Hz]. . . . .	71
A.1	Hammer test 1. . . . .	II
A.2	Hammer test 2. . . . .	III
A.3	Hammer test 3. . . . .	III
B.1	Hammer test 1 displacement. . . . .	IV
B.2	Hammer test 2 displacement. . . . .	V
B.3	Hammer test 3 displacement. . . . .	V
C.1	Orbit plot at 24[Hz]. . . . .	VI

---

---

# 1 | Introduction

## 1.1 Motivation

The demand for energy increases as the global population continues to grow. The world population is estimated to reach 9.7 billion by 2050 [1]. At the same time, the need for energy in developing countries increases as more and more people reach a higher level living standard. Development requires energy and the access to it is an important prerequisite for achieving success in the fight against poverty [2]. It is stated in the United Nations Development Program to end poverty, protect the planet and ensure peace and prosperity for all people [3]. Thus at the same time as energy demand increases, decisive action must be taken to use more environment friendly energy sources. Consequently, the demand for wind power, as well as an ever improving system design is increasing. Figure 1.1 shows how the cumulative power capacity in the European Union has had an continuous incline in the past years.

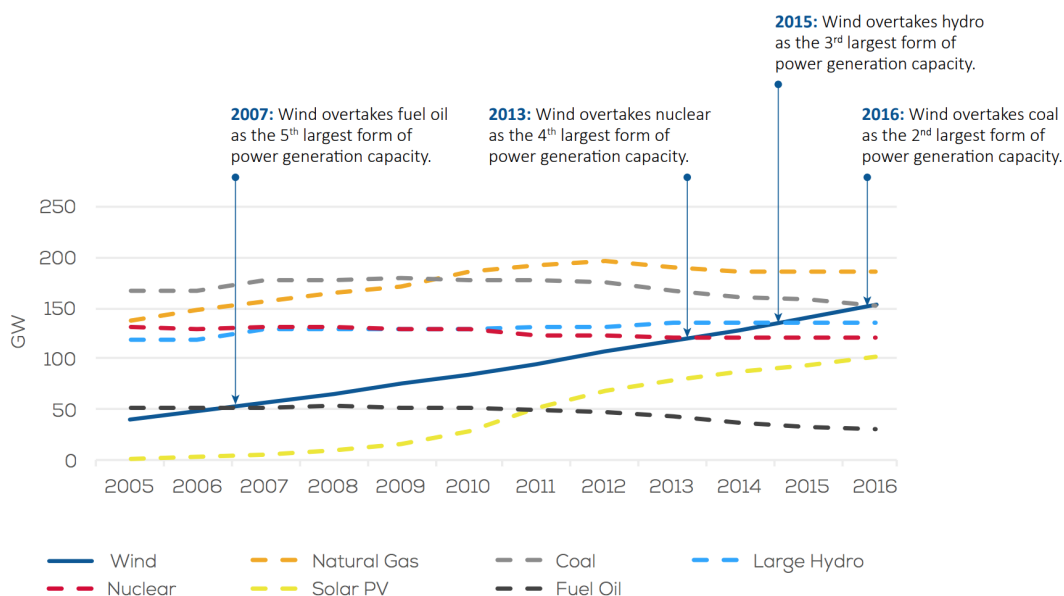


**Figure 1.1:** Cumulative power capacity in the European Union 2005-2016 [4].

By 2016, wind energy had passed coal as the second largest form of power generation capacity. This trend can be seen globally as well, as figure 1.2 over the global cumulative installed wind capacity from 2001 to 2017 shows. Wind energy has been the fastest growing energy technology since the 1990s in terms of percentage of



---

yearly growth of installed capacity per technology source [5].

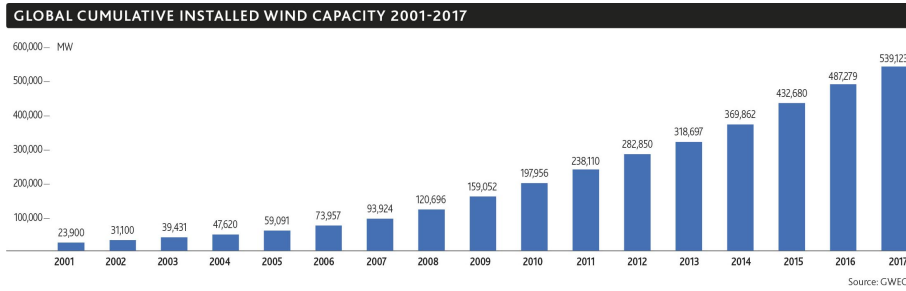


**Figure 1.2:** Global cumulative installed wind capacity 2001-2017 [6].

The decision to move wind turbines offshore, is a promising sign of an even further growth in the wind energy production. Not only offers the ocean space an immense opportunity for installation, is also can be done without doing changes in nature as roads and otherwise bothering the public eye. Another major contributing factor is the wind speed, which is much more stable at sea, as large fetch length can be built up. On the contrary, the Offshore Wind Energy production is a complicated field where different areas of expertise are included. The wind energy producer Ørsted [7] states other issues that have to be worked on simultaneously are:

- Carbon pricing as a driver for investments.
- Collaboration between countries and regulators.
- Competition for full scope of projects.
- Confidence that the green transformation is possible.

Carbon pricing could be viewed as a driver for investments, as the European carbon emissions needs to be reduced by over 95% by 2050 in order to limit the global temperature increase to less than 1.5 % by 2100. In addition, the rapid growth in capacity and turbine size, coupled with a challenging offshore environment with areas that are hard to reach, presents challenges for offshore wind. High operation and maintenance costs are a big issue in the offshore wind production. These costs are dominated by downtime due to failures in the drivetrain, especially the mounted, rotating machinery. If offshore wind energy is to reach its full potential these failures have to be fixed. Condition monitoring represents a way of maintenance that does not involve assumptions of when subassemblies need repair or replacement which is a frequently used maintenance strategy today. Model based CM has been around for a long time and can be done in a variety of ways. Modelling is a way of recreating a system and displaying it in a way that it is easier to and understand and quantify. One of several advantages model based condition monitoring demonstrated, is that the relevant system or process can be portrayed visual and easy understandable [8]. This simplifies communication between partners and different stakeholders that come from multiple disciplines and opens up for a quicker and better way to detect failures and discuss options for improvement. The combination of increased computational power, sophisticated sensors and telecommunications enables a new type of real time data transfer and processing for operation and maintenance. The concept that combines these technologies is a digital twin. This real time simulation

---

of a system and its environment is promising but will also be dependent on good models to build it up in order to improve the state of the art maintenance.

## 1.2 Objective

The main objective of this thesis is to investigate which maintenance an offshore wind turbine drivetrain requires in order to decrease the downtime. Accordingly, existing and new failure detection techniques are reviewed. In addition, the advantages of model-driven condition monitoring are discussed. Furthermore, the new digital twin concept is considered with the aim to review its profitability for offshore wind energy. A case study on a test rig is done in order to investigate some of the benefits in the common used vibration analysis. The overall goal for the thesis is to debate how to improve the fault detection in offshore wind turbines of today.

## 1.3 Background

The utilisation of wind energy has a tradition of at least 3000 years [5] and has become very complex as technology becomes more developed. A modern wind turbine depends on several disciplines, ranging from aerodynamics to structural dynamics, mechanical and electrical. Due to this, the discipline mechatronics has gotten increased attention, due to being an intersection between mechanics, electronics and software design. The demand for renewable energy is increasing as the world population continues to rise and conventional fossil fuel is not a sustainable end solution. As wind turbines deliver a variable level of power depending on the wind speed, moving them offshore opens up for a more efficient use. Moreover, bigger structures will increase the energy output even more. The global wind power capacity is growing but the technology is facing challenges, one of them being expensive operation and maintenance (O&M) cost. The improvement of availability and reliability is important to realise the expected 20 year life of an offshore wind turbine. The bearings in the drivetrain are documented to cause the most downtime and are thus one of the objects of discussion in modern condition monitoring. A digital twin represents the possibility to model different aspects of a system and its environment in simulation models and improve failure detection and thus system optimisation even more. The future energy supply is dependent on a decline in failures in wind turbine. Modelling the degradation of OWTs in a digital twin would be a missing piece in the ever growing knowledge of multi-body simulation and system optimisation of the wind energy generation offshore.

### 1.3.1 History and Development

Wind energy has been used by mankind for a long time. The first wind mill is dated back to the Persian-Afghan border in the year 644 A.D. However, the concept might have been used even earlier than this [9].



**Figure 1.3:** *First wind mill [9].*

Wind mills were further developed in different parts of the world to grind grain, thereof the origin of the expression. An other major application was the drainage of the dikes in the Netherlands. In the middle of the 19th century there existed 200 000 windmills which at the start of the 20th century were replaced by other engines [10]. The modern wind energy use for power generation started shortly before 1900 in Denmark. Out of a strong danish community college movement one wanted to broaden the possibilities for the population in rural areas. The solution became power supply by wind turbines. This was a success and the rural areas in Denmark were among the first worldwide to get access to electricity at the same times as the towns. The danish professor Poul La Cour was a key figure in the transition from the historical windmills to the modern technology of power generating wind turbines. In 1981 he built his first electricity producing wind turbine, shown in figure 1.4 [9].

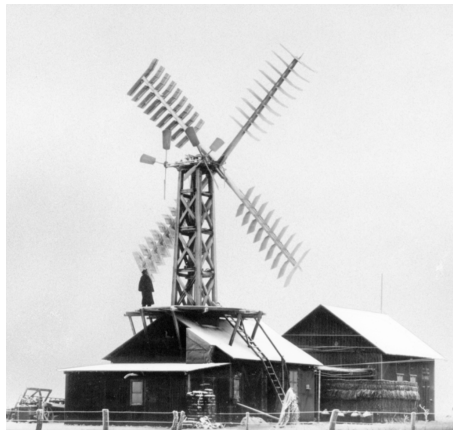


**Figure 1.4:** *Poul La Cour first electricity producing wind turbine [9].*

The wind turbines were displaced by the spread of central coal-fired power plants along with their transmission lines. At times of crisis, as during the World Wars, resourceful engineers regularly resorted to wind power as an independent source of energy and brought it up to date with the latest technology. However, the real starting signal for the continuing boom took place after the first energy crisis in 1973/74. In order to reduce oil dependency, only nuclear power plants should be built in Denmark in the future. As a reaction against these plans, a group of engineers in 1976 came up with the first grid-connected wind turbine. The idea caught on and the most frequent wind turbine layout became a three bladed down-

---

wind horizontal axis (HAWT), as shown in figure 1.5 of a modern HAWT. This is to this day the most common layout [11]. Modern wind turbines are developed to convert wind energy into electricity that is fed to the electricity grid. This is done by converting the kinetic energy in the wind to mechanical energy in the drivetrain shaft which is converted to electrical energy in a generator. The reason a HAWT is preferred over a vertical axis wind turbine (VAWT) is that it achieves higher energy efficiency and thus increases the power productions as well as reducing the expense the system has per kW power generated [12].



*Figure 1.5: Horizontal wind turbine [13].*

### 1.3.2 Offshore

Moving offshore has several advantages, as having an almost infinite area available at a low price [4]. One of the possibilities to reduce the costs in wind energy generation is to increase the turbine size, because this will generate more energy per turbine. Thus, a move of the wind energy production offshore is beneficial [14]. Besides vast areas for big structures, the large areas at sea equal less imperfection in the surroundings to interfere with the acceleration of the wind [15]. Also, the wind at sea has higher velocities and is less turbulent, which is beneficial for the performance of the turbine. Wind can thus gain higher speeds than on land. This is profitable for the energy production, because an increase in wind speed is proportional with an increase of power by power of three [11], as seen in equation 1.1.

$$P = \frac{1}{2}\rho V^3 C_p \quad (1.1)$$

This is also mirrored in the capacity factors, which respectively are  $C_p$ , of 35-45% for offshore and 25-30% for onshore wind turbines [16]. The noise and visual impacts are in addition minimised while the transportation becomes more feasible, considering the transportation and installation of blades with a length of 60m for 5-MW and 90m for 10-MW OWT. Onshore the same transportation and installation requires roads and other facilities as well as planning thoroughly to not interrupt other traffic or life at land [17]. From the 15 638 MW new wind power capacity installed in Europe, 3 154 MW were offshore [4]. With this, 2017 was a record year for wind energy, both onshore and offshore, where offshore grew 101% compared to 2016. Figure 1.6 shows the global cumulative offshore capacity in 2017. Current estimates predict a 60 GW increase in installed capacity by 2025, most in the UK, Germany and China [18]. Offshore installations of more than 3 000 MW in 2017 are a harbinger of thing to come [19].

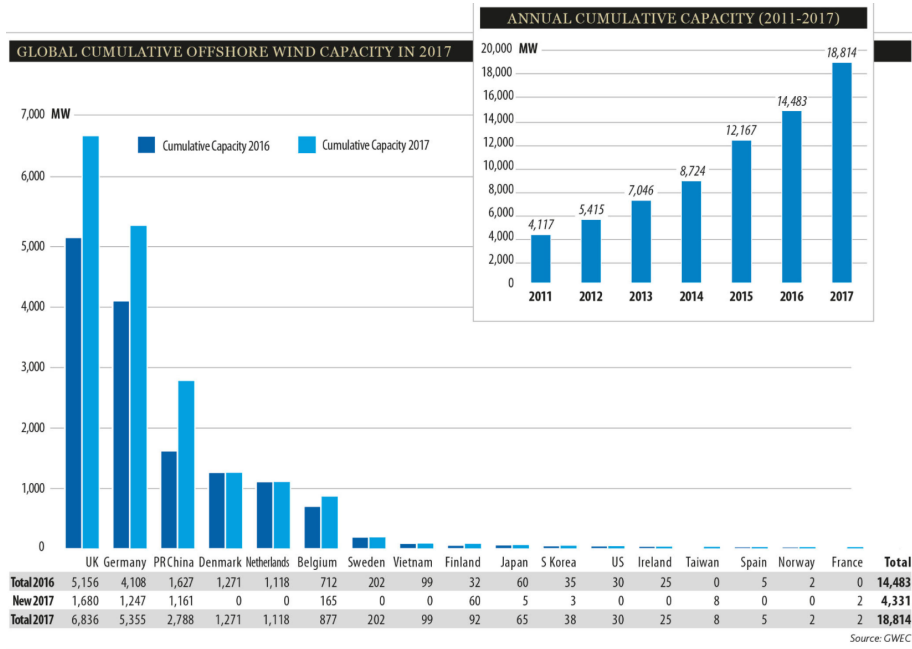


**Figure 1.6:** Global cumulative offshore capacity in 2017 and annual capacity 2011-2017 [20].

However, there are disadvantages about moving the turbines offshore as well. Beside grid connection issues, both the capital expense (CapEx) and operational expense (OpEx) are increased. The CapEx is higher because of more expensive substructure foundations and more complex and expensive installations. The OpEx increases because bad weather can lead to more wear, downtime and tasks like seabed preparation <sup>1</sup>. Several studies claim that Operation and Maintenance costs are estimated to account for 14-30% of the total project life cycle expenditure of an offshore wind farm [21, 22]. This is 75% to 90% of the investment costs. To get a more profitable energy production, identifying the factors for these costs is vital.

### 1.3.3 Layout

There are different variations of offshore wind turbines, most being monopiles. Also floating systems are often chosen because bottom-fixed turbines are depth-limited and some regions do not have shallow, less than 45m, deep sea like Norway, USA and Japan. The main parts of a modern HAWT are the tower, nacelle and blades. The drivetrain is located inside the nacelle, which is shown in figure 1.7 and is a term describing all the components from the blades to the generator. That is, the drivetrain consists of the conversion mechanisms from the main shaft, over the gearbox and to the generator.

<sup>1</sup>Seabed preparation can include actions as protecting against scour.

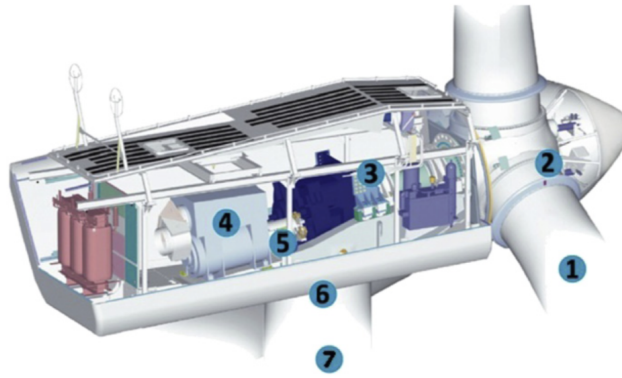


**Figure 1.7:** Main parts of turbine, showing (1) blades, (2) rotor, (3) gearbox, (4) generator, (5) bearings, (6) yaw system and (7) tower [23].

As other wind turbines, wind on the blades creates a thrust force that give lift and therefore rotation to the blades and consequently main shaft. Inside the gearbox this rotational velocity is increased to suit for generating electricity.

### 1.3.4 Drivetrain

The most common drivetrain types consists of a shaft, gearbox and generator and might be viewed as the heart of the wind turbine [24]. The two main drivetrain types are geared and gearless, with geared being the one that covers 85 % of the market. More specific, there are high speed, medium speed (hybrid), direct drive and hydraulic drive, where the latter two have no gearbox. One benefit of a gearbox is that it limits the fatigue life of the components by amplifying the inertia of the generator in power of two and thus making it less sensitive to torque variations. The gears are used to increase the rotational input speed from about 12 rpm to a generator speed at 1200 rpm. The most common gearboxes are high speed gear boxes in the range of 1-90 to 1-120. High speed gearboxes generally consist of three stages of planetary gears and parallel gears. Figure 1.8 shows Nejad et al. schematic layout on a 5-MW gearbox.

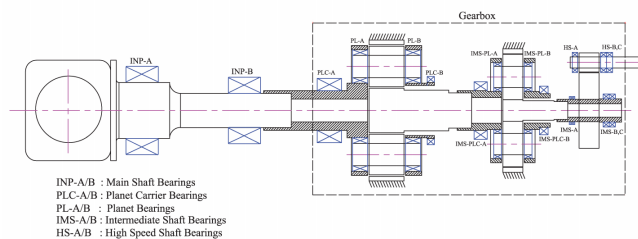


**Figure 1.8:** 5-MW reference gearbox, schematic layout [25].

The compact design and high gear ratios make the planetary gearboxes well fitting for wind turbines. Disadvantages of high speed gearboxes are their long downtime. However, the advantages of proven technology, supply chain and good availability make them profitable and frequently chosen over other alternatives.

### 1.3.5 Failures and Downtime

Offshore wind turbines operate in a challenging environment. As mentioned, the wet and corrosive surroundings will contribute to wear and degradation in parts that are not sufficient protected and also harden the access for installation and maintenance. Understanding the performance and reliability of a wind turbine in order to optimise its operation and maintenance is therefore an important topic. Figure 1.9 shows past and ongoing initiatives collecting and analysing data for performance and reliability of wind turbines in general. It is noticeable how few of the initiatives are on offshore wind turbines. This is one of the reasons data-driven approaches to evaluate OWT are less efficient than in other areas, as further explained in chapter 3.2.

Initiative	Country	Number of WT	Onshore	Offshore	Operational Turbine Years	Start-Up of Survey	End of Survey
CIRCE	Spain	4300	✓		~13,000	~3 years (about 2013)	
CREW-Database	USA	~900	✓		~1800	2011	ongoing
CWEA-Database	China	? (640 WF)	✓		?	2010	2012
Elforsk/Vindstat	Sweden	786	✓		~3100	1989	2005
EPRI	USA	290	✓		~580	1986	1987
EUROWIN	Europe	~3500	✓		?	1986	~1995
Garrad Hassan	Worldwide	? (14,000 MW)	✓		?	~1992	~2007
Huadian	China	1313	✓		547	01/2012	05/2012
LWK	Germany	643	✓		>6000	1993	2006
Lynette	USA	?	✓		?	1981	1986
MECAL	Netherlands	63	✓		122	~2 years (about 2010)	
Muppandal	India	15	✓		75	2000	2004
NEDO	Japan	924	✓		924	2004	2005
ReliaWind	Europe	350	✓		?	2008	2010
Robert Gordon University	UK	77	✓		~460	1997	2006
Round 1 offshore WF	UK	120		✓	270	2004	2007
University Nanjing	China	108	✓		~330	2009	2013
SPARTA	UK	1045	✓		1045	2013	ongoing
Strathclyde	UK	350		✓	1768	5 years (about 2010)	
VTT	Finland	96	✓		356	1991	ongoing
Windstats Newsletter/Report	Germany	4500	✓		~30,000	1994	2004
Windstats Newsletter/Report	Denmark	2500	✓		>20,000	1994	2004
WInD-Pool	Germany/ Europe	456	✓	✓	2086	2013	ongoing
WMEP	Germany	1593	✓		15,357	1989	2008

**Figure 1.9:** Past and ongoing initiatives collecting and analysing data regarding performance and reliability of wind turbines [26].

Martin et al. [27] made a sensitivity analysis of offshore wind farm operation and maintenance (O&M) costs and availability. The study concluded that access and repair costs along with failure rates for both minor and major repairs were important factors for the total costs. The study shows that plant reliability becomes even more important with larger structures, as they are even more prone for failures. Among the fourteen inputs that were found to be important in calculating O&M costs, are failure rates, component cost, repair duration interacting with the shift length. The downtime caused by failing subsystems presents a major challenge. As shown in figure 1.10 by Sheng et al., the subsystem causing the highest downtime is the gearbox [28, 16]. But also other mechanical subsystems in the drivetrain, as the generator and the main shaft and main bearings show high downtimes.



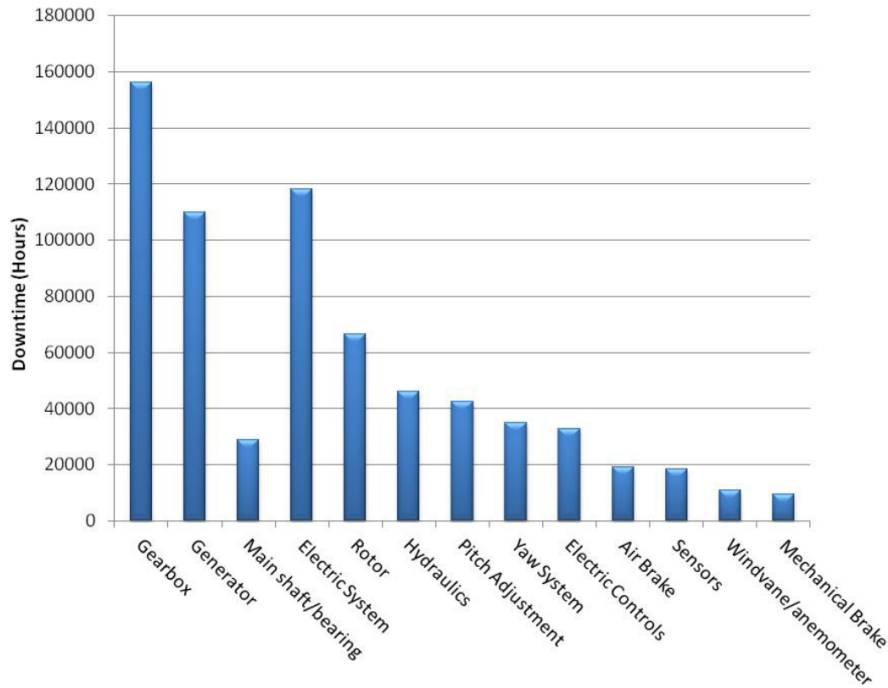


**Figure 1.10:** Downtime caused by wind turbine subsystems [28].

In order to make wind energy more competitive with other energy sources, the reliability has to be increased and the downtime of the turbine reduced. It is believed that condition monitoring (CM) and multi-body simulation by means of a digital twin might be the solution for this and thus the key to make wind energy a competitive option.

## 1.4 Structure of the Thesis

### 1.4.1 Chapter 2

Chapter two aims to explain the most common failure modes in offshore wind turbine drivetrains. Special attention is devoted to the degradation of bearings and their life computation, as they are a major cause of the downtime drivetrains experience today.

### 1.4.2 Chapter 3

This chapter covers fault detection and how condition monitoring is a key method to monitor and improve the fault detection for an offshore wind turbine. The data-driven fault detection as well as the model-based approach are explained and compared.

### 1.4.3 Chapter 4

In chapter four, the idea of a digital twin is reviewed. The architecture, development trend and benefits for the operation and maintenance of an offshore wind turbine are presented.



---

#### 1.4.4 Chapter 5

This chapter seeks to review how previous mentioned selected fault detection methods work and how effective the techniques are in revealing faults. In order to do so, a case study on a test rig with built in errors is completed.

---

---

## 2 | Failure Modes

### 2.1 General

Knowing which failures cause downtime is crucial in order to tailor the condition monitoring, as well as improving the future wind turbine solutions and designs. Failures are permanent interruptions on a system that hinder it from performing the required function, whilst faults are not permitted deviations, either transitory or not, of at least one parameter or property from the standards condition [29].

### 2.2 Failure Studies

When studying the failure modes, it is important to be aware of what data basis they rely on. This is exemplified by looking at two further studies showing the downtime of wind turbine assemblies. The failure and downtime rates for different parts of the wind turbine were studied by Faulstich et al. and showed that the gearbox and drivetrain are subject for both high failure and downtime rates. Figure 2.1 shows databases from Wissenschaftliches Mess- und Evaluierungsprogramm (WMEP) and Landwirtschaftskammer Schleswig-Holstein (LWK).

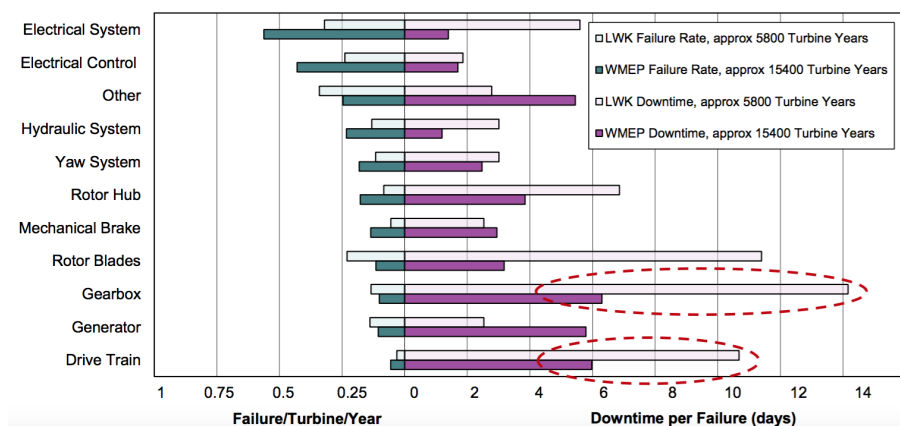


**Figure 2.1:** Failure/turbine/year and downtime from two large surveys of land-based European wind turbines over 13 years [30].

The results for these studies were collected in respectively 1989-2006 and 1993-2006. Even though they collected statistics from wind turbines onshore, the set up is still similar enough to use this knowledge for offshore wind turbines. It is noteworthy

---

that this study shows partly different results than the one shown in figure 1.10. This is due to the first study being by Sheng et al. from 2011 over 27,000 wind turbines. That study mixes both onshore and offshore turbines, ranging from 500 kW to 5MW. Nevertheless, the mechanical downtimes in the subunits of the drivetrain are considerably long in both. Also, figure 2.1 is informative as to showing the difference between the number of failures and the downtime each failure creates. The third study chosen to illustrate the downtime of failures is shown in figure 2.2. This bubbleplot is from a study by Artigao et al. in 2018. This study includes the studies from LWK and WMEP and compares it to nine others. Although other subunits are seen to have high downtimes as well, the drivetrain still shows up to 28 % of downtime levels.

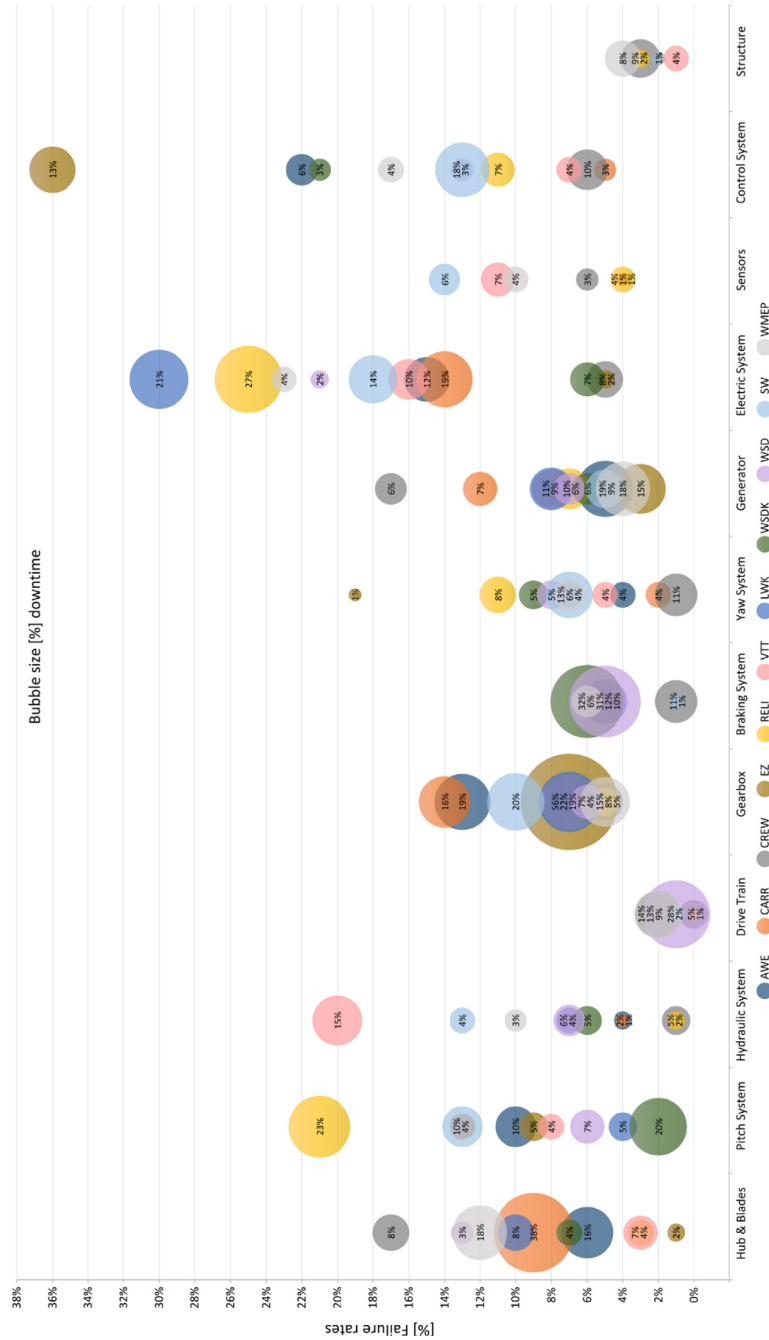


**Figure 2.2:** Failure rates against downtime for all assemblies [31].

It is noticeable that although the electrical systems and control systems might have a higher annual failure rates, the failures in the gearbox and the drivetrain generate a long or longer downtime [30]. These parts are thus of great importance for improving the costs. Moreover, it is noteworthy how varying studies organise the components in the wind turbine differently. The two latter list drivetrain explicit to gearbox, generator and braking system. Here, the drivetrain denotes only the main shaft and the respectively bearings. This can be misleading for someone not familiar with the design of a wind turbine. In this thesis, several failure modes and condition monitoring methods are relevant for several components in the drivetrain. Where it is of importance, the relevant component is specified. When looking into which

components are subject for most failure in the gearbox, the work of Nejad et al. on vulnerability maps for an OWT gearbox is valuable [32]. The reliability for components in the gearbox is not equally distributed. The vulnerability map in figure 2.3 displays the probability of fatigue damage in a 5-MW gearbox, while figure 2.4 shows the same type vulnerability map for a 750-kW gearbox.

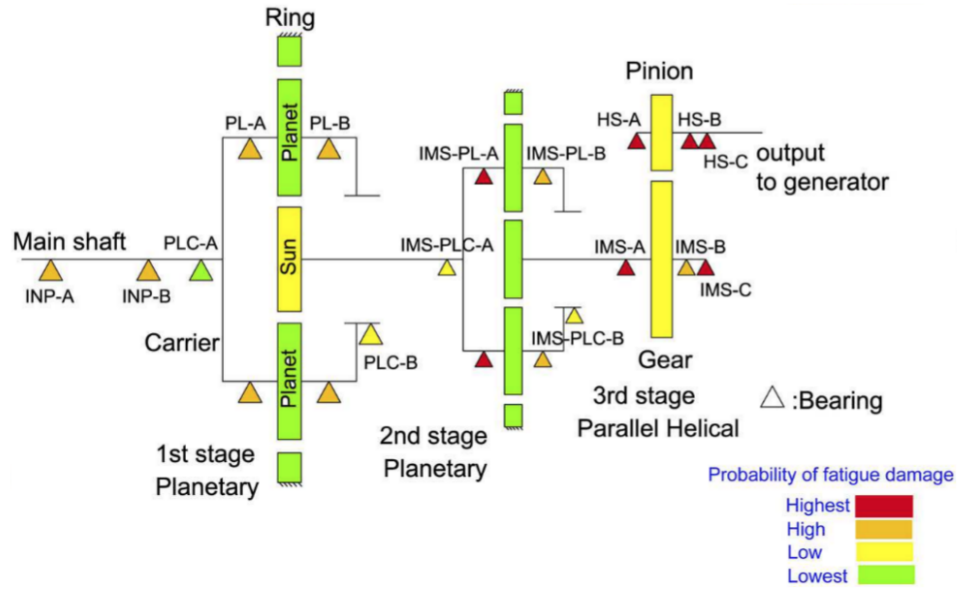


**Figure 2.3:** Vulnerability map for a 5-MW gearbox [33].

An overview like this might be used in the condition monitoring to see where fatigue damage most likely will occur first and thus where monitoring has to be precise. As illustrated here, each gearbox will have variations in vulnerability distributions and should have a designated map. The varying vulnerability might be due to design restrictions as material or geometry limits. Moreover both manufacturing and production errors can lead to differences between turbines with the same design.

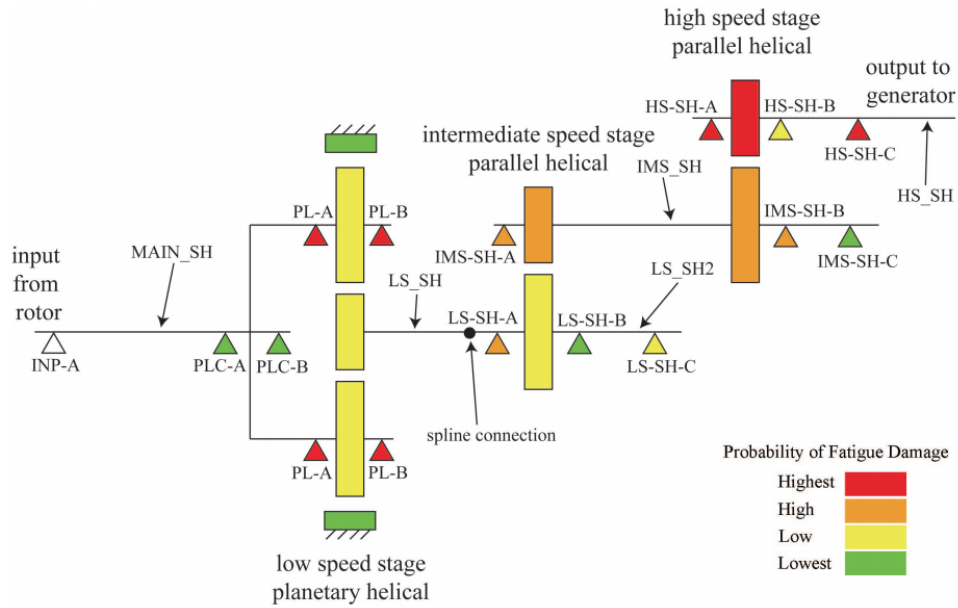


**Figure 2.4:** Vulnerability map for a 750-kW gearbox [34].

## 2.3 Drivetrain Failure Modes

Some of the most frequent, mechanical faults in drivetrains are the following:

- Misalignment
- Imbalance
- Bent Shaft
- Rolling element bearing defect
- Mechanical looseness

### 2.3.1 Misalignment

If the shafts, bearings and couplings are not properly aligned along their centrelines, misalignment is created. There are two types components can be misaligned, either angular or parallel. As shown in figure 2.5, an angular misalignment is when two shafts are joined at a coupling with a degree  $\alpha$ . The parallel misalignment in figure 2.6 has parallel but displaced or offset shafts.

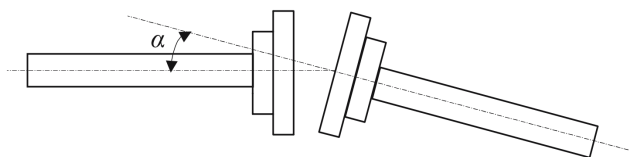


**Figure 2.5:** Angular misalignment [35].

---

The

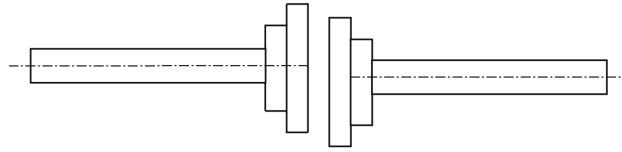


**Figure 2.6:** *Parallel misalignment [35].*

The most common causes for misalignment are:

- Wrong installation, the parts are not proper aligned.
- Improper alignment due to forces from piping an support components.
- Expansion of a component due to temperature changes.
- Shifting in foundation or setting, thus misalignment due to an uneven basis.

The effect of misalignment often is an expedited fatigue. Reason for this being it usually causes the bearing to carry a higher load than it was designed for. This stress is often seen to be applied right below the load carrying surface and is known as spalling. There are also coupled effects to take into account, like a misaligned shaft affecting the bearings [35] which can cause even more damage.

### 2.3.2 Imbalance

Imbalance, or rotating imbalance, is a common drivetrain fault that can affect the machine immensely. It occurs when the centre of mass, also known as the inertia axis of the shaft does not coincide with the centre of rotation, also called the geometric axis. Thus, a deviation in expected distribution of mass ensues. Imbalance can be seen in three different variants, static, coupled and static.

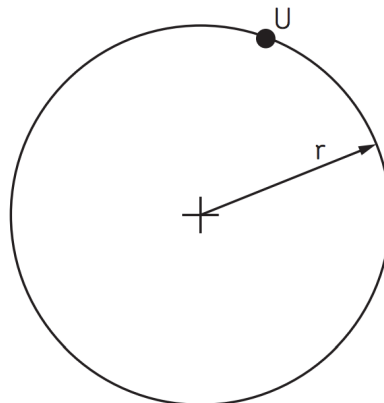


**Figure 2.7:** *Rotor or disk with imbalance  $U$  [36].*

The static imbalance can be observed at rest. This variant is also known as force balance and occurs when the inertial axis is displaced parallel from the axis of rotation. Coupled imbalance is the event where two equal imbalance forces are



---

situated 180 ° from another. The most common of the three types is the dynamic imbalance, which is a combination of static and coupled. The effects the rotating imbalance has on the system can be both vibration and noise. As other faults, it will reduce the life of the bearings and increase the maintenance. Imbalance can be caused by numerous factors, manufacturing errors or a improper build up are among the possibilities. The imbalance can be corrected by either adding, removing, centering or shifting the mass. Thus it can be compensated as well as renewed.

### 2.3.3 Bent Shaft

A bent shaft can be the result from a high torque as well as improper handling during either assembly or transport. A so-called cold bow, which is a shaft that has a high length-to-width-ratio, can also develop a bent shaft when at rest. The bent shaft can cause the bearings to carry a higher dynamic load than they are supposed to. This can lead to a shorter lifetime.

### 2.3.4 Rolling Element Bearing Defect

A rolling element bearing fault defect is seldom a failure that is not caused by another failure. Thus, when detected it has to be looked for other root causes mentioned previous, such as imbalance and misalignment. To repair the issue both bearing and underlying cause have to be overhauled or replaced.

### 2.3.5 Mechanical looseness

Mechanical, rotating looseness occurs when there is too much space between rotating and stationary elements. The causes for looseness might be that the mounting is cracked or broken, or the machine came loose from its mounting. It is also possible that machine component came loose as an manufacturing error. The effect this fault can have is that the affected component can become detached and cause even further damage.

## 2.4 Bearing Degradation

As seen in numerous studies on the contributors to operation downtime, the gearbox is the assembly most crucial to improve in order to enhance the operation time. S. Sheng at the National Renewable Energy Laboratory of the US (NREL) made a study, shown in figure 2.8, that presents the distributions of damages in the gearbox and that bearing failures are dominant.

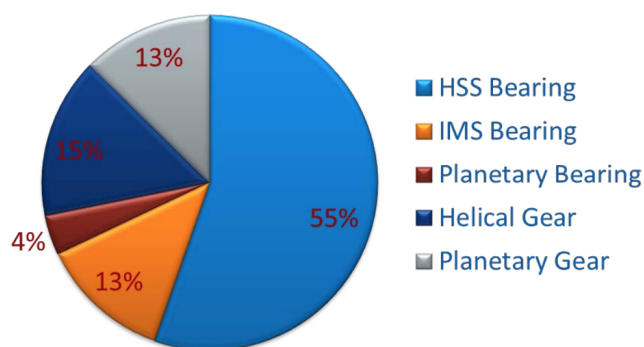


**Figure 2.8:** Distribution of damage locations in the gearbox [37].

This distribution is made as part of the the gearbox reliability database project in 2014 and shows that high-speed shaft (HSS) bearings and intermediate-speed (IMS) bearings contribute with 64 % of the damage [37]. Gears make up 25 % of the damage and are dominated by helical gears. However, since failure starts in the bearings not the gears [38], this study has chosen to focus on them. The gearbox reliability database project collects gearbox failure event data and aims to quantify the magnitude of the failures as well as identifying top failure modes and root causes [28]. Such databases have a big potential, as wind energy at sea still is a quite new technology and one has little historical data to draw conclusions from. Degradation is the expiration of a system by losing one or more properties. The process might be linked to material fatigue, disassembling of compounds as in substance degradation or other. Degradation is often a combination of both the duration and intensity of a process. Figure 2.9 shows a schematic set up of a roller bearing. The terms rolling-contact bearing, anti friction bearing and rolling bearing are all used to describe the class of bearing in which the main load is transferred through elements in rolling contact rather than in sliding contact [39] and which are relevant for an OWT gearbox [40] [41].

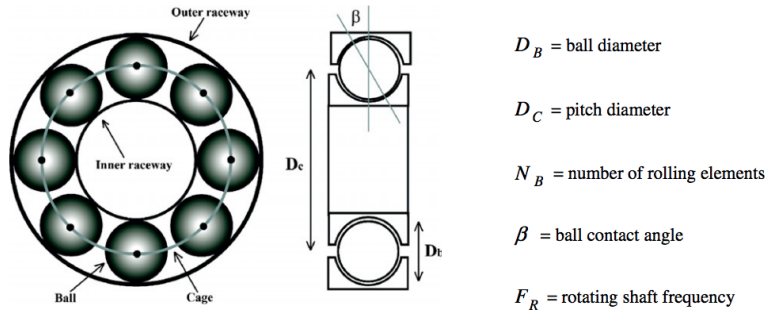


**Figure 2.9:** Schematic roller bearing set up [42].

The degradation of a bearing can be caused by various factors which also can make the bearing fail if these are not taken into account, properly monitored and repaired or replaced. The causes might be extreme or uneven loads as well as kinematic changes, as start, stop and acceleration. Examining the degradation root causes has shown that 71% are axial cracks, 23% spalling and 6% are pitting, as seen in figure 2.8. These values are based on a study on 80 samples and also corresponds to values seen in other literature [43, 44].

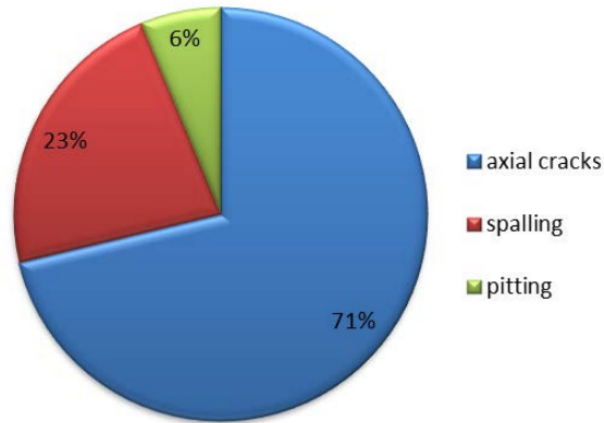


**Figure 2.10:** Distribution of failure modes in the gearbox [37].

### 2.4.1 Axial Cracks and White Structure Flaking

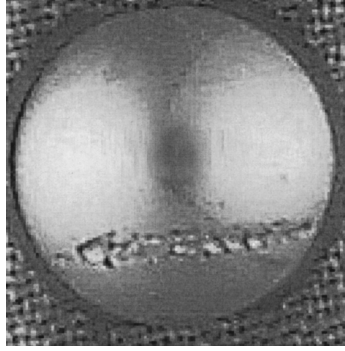
Axial cracks refer to the orientation of the crack as it appears on the raceway of the inner ring in the bearing. These types of cracks have a tendency to propagate to spall or lead to a complete splitting of the ring [45]. The formation of axial cracks, as well as white etching cracks (WECs) with associated micro structural change known as white etching areas (WEAs) causes white structure flaking (WSF). WSF is one of the main prevalent failure modes in gearbox bearing raceways which makes the actual service life of turbine gearbox much lower than the desired 20 years [46]. This phenomena is observed in early stages of the operation, from 6-24 months [47].



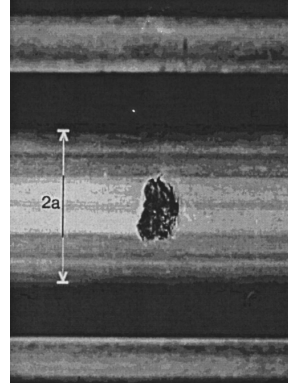
**Figure 2.11:** Axial cracks dominated by high-speed and intermediate-speed stage bearings inner raceway [37].

### 2.4.2 Spalling

Spalling, or fatigue spalling, is the phenomenon when part of the contacting surface between ball and raceway is removed as a result from fatigue cracks that form, propagate and coalesce under operation. This phenomenon is unavoidable in bearings and is the reason why the bearing fails eventually, even though the rolling contact fatigue (RCF) often even exceeds the  $L_{10}$  life which is mentioned later [48, 49, 46].



(a)



(b)

**Figure 2.12:** Fatigue spall in (a) ball bearing and (b) ball bearing raceway [48].

### 2.4.3 Pitting

Pitting is typically associated with tangential shear stress caused by rolling-sliding contact. In bearings this is particularly frequently caused by skidding during unsteady operation [43]. During non steady operation, small holes, 0.1[mm] in depth, are generated on the raceway surface by rolling fatigue [42].

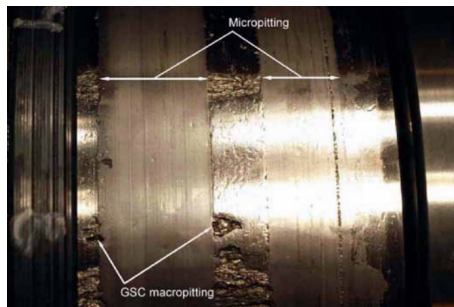


**Figure 2.13:** Micropitting on an intermediate pinion bearing [50].

### 2.4.4 Bearing Life Computation

The life measure of an individual bearing is defined as the total number of revolutions or hours at constant speed of operation until either the failure criterion is developed [41] or the first sign of metal fatigue, spalling, occurs. This might be on a rolling element or the raceway of the inner or outer ring [51]. The American Bearing Manufacturers Association (ABMA) standard states that the failure criterion is the first evidence of fatigue. Large variations are found in the number of cycles until metal fatigue, even on bearing that look identical and under the same conditions [51]. This shows that life estimated for bearings according to the rolling contact fatigue (RCF) is deficient to give a good estimate and a statistical approach should be preferred. Bearing life can be expressed as shown below. Here  $F$  is the dynamic equivalent radial load. It is calculated from  $F = XF_r + YF_a$ , where  $F_r$  and  $F_a$  are respectively the radial and axial loading. The constants  $X$  and  $Y$  are stated by the bearing manufacturer [52].  $L$  the length the load is applied and  $a$  a factor being 3 for ball bearings and  $\frac{10}{3}$  for roller bearings.

$$(FL)^{\frac{1}{a}} = Constant \quad (2.1)$$

---

To estimate the expected bearing life it is possible to use the basic rating life  $L_{10}$  or the SKF rating life  $L_{10m}$ . The basic bearing life is defined as the time 90% of a sufficiently large group of seemingly identical bearings in identical operation conditions will either reach or exceed. This bearing life is used when the operating conditions like lubrication and contamination are known not to have a big effect on the bearing life. Otherwise  $L_{10m}$ , also called SKF rating life is used. Only considering speed and load the basic rating life according to ISO 281 is as follows.

$$L_{10} = \left(\frac{C}{P}\right)^p \quad (2.2)$$

If the speed is constant the expression can be expressed in operating hours as:

$$L_{10h} = \left(\frac{10^6}{60n}\right)L_{10}. \quad (2.3)$$

$L_{10}$  is the basic rating life measured in millions of revolutions, while  $L_{10h}$  is measured in millions of hours.  $C$  is the basic dynamic load rating [kN],  $P$  the equivalent dynamic bearing load [kN],  $n$  the rotational speed [ $\frac{r}{min}$ ] and  $p$  the exponent of the life equation, 3 for ball bearings and  $\frac{10}{3}$  for roller bearings. The bearing life might be dependent on more than the load and bearing size as the basic calculation takes into account. These factors might be lubrication, proper mounting, degree of contamination and other environmental conditions. To take these factors into account, ISO 281 uses a modified life factor,  $a_{SKF}$ . The fatigue limit,  $P_u$ , for a bearing is the load level below which metal fatigue will not occur [53].

$$L_{nm} = a_1 a_{SKF} L_{10} = a_1 a_{SKF} \left(\frac{C}{P}\right)^p \quad (2.4)$$

As seen before, also here the factor can be altered for millions of hours when assuming constant speed:

$$L_{nmh} = \left(\frac{10^6}{60n}\right)L_{nm}. \quad (2.5)$$

$L_{nm}$  is the SKF rating life at 100- $n$  % reliability [millions of revolutions],  $L_{nmh}$  the SKF rating life at 100- $n$  % reliability [operating hours],  $a_1$  the life adjustment factor for reliability,  $a_{SKF}$  the SKF life modification factor. The factor  $n$  is the failure probability. However, this approach to bearing life computation has not shown to be adequate to describe the bearings. Premature failures still happen frequently and the wind industry is searching for improved models to detect the process of it.

---

---

## 3 | Fault Detection and Condition Monitoring

### 3.1 General

Condition monitoring (CM) is the collection, storage, comparison and evaluation of data from a machine in operation to monitor the condition of the system while running. It includes thus both detection and diagnosis of faults and failures. The classical maintenance theory describes the field of maintenance as either corrective or preventive [54]. Corrective maintenance is carried out after a fault or failure has already happened and been detected. This correction requires unscheduled work and generates downtime because a repair has not been planned and there might be a need for refurbishment or replacement of components. CM is preventive as well as predictive because it seeks to analyse the sampled data to predict when future replacement or repair should be done. The monitoring of the condition is thus a maintenance method for early detection of faults and failures to both minimise downtime and maximise productivity [55]. Hence, condition monitoring is the most fitted type of maintenance for an offshore structure. This method allows maintenance to be scheduled or that other actions are taken to prevent consequential damages. It also allows for conditions to be found before they develop into a major failure. In addition to enabling preventing big failures it also allows personnel to order spare parts in advance, schedule repair and plan how to use the downtime effectively [56]. This concept is shown in figure 3.1. CM aims to increase lifetime expectancy of components while reducing the OpEx. As wind turbine technology experiences a rapid growth with respect to market share, size and technological design, the operation and maintenance costs determine whether the production is efficient compared with other power plants [57].

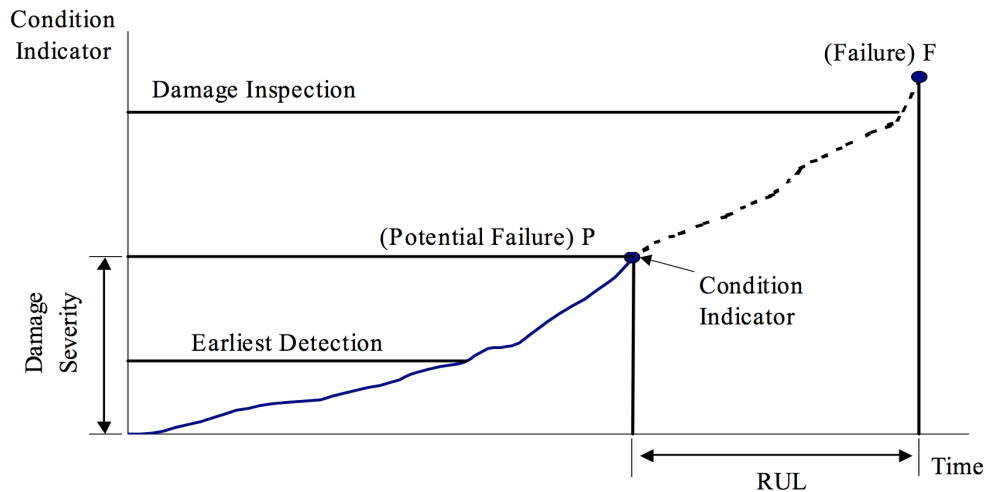


**Figure 3.1:** Condition monitoring concept [58].

A number of commercial wind turbine condition monitoring techniques are available already. Multiple of them are developed by companies with a long experience in condition monitoring, like GE Bently Nevada, SFK, Brüel & Kjær, Gram & Juhl and Prüftechnik. Often these strategies are made in the same manner as for other conventional rotating machines. The majority of these are vibration-based systems, with some being in combination with fibre-optic strain gauge and oil particle counters for an improved result [59, 60]. Because the drivetrain is such an important system, the focus in wind turbine monitoring has been the shaft, main bearings, gearbox and generator. For this, spectral analysis techniques are frequently used. Despite the efforts, to date the CM methods have not shown improving availability and false alarms are still an issue. These false alarms are the basis for ineffective fault reports which make it hard to gain knowledge of the data. The Supervisory Control and Data Acquisition (SCADA) system monitors alarms and signals and is used in all wind farms today. The registration of signals commonly occurs at a 10 min interval in order to get the transmitted data bandwidth from the wind turbine [61]. Although parameters like active power output, average nacelle temperature and turbine and generator shaft speeds are measured [62, 61], SCADA is no CM method in its own. Rather, it is an operational monitoring method. An additional misconception, commented in a technical report about wind turbine drivetrain CM testing by Sheng et al. [28] is the operators expectation to what one CM system can detect. In order to keep track of the varying parameters in comprehensive system like an OWT, various CM techniques and models have to be combined to create a complete condition monitoring solution. This development of the CM has to happen at the same pace the turbines develop and change. Models can help understand and combine technique and insight in different aspects of the system. Condition monitoring models can be divided into two main categories, data-driven and physical. What these include and how they are used for drivetrains is explained in this chapter. It is noticeable that this separation does not apply to all CM methods, as model are build on data on the line between a simple graph or figure and a model can be hard to draw for some techniques. However, it is applicable for many methods and can thus be a helpful way in understanding as well as improving condition monitoring.



---

## 3.2 Data-Driven Fault Detection

The data-driven or data-based approach is the most common condition monitoring today. The associated methods vary from simple and known concepts to complex computations. It is often done by using a certain acceptable limit for a parameter like a specific temperature that can not be surpassed in order to secure a safe operation. An example for this can be seen in figure 3.2, from a work on offshore wind turbine gearbox replacement. Here the red indicates the healthy state for data 4 months after replacement, while the blue is a warning state 4 months prior to replacement.

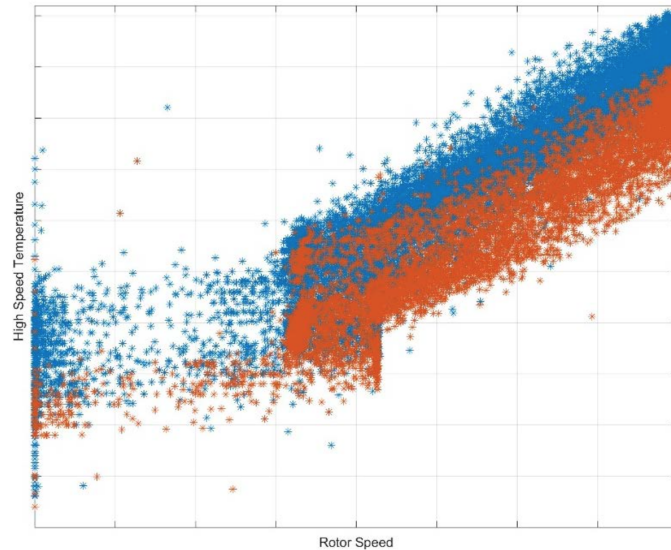


**Figure 3.2:** A plot of the high speed temperatures at different rotor speeds [63].

Thresholds used in the data-driven approach is often obtained from data gathered in earlier cases and studies. A frequently used argument for the data driven approach is that the necessary process information can be extracted directly from huge amounts of data [64, 65, 66, 67]. Often it also more simple and thus less costly and with a low design effort compared to the model-based condition monitoring in chapter 3.3. Following, data-based or statistical methods are frequently used for process monitoring in various industrial applications [68, 69, 70, 71, 72, 73]. There are multiple parameters and proportionately many measuring techniques in the data-driven condition monitoring. Some of the most relevant for a wind turbine drivetrain are reviewed in the following subchapters. However, the data-driven approach is seen to have challenges in monitoring an offshore wind turbine. It is complicated to include and combine loads being both varying and non-linear as well as the overall interaction between different components on each other. Furthermore, the methods relies on data that comes from an earlier state, other systems or numerical formulas instead of the state and characteristics of the actual system. In case of big structures with many parts and thus even more parameters, it becomes increasingly important to take into account system-specific values to take optimised decisions. In addition, the offshore wind turbines are still continuously developing. It follows that there does not exist a comprehensive data basis to choose from yet. In the case of bearings in the drivetrain, it is debatable how many sensors one should install in order to get all the information needed to monitor them.

---

### 3.2.1 Visual

Measurement of visual indicators can be very informative for machinery components. Visual inspection of a system in operation can nevertheless be challenging as it might be difficult to get to or it is hard to see because important parts are behind some sort of barrier [74]. A stroboscope is a tool which uses glimpses of light to survey rotating machinery. The flashing from a strobe light at a proper period can give the impression that the part is frozen in time and thus capture the relevant part [75]. An endoscope might be used to take pictures of the internal parts of a machine. Both of these are used without having to stop the whole operation which saves both time and money.

### 3.2.2 Temperature

Temperature monitoring can also be very revealing about the health of the system and is used in several analyses. The measurements can be taken with many different sensors and used for both preventive and predictive maintenance. The most common sensor types are resistance temperature detectors (RTDs), resistant thermometers and optical pyrometers [76, 77]. Every component has a operational temperature range that it needs for correct functioning. Due to this, there can be set thresholds, where temperatures above it can be viewed as signs of faults. The most common reasons for such failures are bad electrical connection or mechanical wear [76, 78]. Disadvantages with using temperature monitoring is a slow development, where fault detection in some cases might be too late. On its own it might not be viewed as an effective condition monitoring for the drivetrain of a wind turbine. As temperature varies with load, it has to be considered that the temperature can be influenced by the surroundings. Accordingly, it has to be taken into account how much nearby parts increase in temperature to distinguish between a higher load and actual fault in component. A simple approach is to monitor the difference between temperatures, since a higher load would affect both and thus not change the interval.

### 3.2.3 Lubrication and Oil Debris

A good lubricant state is important in order to reduce downtime and increase the life of rolling bearings which are the most normal in OWT. It is nevertheless not viewed as a main technique to use for condition monitoring, due to being a slow method. The cleanness, viscosity and temperature of the oil gives insight in how the gearbox is performing. This makes the oil and lubrication analysis an important CM approach. As the wind turbine operates, bearings and gears will wear down and cause debris. As these particles accumulate, they end up in the oil filter [58]. The metallic debris detection in the oil can be done both online and offline. The online system uses sensors installed on the structure, while the more common choice, offline, relies on periodic samples. The periodic offline samples go through a lubrication analysis which can be quite slow. Therefore, online monitoring is gaining interest, because although being more expensive, provides a direct control of the lubrication condition. The monitoring of oil is done by multiple purpose sensors, the same as used in generators [79]. The types of sensors for oil CM are shown in table 3.1.

---

**Table 3.1:** *Types of sensors for oil condition monitoring.*

<b>Sensor Type</b>	<b>Measures Parameter</b>	<b>Reference</b>
Quality and properties	Electrochemical impedance spectroscopy (EIS)	[80]
Viscosity	Kinematic viscosity	[81]
Humidity	Percentage of water in lubricant	[82]
Particle concentration	Particle size distribution	[83, 84]
Conductivity	Electrical conductivity level used to monitor oil oxidation rate	[85, 86, 87]
Dielectric constant	Dielectric constant	[84, 88]

Among the online monitoring methods are particle count, temperature and viscosity monitoring, while offline is oil filter analysis for flow and cleanness [89]. Existence of wear and faults in the different parts can be done through taken into account that each element has different kind of particle-characteristics. Content that may alter the lubricant condition is water content, metallic content, oxidation and fuel contamination [90]. The life expectancy of a gearbox can be respectively increased or reduced with up to 50 % depending on the how clean the oil is. The cleanness is in addition important to detect mechanical faults.

**Table 3.2:** *Methods for lubrication analysis in wind turbine gearboxes.*

<b>Method</b>	<b>Reference</b>
Oil debris count and size detection	[58]
Lossy Mode Resonance (LMR) based optical fiber refractometer	[91]
Chamber for HALT/HASS for oil sensor properties assessment	[92]
Online lubrication oil CM and RUL prediction using viscosity and DC sensors along with a particle filtering technique	[93, 94]

Sanches et al. [91] fabricated and characterised an optical fiber refractometer based on Lossy Mode Resonance (LMR) for gearbox synthetic lubricant degradation. The work concludes that thinner coating results in higher sensitivity. Coronado et al. [92] investigates High Accelerated Life Test (HALT)/Highly Accelerates Stress Screening (HASS) test chamber where oil sensors properties can be assessed. As the goal is to recreate the environment in which the gearbox of a wind turbine operates, the study is done under varying operating temperature and vibration levels. It is shown that temperature indeed alters the results. Zhu et al. [94] studied using online sensors in order to investigate lubrication CM and degradation.

### **3.2.4 Acoustic Emission**

In general, acoustic emitted signals are either of mechanical or aerodynamic sort. The sound is created by interaction of turbine components and air flowing over the blades. Among the sources for AE there are the generation and propagation of cracks which have been seen to be some of the main ways bearings degrade. In other words, AE is the structural alteration under mechanical or thermal rapid stresses causing a rapid release of strain energy [95]. Figure 3.3 shows a typical AE burst signal.

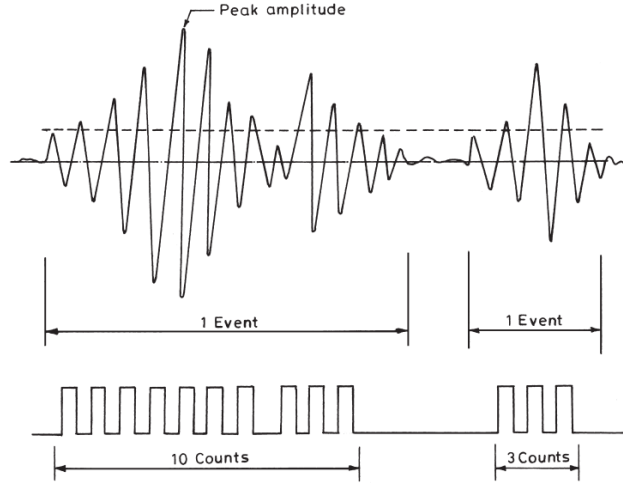


**Figure 3.3:** A typical acoustic emission burst signal [96].

The subject of study are high frequencies from 100[kHz] to 1[MHz] [97, 98, 99]. Because mechanical rotating systems have a specific, signature vibration [100], they also have an acoustic signature. This can be used to detect alterations in the AE, which will indicate deterioration of the component. This is why acoustic emission is very suitable for detecting shaft cracks and bearing faults. The accuracy in fault detection depends on sound pressure and sound intensity data [101, 102] and can be interrupted by other component noise, which is a challenge when using AE for condition monitoring. Sensors in acoustic measurement are attached by flexible glue with low attenuation to "listen" to the component [103]. Sound level meters are used to obtain information [99, 103]. Depending on the noise characteristics, the signal can further be divided into tonal, low frequency, broadband and impulsive sound [99]. These noise readings are used to predict possible faults, based on the higher frequency components. The AE are measured with a transducer, primarily the piezoelectric type, a preamplifier and a signal-processing unit. The most common parameters measured are ringdowns, counts, events and peak amplitude of the signal. Table 3.3 shows an overview over methods used for CM in wind turbine gearboxes.

**Table 3.3:** Methods for acoustic emission condition monitoring of wind turbine gearboxes.

Method	Reference
LabView-based <sup>1</sup> online gearbox monitoring system	[104]
DRFF and DBMs <sup>2</sup> for 11 different gearbox operating conditions	[105]
Heterodyne technique with TSA <sup>3</sup> and Kurtosis	[106]
Comparative study between AE and vibration analysis for wind turbine gearbox fault detection	[107, 108]
Time of Arrival (TOA) with Continuous Wavelet Transform (CWT) on Morlet waves to localise faults	[109]

<sup>1</sup> Laboratory Virtual Instrumentation Engineering Workbench

<sup>2</sup> Deep Random Forest Fusion, Deep Boltzmann Machines

<sup>3</sup> Time Synchronous Averaging

The LabView-based online monitoring system for CM fault detection and CM in

---

a gearbox was designed by Wei et al. [104]. Que et al. introduces Heterodyne techniques to preprocess acoustic emission signals to detect faults in [106]. Later spectral Kurtosis and Time Synchronous Averaging (TSA) were suggested for feature extraction and fault detection in gears. The sampling rate was reduced from a MHz order to a kHz order by using this Heterodyne technique and make an effective fault detection in gear teeth possible. Li et al. introduced using the Deep Random Forest Fusion (DRFF) for gearbox fault detection [105]. This is an advanced application, where the wavelet packet transform is used to extract statistical parameters. Deep Boltzmann Machines (DBMs) were used for deep representation of these parameters. Qu et al. investigated partial gearbox tooth cut faults in [107]. Elasha et al. studied bearing defect of wind turbine gearbox [108]. While vibration analysis can be affected by mechanical resonance, AE was here shown to be capable of isolating damage levels. Acoustic emission can also be used to detect and localise gear faults. Some of the drawbacks for Acoustic Emission for condition monitoring is that wide bandwidth is costly to measure and analyse. Furthermore, the nacelle is not ideal to collect acoustic data due to the noise [61].

### **3.2.5 Electrical Effects**

The monitoring of electrical effects can detect changes that might be caused by fatigue, cracks and delamination. This is due to electrical resistance varying with stiffness for some components. Voltage and current analysis is used to seek for unexpected changes and deviations. [101]. Although electrical effect monitoring is a common CM method for rotating, electrical machines, it has not been used in wind turbines yet, due to too few studies on this application [61]. Among the available techniques for the monitoring of electrical effects are velocity measurements, discharge measurements, oil analysis and contact force measurements. All of them are used to detect medium or high voltage grid, transformers, switches or cabling isolation faults. They have in common to not interfere with the operation of the wind turbine [101, 110, 103].

### **3.2.6 Shock Pulse**

The shock impulse method (SPM) detects mechanical shocks that are caused when a ball or roller in a bearing comes in contact with debris in the bearing or a damaged area of raceway [111]. These shocks are transmitted through the surrounding bearing housing and detected by a piezoelectric transducer. The shock pulse magnitude is effected by the bearing size, its condition, the speed and to some extent the load [112].

### **3.2.7 Vibration Analysis**

Vibration measurements are powerful techniques to detect and diagnose fault in drivetrains. It is a widely used method in several industries for monitoring a variety of machines and their components [101, 113, 114]. Vibrations are a natural part of every machine, thus also the drivetrain. Decisive is the degree of vibration and in which part of the system they occur. Analysing these fluctuations gives a picture of the systems health and is important in order to understand and be able to prevent the machine to fail prematurely [115]. The two main types of vibration are free vibration where the total energy stays constant over time and forced vibration which is forced to vibrate at a specific frequency by a periodic force input. All vibrations are a combination of forced and resonant vibration. The forced vibration can be

---

caused by ambient excitation, external loads, internally generated forces or imbalance. Resonant vibration develops when the natural modes of vibration are excited. Typically, the vibration response is amplified over the level of deflection, strain or stress that comes from static loading, as a result from resonant vibration. Vibrations are often the first sign of a potential machine failure. Abnormal vibrations can be caused by imbalance, misalignment, loose parts, rolling bearings and gear damage. Instruments to analyse vibrations can as the other tools help detected a problem before it becomes a big failure. The vibration magnitude can be registered as displacement, velocity or acceleration. The sensors used for measuring vibrations rigid mounted to the component of interest are chosen depending on their frequency range. Accelerometers are used for high frequencies, while respectively velocity sensors and position transducers are used for medium and low frequencies [103]. In DNVGL-SE-0439, the certification of condition monitoring from 2006, shows the frequency ranges that are relevant for a wind turbine. The document also provides information over the sensor technology and the handling of sensors among others. For bearings, the number of sensors to measure the vibration varies with bearing type and function. ISO 1337-1 on vibration condition monitoring gives the general procedures for the field. Here, there are also found the typical transducers for measuring. Moreover, ISO 10816-21 provides evaluation of machine vibration by measurements on non-rotating parts in a horizontal axis wind turbine with gearbox. This is beneficial in order to compare evaluations of vibration measurements. A limiting factor for vibration analysis can be that the vibration spectrum is less efficient for bearing fault during the incipient phases of bearing [101, 116, 117]. The analysis of vibration can be both data-based and model-based, as the Root Mean Square (rms) analysis and the Fast Fourier Analysis (FFT) respectively. This field shows how these fields also often overlap when using a graph to visualise data. The FFT is further reviewed in subchapter 3.3.1. Statistical condition indicators can be used to extend what information can be extracted from the vibration signals. Among these are along the mentioned rms, peak-to-peak, crest factor, kurtosis and sideband factors [118, 119]. To underline how various the vibration analysis methods for fault detection are, some are showed in table 3.4.

---

**Table 3.4:** *Methods for vibration analysis in wind turbine gearboxes.*

<b>Method</b>	<b>Reference</b>
Vibration analyses to early fault detection on bearings.	[120]
Bearings monitoring based on TESPAP (Time Encoded Signal Processing and Recognition), vibration and envelope analysis.	[121]
Real time vibrations-based method to detect, localise, and identify a faulty bearing.	[122]
Frequency domain, percent power, peak rms, sequential forward search algorithm and adaptive neuro fuzzy inference systems to detect and identify faults on bearings.	[123]
Fault estimation algorithm based on artificial neural network (ANN), envelope analysis, Hilbert Transform and Fast Fourier Transform to detect bearing faults.	[124]
Local mean decomposition technology and multiscale entropy to diagnose roller bearing faults.	[125]
Envelope extraction and independent component analysis for faults detection on rolling element bearing.	[126]

---

**Root Mean Square** The rms can be one of the ways to measure the magnitude of vibration, which as mentioned is a very important parameter for the condition monitoring of the drivetrain. For the rms, the vibrations are classified according to its peak to peak acceleration. This can be calculated by equation 3.1. Here N is the total number of samples whilst  $x(i)$  are the sampled data values.

$$rms = \sqrt{\left[ \frac{1}{N} \sum x^2(i) \right]} \quad (3.1)$$

Velocity measurements are well fitted for detecting and analysing low frequency rotational faults, like misalignment, imbalance, bent shaft and looseness. The International Standard for ISO 20816-1 "Mechanical vibration - Measurement and evaluation of machine vibration" shown in table 3.5 presents the range of typical values for the zone A/B, B/C and C/D boundaries for non-rotating parts. This ISO classification can be used to determine the severity levels of measurements like this. When using standards like these it is to keep in mind that the levels of machinery and environments have to be considered as well.

**Table 3.5:** Range of typical values for the zone A/B, B/C and C/D boundaries for non-rotating parts

Range of typical zone boundary values for non-rotating parts				
r.m.s. vibration velocity mm/s				
0,28				0,28
0,45				0,45
0,71				0,71
1,12	Zone boundary A/B 0,71 to 4,5			1,12
1,8				1,8
2,8		Zone boundary B/C 1,8 to 9,3		2,8
4,5				4,5
7,1			Zone boundary C/D 4,5 to 14,7	7,1
9,3				9,3
11,2				11,2
14,7				14,7
18				18
28				28
45				45

NOTE 1 This table only applies to machines for which specific International Standards have not been developed and for which there is no suitable experience available.

NOTE 2 Small machines (e.g. electric motors with power up to 15 kW) tend to lie at the lower end of the range and large machines (e.g. prime movers with flexible supports in the direction of measurement) tend to lie at the upper end of the range.

The explanation for the different zones is in the standard given as follows:

- A *The vibration of newly commissioned machines normally falls within this zone.*
- B *Machines with vibration within this zone are normally considered acceptable for unrestricted long-term operation.*
- C *Machines with vibration within this zone are normally considered unsatisfactory for long-term continuous operation. Generally the machine may be operated for a limited period in this condition until a suitable opportunity arises for remedial action.*
- D *Vibration values within this zone are normally considered to be of sufficient severity to damage the machine.*

**Campbell Diagram** The Campbell diagram is plot of the natural frequencies as a function of rotational speed. The frequencies of the forcing excitation functions are superimposed on it [127, 128]. This representation is also called resonance diagram because if a natural frequency, marked by a horizontal line, crosses a mesh frequency within the vertical line that represents the operational speed range, resonance might occur [129]. It is one of the most important tools for understanding the dynamic behaviour of a rotating system as the shaft in the drivetrain and also used in the case study in chapter 5.

**Orbit Plot Analysis** The orbit plot analysis is suited for harmonic motion and fault detection in OWT bearings. The plot of the shaft motion in journal bearings obtained from feeding feeding horizontal and vertical vibration signals in horizontal and vertical amplifiers of an oscilloscope indicates failure as well as severeness of eventual faults [130]. Figure 3.4 shows four different orbit plots from two proximity probes for normal condition, misalignment, severe misalignment and rubbing. The



orbit plot shows the motion of centre of the shaft. When presented in a diagram, the centre of the figure tends to be in origo, although this is no requirement for a fault free system.

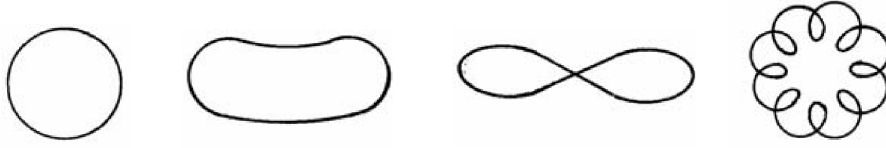


**Figure 3.4:** Typical orbit plots from two proximity probes for respectively normal condition, misalignment, severe misalignment and rubbing [130].

### 3.2.8 Stator Current

Stator current harmonic measurements have been appearing as an alternative for the measurement of vibrations [131], because the vibration sensors are delicate and expensive. It has been suggested that monitoring of the stator current might give the same indications [132]. This method is based on the load torque variations caused by the bearing fault as well as introduction of a particular radial rotor movement [133]. Ball bearing defects result in radial motion between the rotor and stator, that can be measured. These vibrations can be seen in context to stator current since any air gap eccentricity will lead to anomalies in the air gap flux density [130]. The frequencies at which these stator currents are generated can be seen in equation 3.2.

$$f_{brg} = |f_3 \pm m f_{vd}| \quad (3.2)$$

Here,  $f_{brg}$  is the bearing frequency,  $f_e$  the electric supply frequency,  $m=1,2,3\dots$ , and  $f_{vd}$  is the bearing element vibration defect frequencies.

### 3.2.9 Multivariate Statistical Analysis

The Multivariate statistical analysis (MSA) includes statistical techniques that allow investigations into the relationship along multiple variables recorded simultaneously [134]. Multivariate methods can reduce and simplify large big data sets as well as developing models for data prediction. The methods can also be used for constructing and testing various hypotheses concerning the data set. MSA is based on the probability model multivariate normal distribution. This is a much used probability distribution describing data that usually is around a central value with no bias beside it [135]. The central limit theorem, stating that the mean of a sufficiently large number of independent random variables will be approximately normally distributed is important considering this distribution [136].

### 3.2.10 Limitations Data-Driven

One of the issues data-driven methods cause, is that basing the CM of a part on a threshold is a very rigid approach. It is reliant on comprehensive studies to already exist to find out what should be measured and what the threshold should be. It also excludes unforeseen events as well as interactions between the components and the environment and components. The data-driven approach is a classic and well established maintenance strategy in several industries. It is very well fitting for systems that equal and are produced in big numbers. They usual also have in common that there is big data- set for them, samples over a long time. This is the

reason for why the approach might not be the best for components in offshore wind turbines and the system as a whole. These are systems that are relatively new, thus there is not much data to use to determine statistics and limits from. Moreover, an OWT is not a simple system that is produced in a big number. As today, they are manufactured individually. Being a new system, they change all the time and new concepts are tried out.

### 3.3 Model-Based Approach

Model-based approach is in thesis interpreted as using a model of a system to understand it better, monitor and learn from it in order to improve the fault detection and condition monitoring of it. Figure 3.5 shows a general model-building process. It showcases how the model is based on both data and estimation with feedback from model check to identification.

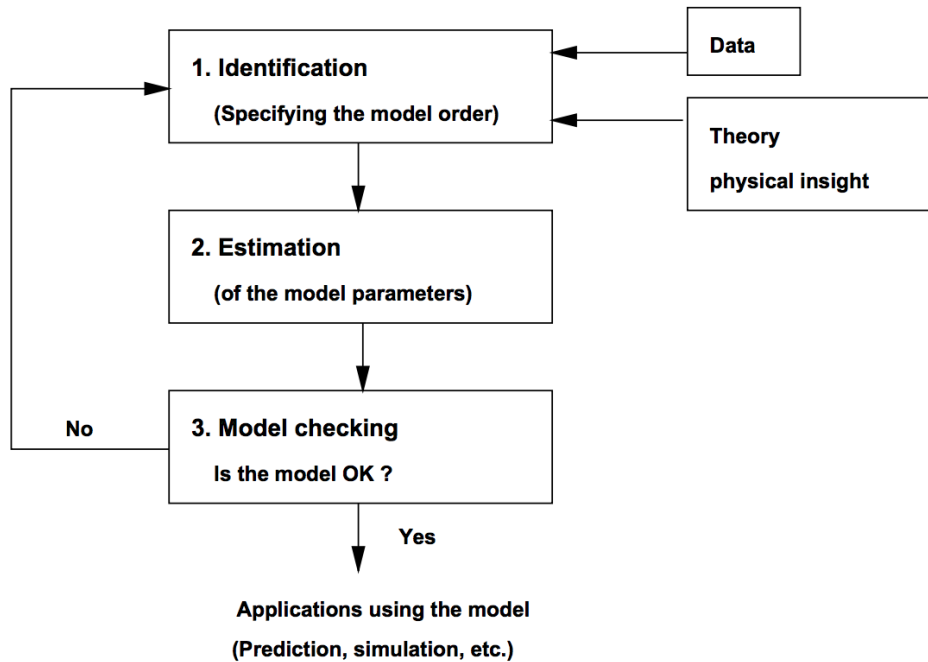


**Figure 3.5:** Model building in general [137].

The term model can be used on everything that seeks to show features of the reality and can be divided into physical models and more numerical ones, like linear regression. This thesis is mainly concerned with a physical model-driven approach, which also often is the associated term for model. The approach opens up for a smarter condition monitoring, because one can model everything of interest without including less important or less valuable information. With the knowledge of the system a model can be built that reflects how the system actually will react and at which time possible changes, alterations should be made. This is in contrast to the classical check ups according to fixed intervals that has been normal for wind turbines. A model also opens for a better predictive maintenance by letting the system be tested and simulated for alternative scenarios to learn how it will react.

---

The most advanced kind of model we know of today is the digital twin, which is discussed in chapter 4.

### 3.3.1 Fast Fourier Transform Spectrum Analysis

One example of a model-based approach is the Fast Fourier Transform Spectrum Analysis when analysing vibrations. This is a spectrum analysis that is frequently used in vibration analysis. It helps analysing the vibration amplitudes at various frequencies on the FFT spectrum. By this the specific frequencies at which there are excessive vibrations or other deviations can be found and checked. The running speed normally is the first significant peak in the spectrum. Furthermore, it is important to determine the fault severity. A high vibration might not be harmful for every component, while some already are outside an acceptable limit at small changes. It can be useful to compare the obtained amplitudes with previous measurements or similar components taken at the same operation conditions to look for changes. If available, results can also be compared with baseline measurements. Faults in the drivetrain can be caused by a variety of reasons, further explained in chapter 2.3 about drivetrain failure modes. The diagnoses of some of these are explained in the rest of this chapter based on a SFK manual on spectrum analysis [36]. In this manual, general indicators to identify and verify suspected fault frequencies are explained. Common for the detection by FFT spectrum is that for phase measurement, all values are  $\pm 30^\circ$  due to mechanical variance.

- Misalignment
- Imbalance
- Bent Shaft
- Rolling element bearing defect
- Mechanical looseness

**Misalignment** Often overall vibration values, as well as phase measurements, are used to distinguish between the different types of misalignment and imbalance. A frequently used approach is to compare the values between 2x, which indicates misalignment and 1x, which indicates imbalance. Misalignment can be indicated as a 2x amplitude that is 30% to 200% as big as 1x. In case of severe misalignment, multiple harmonics from 2x to 10x of running speed can be viewed. This also is the case for a vibration amplitude that is increased two or three times in the horizontal plane. Phase measurements are a further method to diagnose misalignment. To detect an angular misalignment, a phase shift of  $180^\circ$  in the axial position is to be found across the coupling or the machine. The parallel misalignment is seen by a phase shift of  $180^\circ$  in the radial direction. The most common misalignment, being a combination of angular and coupled misalignment is recognised by a phase shift of  $180^\circ$  in the axial or radial position across the coupling or machine.

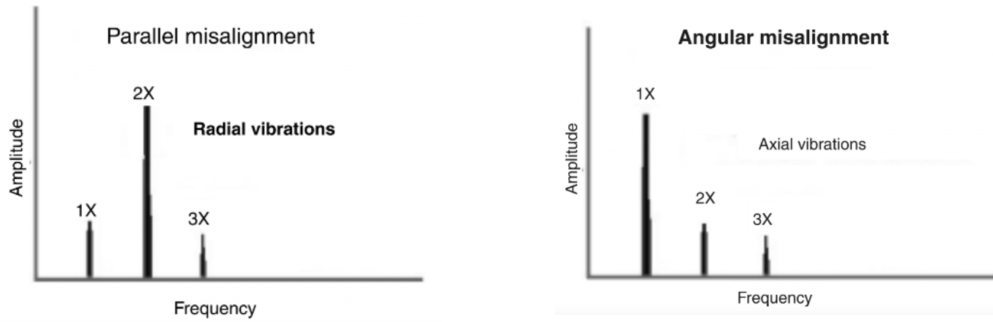


**Figure 3.6:** FFT indicating respectively parallel or angular misalignment [138].

**Imbalance** Static imbalance can be measured at rest. Coupled imbalance is found by looking for a  $180^\circ$  out-of-phase reading from opposed ends of the shaft [36]. Further characteristics to look for are that the amplitude increases with speed and that there is a single frequency vibration whose amplitude is the same in all radial directions. Imbalance will create a sinusoidal movement occurring at frequency of one per revolution (1x). Unless the imbalance is severe, the spectrum will not show harmonics of 1x running speed. Since a pure imbalance causing vibration is an once per revolution sinusoidal waveform, a high 1x amplitude will show up in a FFT-spectrum. Specific for imbalance is that there are no other harmonics produced. As a generalisation, signals with harmonics above once per revolution are often assumed to not to be imbalance. Nevertheless, also harmonics can occur as imbalance increases or when horizontal and vertical support stiffness differs by a large amount. Of the phase from the vertical and horizontal measurements differ by  $90^\circ$ , while the majority of the vibrations is in the radial plane. The third way one can detect imbalance is if the machine has an overhung mass and the axial phase measurements across the machine are in phase while the primary vibration plane is both axial and radial. There also might be imbalance if the radial measurements 1x amplitude is high while harmonics other than vane passing are less than 15% of the height of 1x. Obviously also an increasing force coming from imbalance can be harmful for the bearings as specified load might exceed.

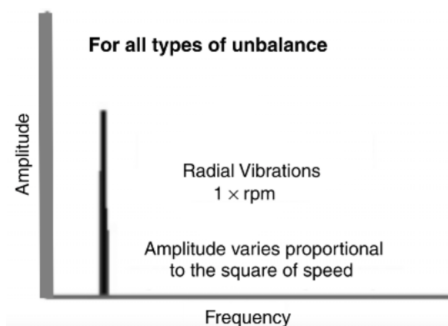


**Figure 3.7:** FFT indicating imbalance [138].

**Bent Shaft** The vibration signature of a bent shaft is similar of that to a misalignment, thus 1x divided by 2x amplitude. The high 2x peak can span from 30 % to 200% of the 1x amplitude. Phase measurements can be helpful in distinguishing the two fault root cases. If a  $180^\circ$  phase difference in the axial direction across the machine occurs, this is a sign for a bent shaft.

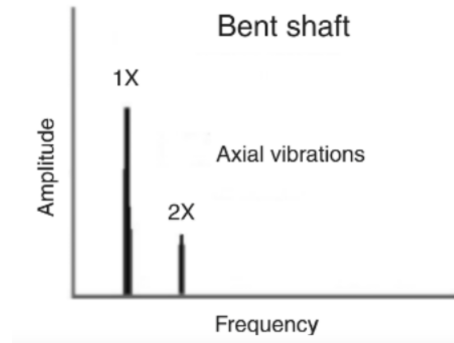


**Figure 3.8:** *FFT indicating bent shaft [138].*

### Rolling Element Bearing Defect

To detect rolling element bearing defects is just the first step, since this seldom is the root cause. Other mentioned fault are more frequently the cause of bearing defects.

**Mechanical looseness** A distinct feature for the mechanical looseness are random and unorganised harmonics, with peaks at for instance 2x, 3x, 4x, 5x etc or 3x, 3.5x, 4x, 5.5x, 6x and so on. Common for these are that they are a string of rotating frequency harmonics or 50° rating frequency harmonics at increased amplitudes. This series consists of three or more parts synchronous multiples of the running speed. Their peaks are greater than 20° of the 1x. Other than mechanical looseness, this also can be a sign of an improper fit between components. Moreover, if there is no coupling or belt and thus the machine is rigidly connected, this can also be a sign for mechanical looseness.

### 3.3.2 Multi-Body Simulation

Multi-body simulation (MBS) is the term describing the simulation of a system divided into different bodies of dynamic and rigid parts. It is worth repeating that a model will be as accurate or inaccurate as preferred. Systems such as OWTs are complex and it will not always be beneficial to be as detailed as possible. Too many factors can disturb from the most important contexts and answers. It is important to thoroughly investigate what the goal with the model is and which parts are of importance. MBS is a powerful tool for the load and dynamic response analysis of wind turbine gearboxes [25]. Multi-body simulation is modelling systems in order to understand, improve them or more has existed for a long time. The model based approach goes beyond what the data-based approach can do, which is the foundation in traditional condition monitoring. Multi-body simulation is beside the Finite Element Method (FEM) [139] and the semi-analytical approach described by Nejad et al. [140] the numerical method used for the dynamical analysis of rotating components in gearboxes and contact analysis. Although the FEM is more accurate, the MBS can be preferred because it is faster and still accurate enough for many applications [141]. With this kind of simulation one can generate and solve virtual 3D models for predicting and visualisation of motion, coupling forces and stresses. The goal for an analysis of a wind turbine drivetrain might vary from noise control to a stability analysis. It is important to look at the natural frequencies of the system, as well as noise and vibration analysis and dynamic loads. The importance of such a multi-body simulation is increasing as the demand for the functionality of condition monitoring increased simultaneously as systems become more advanced.

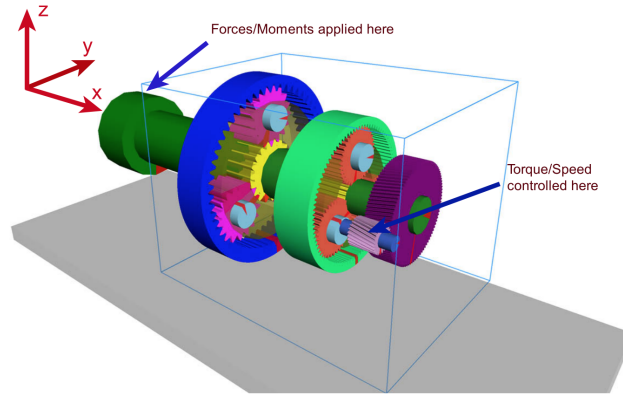


**Figure 3.9:** 5-MW gearbox MBS model [33].

Figure 3.9 shows how a MBS for a 5-MW reference gearbox looks. It is designed for offshore development by Nejad et. al [33]. The gearbox is built as a typical design type in a wind turbine with a gearbox consisting of three stages, two planetary and one parallel stage gear. When working on a MBS for an OWT there has to be performed a global analysis as well as local analysis to take into account all relevant forces on the system. The global analysis concerning global motions and forces, as hydrodynamic and aerodynamic loads are analysed to ensure they are under both the Fatigue Limit State (FLS) and the Ultimate Limit State (ULS). Whilst looking at the global perspective of the system, the drivetrain often is modelled as 1 degree of freedom (DoF) in order to observe its first torsional frequency. For the local analysis of the drivetrain, the found forces are applied on MBS model of the gearbox. There are specific challenges one has to overcome when performing a dynamic analysis of rotating components, gears and bearings, and the analysis of the contact between their parts [142]. The contact between the gear teeth is where power is transferred. In a MBS model the gearbox is a system of either rigid or flexible bodies interconnected with appropriate force elements [143, 144]. The degree of freedom of the bodies are described by joints which shows both location of its respective body and DoF with respect to the body in which its located. Moreover, force elements are used for springs, dampers and contact elements to show how forces are transmitted through a body. Here Guo has a table of MBS recommended modelling methods in MBS [145].

**Bearing Model in MBS** Bearings are often modelled as force elements representing their stiffness when being in a gearbox MBS model [33]. Because calculating the stiffness in the bearing represents a challenge it is crucial to use either data from experiments or FEM models to validate the obtained values [146]. The reason why the damping often is neglected is that bearing damping value varies from 0.25% to 2.5% of the stiffness [147]. A gearbox bearing should for example be modelled as a stiffness matrix. Nejad et al. [25] for instance modelled the bearings with a linear diagonal stiffness as seen in the matrix below.

---


$$\mathbf{K} = \begin{pmatrix} K_x & 0 & 0 & 0 & 0 & 0 \\ & K_y & 0 & 0 & 0 & 0 \\ & & K_s & 0 & 0 & 0 \\ & & & K_\alpha & 0 & 0 \\ & sym. & & & K_\beta & 0 \\ & & & & & K_\gamma \end{pmatrix} \quad (3.3)$$

### 3.3.3 Modal Analysis

The modal analysis is the study of the dynamic characteristics of a system. The objective for it is to obtain a numerical description of the structures dynamic or vibrational behaviour [148]. Since more advanced modelling of the offshore wind turbine requires comprehensive knowledge about its structural dynamic behaviour, there has been an increased interest on the identification of system parameters by this method.

**Modal parameters** Modes are determined by material properties mass, stiffness and damping, as well as boundary conditions and are thus inherent properties of a structure. These modal parameters are natural frequencies, damping ratios and mode shapes. Resonance plays an important role in the modal analysis as it is important to identify and quantify the resonances of a structure. For this, the determination of modal parameters is frequently used. The response to reaching resonance is either a sharp maximum of the magnitude of the vibration or a phase shift that is 180° as the frequency passes resonance and 90° at resonance. These responses are distinct phenomena and can be used to determine the defining modal parameters. The damping ratio gives how much vibration energy is dissipated through either friction damping or viscous damping. Mode shapes provide a graphical representation of how a structure is moving at its natural frequencies by being vectors describing the relative motion between two or more degrees of freedom [149]. If a material property like mass changes, the vibration of the system will also change, as the modal parameter has been altered. Modes are further characterised to be flexible body or rigid body modes [150]. A structure can have six rigid body modes, three translational and three rotational modes. Modes are used to characterise resonant vibration. Near the natural frequency of a mode, the mode shape of resonance will be the dominant one. This resonance movement is identified by excessive, sustained, oscillatory motion at proper conditions. Resonant vibration is generated by the interaction between elastic and inertial properties of the material the structure is made of. In structures and operating machinery, this is often a contributing factor if not the main reason for failures [150]. The operation deflection shape (ODS) is defined as any forced motion of either two or more points on a structure. A shape is defined by specifying two or more points or the motion of one point relative to another. Motion is a vector quantity, thus having a location and direction. Another term for motion at a point in a direction is degree of freedom (DoF).

**Experimental Modal Analysis** The Experimental Modal Analysis (EMA), also known as modal testing, uses the measured input excitation and vibration response to determine the modal parameters through either the frequency response function (FRF) or impulse response function (IRF) [151]. The frequency response function is a measurement that is used to isolate the inherent dynamic properties of a me-

chanical structure. From this, the modal parameters can be obtained. The impulse response function on the other hand utilises that a defect on a surface of a rolling element will produce an impulse when striking another surface [152]. This impulse will occur periodically with a frequency uniquely determined by the defect location as the bearing rotates. The requirement to use the EMA is that it must be possible to excite the system by a measurable excitation force, like by the stroke of a hammer. This excludes big structures like ships or wind turbines. As the name *experimental* initiates, the EMA is often done in a laboratory in a more or less artificial environment. All experimental modal parameters are obtained from measuring operating deflection shapes. The most used EMA is impact testing, also known as hammer test. A system is struck with a hammer and thereby forced out of equilibrium. As the system returns to its initial position, the motions are observed and analysed. An equation of motion (EOM) is a way of describing a system numerically. The EOM of the simple spring-mass-damper system, a good approximation of a bearing, can be represented by 3.4. It is noteworthy that it is chosen to consider translational movements in this section. The reason for this is that this is often the preferred option in the industry, because they are much more easy to measure than torsional. It is also more costly to take torsional measurements. In these equations  $x(t)$  is the displacement,  $m$  the mass,  $k$  the stiffness factor and  $c$  the damping factor.  $F(t)$  is the force applied to the system.

$$m\ddot{x}(t) + c\dot{x}(t) + kx(t) = F(t) \quad (3.4)$$

The mass,  $m$ , is often stated by the manufacturer. The natural frequency is found by observing the periods in this transient, decaying phase and through spectral analysis of FFT. The natural frequency can be converted to angular velocity by using that  $\omega_n = 2\pi f_n$ . The natural stiffness can be obtained when knowing both mass and natural frequency.

$$\omega_n = \sqrt{\frac{k}{m}} \quad k = \omega_n^2 m \quad (3.5)$$

There are different kinds of damping. Figure 3.10 shows how critically-, over- and under damped 1DoF systems behave in a decay test like done in a hammer test.

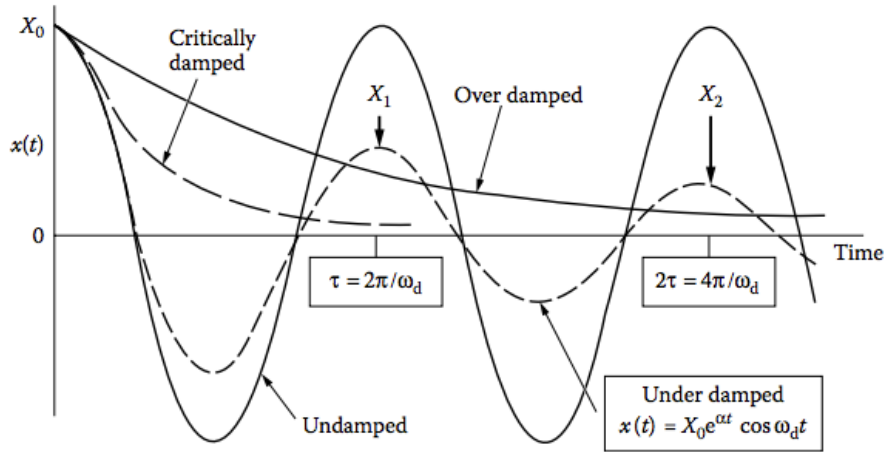


**Figure 3.10:** Motion types for the unforced 1-DoF system [153].



The translational damping coefficient,  $c$ , is found by knowing the damping ratio  $\zeta$  and the natural frequency as seen in equation 3.6.

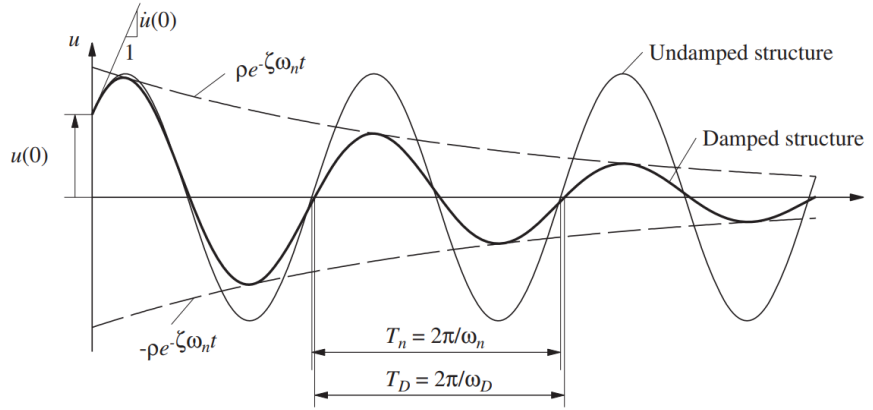
$$c_c = 2m\zeta\omega_n \quad (3.6)$$

The logarithmic decrement  $\delta$ , considers the decrease of the amplitude in a response. It is expressed as seen in equation 3.7.

$$\delta = \ln \frac{X_1}{X_2} = \frac{2\pi}{\omega_d} \frac{c}{2m} \quad (3.7)$$

$$\omega_d = \omega_n \sqrt{1 - \zeta^2} \quad (3.8)$$

$X_1$  and  $X_2$  are amplitudes that can be found by when plotting displacement versus time after a hammer test.  $\omega_d$  the frequency of damped vibration which also is explained by figure 3.11.



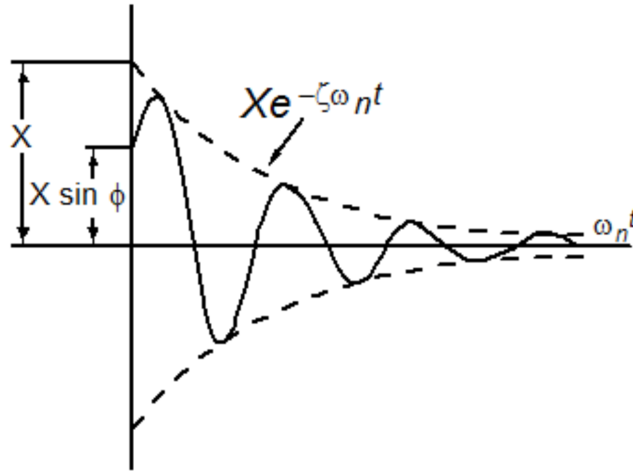
**Figure 3.11:** Effects of damping on free vibration [154].

Table 3.6 shows how the condition of the motions can be expressed by the damping ratio. If the damping is very small, thus  $\zeta$  is small, equation 3.7 is simplified to 3.9.

**Table 3.6:** Conditions for varying damping factors.

Damping ratio $\zeta$	Condition
0	Undamped
$[0, 1]$	Underdamped
$>1$	Overdamped
1	Critically damped

$$\delta \approx 2\pi\zeta \quad (3.9)$$



**Figure 3.12:** Damped vibration with  $\zeta < 1.0$ .

Figure shows the damped vibration with  $\zeta < 1.0$ . As the damping in most mechanical structures is very difficult to establish, the solution often is to rely on the decay of vibration for free vibration. The rate of the decay is then used to find the logarithmic decrement for the damped system from which the actual damping parameters can be obtained [155]. A expression for the amplitude of a system with free damped vibrations is given in equation 3.10.

$$x = X e^{-\zeta \omega_n t} \sin(\sqrt{1 - \zeta^2} \omega_n t + \phi) \quad (3.10)$$

$$\delta = \ln\left(\frac{x_i}{x_{i+1}}\right) = \ln\left(\frac{e^{-\zeta \omega_n t_i} \sin(\sqrt{1 - \zeta^2} \omega_n t_i + \phi)}{e^{-\zeta \omega_n (t_i + T_d)} \sin(\sqrt{1 - \zeta^2} \omega_n (t_i + T_d) + \phi)}\right) \quad (3.11)$$

$$\delta = \ln\left(\frac{x_i}{x_{i+1}}\right) = \ln\left(\frac{e^{-\zeta \omega_n t_i}}{e^{-\zeta \omega_n (t_i + T_d)}}\right) \quad (3.12)$$

**Operational Modal Analysis** OMA has been used since the early 1990's and is still a very relevant method to analyse large structures as buildings or in this case offshore structures. This technique is an output only modal analysis. Here, the structure's normal operating conditions are used as the input excitation to determine the modal parameters. Thus, it does not interrupt the normal operation and will, opposed to the EMA, have the true structural boundary conditions. As there is no artificial excitation required, the actual excitation forces, including harmonics are taken into account. The modal parameters obtained from such a method describe the structure's true service state. Moreover, the OMA can be used for testing the structure, detecting damage, analysing fatigue and document vibration levels. The the method's limitations include unscaled mode shapes, consequently modal participation factors can not be calculated. Further limitation OMA displays are unscaled excitation forces and harmonic contamination. Latter may be caused by rotating machinery introducing false modes that can be incorrectly identified.

**OMA Assumptions** Operational modal analysis is based on the assumption that input excitation is Gaussian white noise stochastic process. This implicates that the

input excitation has the same energy at all frequencies and all modes are excited equally. This is a simplification, because exciting all frequencies with the same energy is not usually possible in the real world. As a compensation, the unknown forces are modelled as the result of the presumed white noise passed through a linear and time invariant excitation filter. This implies that the response which is measured will be a combination of both the structural system and the excitation filter. Thus, the information in the modes of the system also includes no non-physical modes like noise and harmonics.

**Modal Parameter Identification Techniques** To identify the modal parameters from just the output measurements one can choose from multiple techniques. Frequency domain techniques include the Least Square Complex Frequency (LSCF) and Frequency Domain Decomposition (FDD). Among the time domain techniques are Stochastic Realisation-based and Stochastic Subspace-based techniques as well as Auto-Regression Moving Average (ARMA) and Natural Excitation Technique (NExT)[151]. Depending the application, the techniques have their advantages and disadvantages.

### 3.3.4 Inverse Method

Inverse methods aim to solve a problem in an opposite order, that is starting with an output to find an input. While the modal analysis will be helpful to find the mass, damping and stiffness matrix for an EOM of a drivetrain or bearing, the inverse method could be used to find the excitation force. For a model of a bearing, the force is a crucial to be able to propose how quickly the degradation will precede and how long the remaining useful life (RUL) of the component is. There are both direct, inverse methods and more indirect, regularised inverse methods. This subsection reviews the theory of inverse methods and some approaches to find the excitation force for a simple model of a bearing in a drivetrain. When applying this to a multibody-simulation, this commonly is called the input force vector method. For a bearing the output will be the velocity or acceleration. From this the inverse method is used to find the force. This information can then be used to generate SN-curves for a bearing and thus estimate its remaining useful life, RUL.

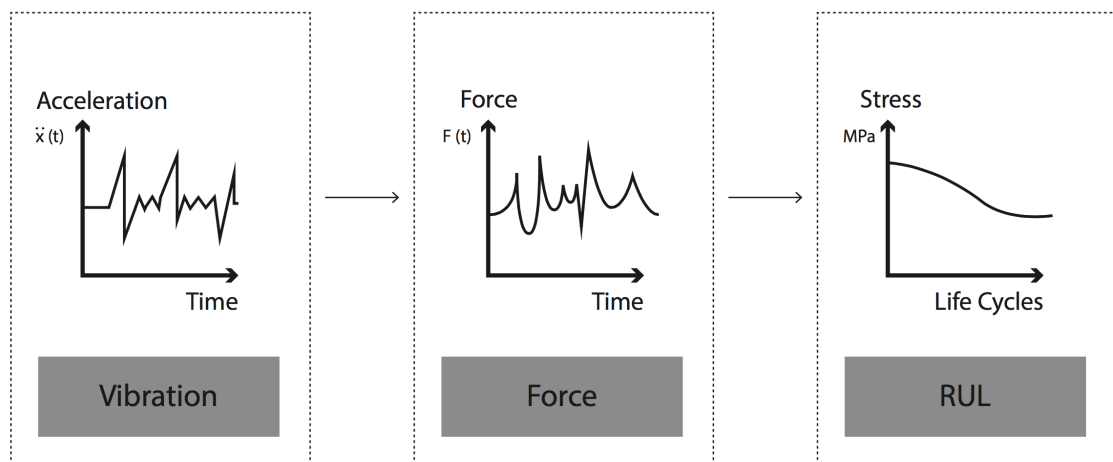


**Figure 3.13:** Methodology of inverse vibration analysis for RUL calculation.

**Direct Methods** Direct methods make use of the numerical or physical model to

formulate the inverse problem without manipulation of any other additional constraints. Methods like this can be carried out in a time as well as a frequency domain. It is noticeable that the behaviour of a structure is often nonlinear, making the numerical model of it restricted to a linear part of the behaviour and being an estimate only. For the sake of clarity, the suggested approaches are here limited to 1DoF and 2DoF spring-mass-damper systems. Also, only harmonic motions are considered.

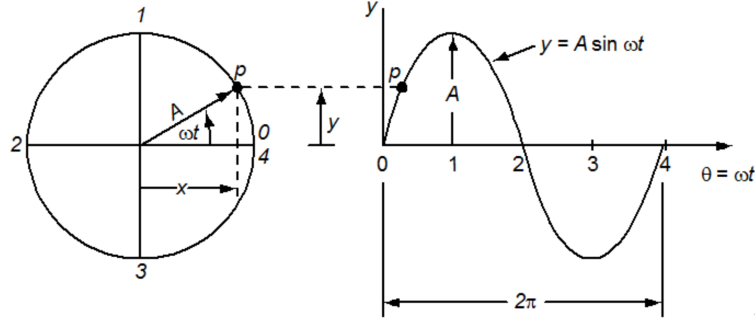


**Figure 3.14:** Harmonic movement description.

Assuming parameters  $k$ ,  $c$  and  $m$  are found by the Experimental Modal Analysis (3.3.3), the remaining terms force, displacement, velocity and acceleration have to be found otherwise. One approach is to use the data set of accelerations obtained when measuring the movements of the bearings. By double deriving an average of the accelerations,  $\ddot{x}_{average}$ , an approximate value for the displacement is found. This calculated  $x$ ,  $x_{calc}$ , can be inserted in the equation of motion for a 1DoF spring-mass-damper system shown in equation 3.13.

$$x_{calc} \longrightarrow F_{calc} = m\ddot{x} + c\dot{x} + kx \quad (3.13)$$

A similar approach is done by Böswald et al. [156] on output-only modal analysis. This study is on ground and flight vibration testing of aeroplanes, but the process is nevertheless relevant. A key element in the study is that the total response is separated into quasi-static response due to deflection of the support DoFs as well as a relative dynamic response excited by equivalent effective excitation forces. These assumption are partly transmissible for a drivetrain in an OWT. Furthermore, the relative dynamic response can be viewed as if the effective excitation forces act on the system with fixed support DoFs. The analysis done in this study requires partitioning of the whole system into unconstrained DoFs, denoted with index  $a$ , and forced vibration DoFs, with index  $b$ .

$$\begin{bmatrix} M_{aa} & M_{ab} \\ M_{ba} & M_{bb} \end{bmatrix} \begin{Bmatrix} \ddot{x}_a \\ \ddot{x}_b \end{Bmatrix} + \begin{bmatrix} C_{aa} & C_{ab} \\ C_{ba} & C_{bb} \end{bmatrix} \begin{Bmatrix} \dot{x}_a \\ \dot{x}_b \end{Bmatrix} + \begin{bmatrix} K_{aa} & K_{ab} \\ K_{ba} & K_{bb} \end{bmatrix} \begin{Bmatrix} x_a \\ x_b \end{Bmatrix} = \begin{Bmatrix} 0 \\ 0 \end{Bmatrix} \quad (3.14)$$

By using the effective excitation forces, the relative dynamic response can be calculated for the unconstrained DoFs.

---


$$\begin{aligned}
[M_{aa}] \{\ddot{x}_a\}^{rel} + [C_{aa}] \{\dot{x}_a\}^{rel} + [K_{aa}] \{x_a\}^{rel} &= \{F\} \\
\{F\} &= ([M_{aa}] [K_{aa}]^{-1} [K_{ab}] - [M_{ab}]) \{\ddot{x}_b\} + \\
&([C_{aa}] [K_{aa}]^{-1} [K_{ab}] - [C_{ab}]) \{\dot{x}_b\}
\end{aligned} \tag{3.15}$$

Assuming the displacements are measured, but only the masses are stated by the manufacturer, an approach like done in Rayleigh's method can be used. This method uses expressions for the potential and kinetic energies [56] to approximate a value for the natural frequency. This can be reordered to find  $k$  and  $c$ . Expressions for the potential and kinetic energies are given as:

$$T = \frac{1}{2} \dot{\vec{x}}^T [m] \dot{\vec{x}} \tag{3.16}$$

and

$$V = \frac{1}{2} \vec{x}^T [k] \vec{x}. \tag{3.17}$$

In order to find the natural frequencies, it is moreover assumed that the harmonic motion is expressed as follows.

$$\vec{x} = \vec{X} \cos \omega t \tag{3.18}$$

Here  $\vec{X}$  represents the vector of amplitudes, thus the mode shape, whilst  $\omega$  denotes the natural frequency of vibration. In case the system is conservative, the maximum kinetic and potential energy will be even.

$$T_{max} = V_{max} \tag{3.19}$$

By inserting equation 3.18 in to 3.17 and 3.16, it is obtained that

$$T_{max} = \frac{1}{2} \vec{X}^T [m] \vec{X} \omega^2 \tag{3.20}$$

$$V_{max} = \frac{1}{2} \vec{X}^T [k] \vec{X}. \tag{3.21}$$

Hence, by equating  $T_{max}$  and  $V_{max}$  it is found that

$$\omega^2 = \frac{\vec{X}^T [k] \vec{X}}{\vec{X}^T [m] \vec{X}}. \tag{3.22}$$

Here, the right hand side is known as Rayleigh's quotient and is denoted  $R(\vec{X})$ . For a 2DOF freedom system this can be written as:

$$\begin{bmatrix} \omega_1^2 \\ \omega_2^2 \end{bmatrix} = \frac{\begin{bmatrix} x_1 & x_2 \end{bmatrix} \begin{bmatrix} k_1 \\ k_2 \end{bmatrix} \begin{bmatrix} x_1 \\ x_2 \end{bmatrix}}{\begin{bmatrix} x_1 & x_2 \end{bmatrix}} \tag{3.23}$$

A third approach to expressing the force is done by starting with expression 3.24 for a 2DoF spring-mass-damper system.

$$\begin{aligned}
m_1 \ddot{x}_1 + k_1 x_1 + k_2 (x_1 - x_2) &= 0 \\
m_2 \ddot{x}_2 + k_2 (x_2 - x_1) + k_3 x_2 &= 0
\end{aligned} \tag{3.24}$$

---

Using a matrix notation, this changes to equation 3.25.

$$\begin{bmatrix} m_1 & 0 \\ 0 & m_2 \end{bmatrix} \begin{Bmatrix} \ddot{x}_1 \\ \ddot{x}_2 \end{Bmatrix} + \begin{bmatrix} k_1 + k_2 & -k_2 \\ -k_2 & k_2 + k_3 \end{bmatrix} \begin{Bmatrix} x_1 \\ x_2 \end{Bmatrix} = \begin{Bmatrix} 0 \\ 0 \end{Bmatrix} \quad (3.25)$$

Considering harmonic vibrations to get equation 3.26.

$$\begin{aligned} x_1(t) &= x_1 \sin(\omega t) \\ x_2(t) &= x_2 \sin(\omega t) \end{aligned} \quad (3.26)$$

Substituting this into equation 3.25 and get:

$$-\omega^2 \begin{bmatrix} m_1 & 0 \\ 0 & m_2 \end{bmatrix} \begin{Bmatrix} \ddot{x}_1 \\ \ddot{x}_2 \end{Bmatrix} + \begin{bmatrix} k_1 + k_2 & -k_2 \\ -k_2 & k_2 + k_3 \end{bmatrix} \begin{Bmatrix} x_1 \\ x_2 \end{Bmatrix} = \begin{Bmatrix} 0 \\ 0 \end{Bmatrix} \quad (3.27)$$

$$\begin{bmatrix} k_1 + k_2 & -k_2 - m_1\omega^2 \\ -k_2 & k_2 + k_3 - m_1\omega^2 \end{bmatrix} \begin{Bmatrix} x_1 \\ x_2 \end{Bmatrix} = \begin{Bmatrix} 0 \\ 0 \end{Bmatrix} \quad (3.28)$$

For a non-trivial solution:

$$\text{determinant} \begin{bmatrix} k_1 + k_2 & -k_2 - m_1\omega^2 \\ -k_2 & k_2 + k_3 - m_1\omega^2 \end{bmatrix} = 0 \quad (3.29)$$

$$\omega_n^2 = \lambda \quad (3.30)$$

$$\begin{aligned} (-m_1\lambda + k)(-m_2\lambda + k) - k^2 &= 0 \\ m_1m_2\lambda^2 - (m_1m_2)k & \end{aligned} \quad (3.31)$$

$$\lambda = \frac{(m_1 + m_2)k}{m_1m_2} = \omega_n^2 \quad (3.32)$$

$$\frac{x_1}{x_2} = \frac{k}{-m_1\omega_n^2 + k} = \frac{1}{1 - \frac{m_1}{k}\omega_n^2} \quad (3.33)$$

$$\begin{aligned} \varphi_1 &= 1 \\ \omega_n^2 &= 0 \end{aligned} \quad (3.34)$$

$$\varphi_2 = \frac{1}{1 - (\frac{m_1}{m_2} + 1)} = \frac{-m_2}{m_1} = \frac{x_1}{x_2} \quad (3.35)$$

$$\varphi_i = \begin{Bmatrix} \frac{-m_2}{m_1} \\ 1 \end{Bmatrix} \quad (3.36)$$

A study done by Oh et al. [157] shows that when knowing the mode shapes and assuming the displacement, a relation for obtaining the force can be found. The last approach examined in this section is a mounted rotating machinery support with an imbalance shown in figure 3.15. It is based on the descriptions of how a system will act under forced vibration excited by a harmonic force. This can be viewed as a stylised offshore wind turbine bearing, as imbalance is a common reason for the excitation of vibrations in rotating machinery.

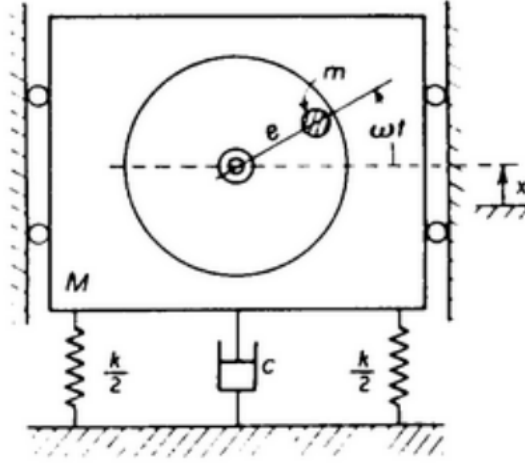


**Figure 3.15:** 1DoF mounted rotating machinery with imbalance.

Although pure harmonic vibrations seldom are the root cause, the thought process for this assumption can help understanding the response of a system under similar circumstances [155]. When only considering a spring-mass-damper system allowed to move in vertical direction that can be excited by a small imbalance with mass  $m$ , a equation for the mass expressed by the parameters of the system can be found. The non-rotating mass  $(M - m)$  has displacement  $x$  relative to a static equilibrium position. It follows that the displacement of the eccentric mass  $m$  is

$$x + e \sin(\omega t). \quad (3.37)$$

Thus, the equation of motion can be expressed as

$$\begin{aligned} (M - m)\ddot{x} + m \frac{d^2}{dt^2}(x + e \sin(\omega t)) &= -kx - c\dot{x} \\ M\ddot{x} + c\dot{x} + kx &= me\omega^2 \sin(\omega t). \end{aligned} \quad (3.38)$$

Hence, the stationary solution can be rewritten as

$$x = X \sin(\omega t) - \phi. \quad (3.39)$$

With  $X$  and  $\phi$  being

$$X = \frac{me\omega^2}{\sqrt{(k - m\omega^2)^2 + (c\omega)^2}} \text{ and} \quad (3.40)$$

$$\phi = \arctan \frac{c\omega}{k - m\omega^2}. \quad (3.41)$$

A prediction of the response excitation with rotating imbalance can be found by equation 3.42.  $X$  is the response amplitude,  $m$  the eccentric mass.

$$\frac{MX}{me} = \frac{\left(\frac{\omega}{\omega_n}\right)^2}{\sqrt{\left(1 - \left(\frac{\omega}{\omega_n}\right)^2\right)^2 + \left(2\zeta \frac{\omega}{\omega_n}\right)^2}} \quad (3.42)$$

---

In previous studies such a system has been assigned the EOM 3.43.

$$M\ddot{x} + k\dot{x} + cx = (mew^2)\sin(\omega t) \quad (3.43)$$

Here M is the mass of the support, m the mass of the imbalance and e the distance from the centre of rotation to the imbalance. Because this only takes into account on failure, it would be beneficial to find ways to express the misalignmnet and other possible faults as well, seen as respectively  $B\sin(2\omega t)$  and  $C\sin(3\omega t)$ .

$$M\ddot{x} + k\dot{x} + cx = A\sin(\omega t) + B\sin(2\omega t) + C\sin(3\omega t) \quad (3.44)$$

The distribution is due to their respectively peaks are at 1x, 2x and 3x when considering fault detection in the FFT analysis. This ratio varies between systems and in some the force-element might entirely be imbalance [138]. Considering the two most frequent fault, imbalance and misalignment, by doing a Fast Fourier Transformation on the data set, the weighting of these two elements could be found. Ultimately, these values could be used to explore the excitation force.

**Regularisation Methods** Regularisation is the process of introducing additional constraints with the aim to solve an ill-posed problem or to prevent over-fitting [158, 159]. While well-posed problems have an unique solution that changes as the initial conditions changes, ill-posed problems do not fulfil these requirements. Most regularisation methods for computing stable solutions to inverse problems involve a trade-off between the "size" of the regularised solution and the quality of the fit that it provides to the given data. The various regularisation methods are distinguished by how they measure these quantities, and how they decide on the optimal trade-off between the two quantities. Singular values of a matrix as seen in 3.45 accumulate at the origin before they gradually decay to zero. This makes the matrix severely ill-conditioned, which is the reason for them also being known as linear discrete ill-posed problems [160].

$$Ax = b, \quad A \in \mathbb{R}^{m \times n}, \quad x \in \mathbb{R}^m \quad (3.45)$$

Often the right hand side b of problems like this is contaminated by an error  $e \in \mathbb{R}^m$  which can originate from measurement inaccuracies or discretization. Let  $\bar{b}$  denote the unavailable error-free representative of vector b as seen in 3.46.

$$b = \bar{b} + e \quad (3.46)$$

The goal is then to determine a solution av  $\bar{x}$  of an error free linear system of equation 3.47.

$$A\bar{x} = \bar{b} \quad (3.47)$$

$\bar{x}$  is determined by computing an approximate solution  $\hat{x}$  of the available linear system as  $\bar{b}$  is not available. It is noticeable that solution  $\hat{x}$  itself is not a good approximation of  $\bar{x}$ , because the ill-conditioning character of A as well as the error e. A solution to this is typically to replace the linear system by a nearby system that is less sensitive to perturbations of the right hand side which then gives an solution that will be an approximate solution  $\bar{x}$ . This replacement is often called regularisation. The two most common regularisation methods are the Truncated



---

Singular Value Decomposition (also called spectral cut-off regularisation) and the Tikhonov regularisation (also called ridge regression or Wiener filtering) [161]. Both of these methods are dependent on the choice of regularisation parameter in order to result in a good solution. For instance, the Tikhonov regularisation deals with linear, discrete, ill-posed problems [162, 163, 164]. Tikhonov regularisation is a much applied regularisation method which replaces the ill-posed problem by a nearby well-posed problem. The Tikhonov regularisation operates like a smooth filter on the eigenvalues. This approach is adjusted by a parameter which can be found with a L-curve, which is described later. In its simplest form, the Tikhonov regularisation replaces the linear system of equation by the minimisation equation 3.48 [160].

$$\min_{x \in \mathbb{R}^n} \{ \|Ax - b\|^2 + \lambda^2 \|x\|^2 \} \quad (3.48)$$

Here  $\lambda$  is the regularisation parameter, which for any  $\lambda > 0$  gives the minimisation problem 3.48 an unique solution.

$$x_\lambda = (A^T + \lambda^2 I)^{-1} A^T b \quad (3.49)$$

Let  $A = U \sum V^T$  be the singular value decomposition of A. The regularised solution  $x_\lambda$  is then given by equation 3.50.

$$x_\lambda = \sum_{i=1}^n f_i \frac{u_i^T b}{\sigma_i} v_i \quad f_i = \frac{\sigma_i^2}{\sigma_i^2 + \lambda^2} \quad (3.50)$$

The solution and residual norms for  $x_\lambda$  are given by equations 3.51 and 3.52 [165].

$$\|x_\lambda\|^2 = \sum_{i=1}^n f_i^2 \frac{(u_i^T b)^2}{\sigma_i^2} \quad (3.51)$$

$$\|r_\lambda\|^2 = \|b - Ax_\lambda\|^2 = \sum_{i=1}^n (1 - f_i)^2 (u_i^T b)^2 \quad (3.52)$$

The Tikhonov regularisation seeks for some  $x_\lambda$  to provide a small residual  $\|r_\lambda\|$  as well as a moderate value of the penalty term  $\|x_\lambda\|$ . As can be seen from the equations above,  $\|r_\lambda\|$  and  $\|x_\lambda\|$  are respectively increasing and decreasing functions of  $\lambda$ . There are two main categories for determining a suitable regularisation parameter, either not requiring any knowledge of the error norm or having knowledge or a good estimate of  $\|e\|$  [160]. Equation 3.53 shows an other way of viewing the Tikhonov regularisation.

$$\min_M \{ \|GM - R\|^2 + \lambda \|LM\|^2 \} \quad (3.53)$$

Here  $\lambda$  is the regularisation parameter, L is the regularisation matrix and  $\|\cdot\|$  denotes the Euclidean norm. The regularisation parameter has to ensure that the two terms in equation 3.53 are of the same order of magnitude. In case  $\lambda$  is chosen too small, the solution will be unstable. Contrarily, a too large value of the parameter will cause inaccuracy in the solution. Thus, for a reliable solution, the determination of  $\lambda$  is critical. The solution of the load vector M is minimising the equation. The regularisation matrix L describes the presumed smoothness of the solution. Equation 3.54 shows the 1st order regularisation matrix [166].

$$L = \begin{bmatrix} -1 & 1 & 0 & \dots & 0 \\ 0 & -1 & 1 & \dots & 0 \\ \vdots & \vdots & \ddots & \ddots & 0 \\ 0 & 0 & 0 & -1 & 1 \end{bmatrix} \quad (3.54)$$

The L-curve is a log-log plot of the norm of a regularised solution versus the norm of the corresponding residual form [165]. It is used to determine the the optimal level of regularisation [167]. The regularisation factor should balance between  $\|r_\lambda\|$  and  $\|x_\lambda\|$  quantities. This is why it is also known as  $(\|r_\lambda\|, \|x_\lambda\|)$  curve [160]. It is the characteristic shape that gives the curve its name. In case of under-regularisation, when  $\lambda$  is very small changes in the solution norm occur faster than changes in residual norm. This gives the vertical line. The horizontal line comes from an over-regularisation when  $\lambda$  is very big and the residual norm is very sensitive to small changes in  $\lambda$  while the solution norm is relatively constant. The corner of the curve, and the associated  $\lambda$ , which is the transition between these regions shows the optimal regularisation [168]. A limitation to consider is that a smooth solution is likely to give a poor performance [169, 170]. Figure 3.16 shows a schematic example of a L-curve plot for a TGSVD or Tikhonov regularisation.

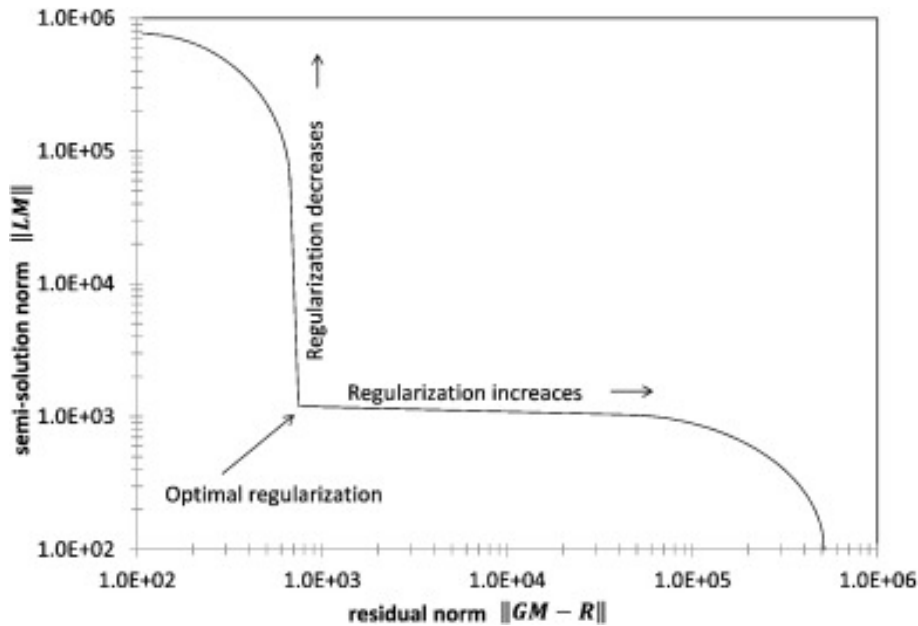


**Figure 3.16:** A schematic L-curve plot for TGSVD or Tikhonov regularisation, where the norm of the semi-solution is plotted against the norm of the residual. The optimal level for regularisation is obtained with the parameter value corresponding to the corner of the curve [167].

### 3.4 Remaining Useful Life

A correct estimation of the remaining useful life (RUL) of components as well as the whole system is very important in order to plan maintenance operations.

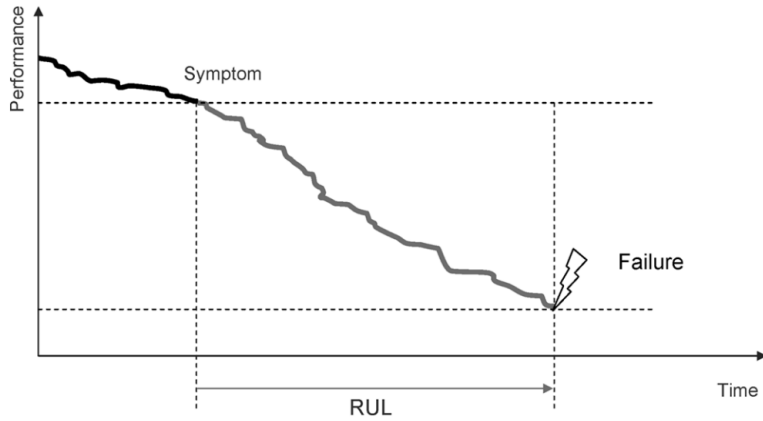


**Figure 3.17:** Illustration of RUL [171].

An offshore wind turbine can be challenging to get to, due to both location and changing weather, making the RUL estimation even more important. Figure 3.17 gives a simple illustration of how the RUL is the time from symptom to failure. The maintenance action should be completed before the failure occurs. When focusing on the downtime prone bearings in the drivetrain it can be interesting to view the framework the already mentioned monitoring and modelling is in. Figure 3.18 shows the RUL estimation steps. In the image 3.17 by Medjaher et al., the steps are divided into a offline and online phase, respectively the learning phase and exploitation phase. From the model selection one can get the RUL estimation. This also applies to the approach mentioned in this thesis, where figure 3.13 shows how data from vibration analysis in the drivetrain can be used to calculate the force which than can be used in a SN-curve to estimate the RUL. The SN-curve is a graph of the magnitude of the cyclic stress on a component against the logarithmic scale of cycles to failure. Equation  $(FL)^{\frac{1}{a}} = Constant$  on the life of a bearing is a form of a single SN curve formulation. To calculate the remaining life, the excitation force thus has to be known.

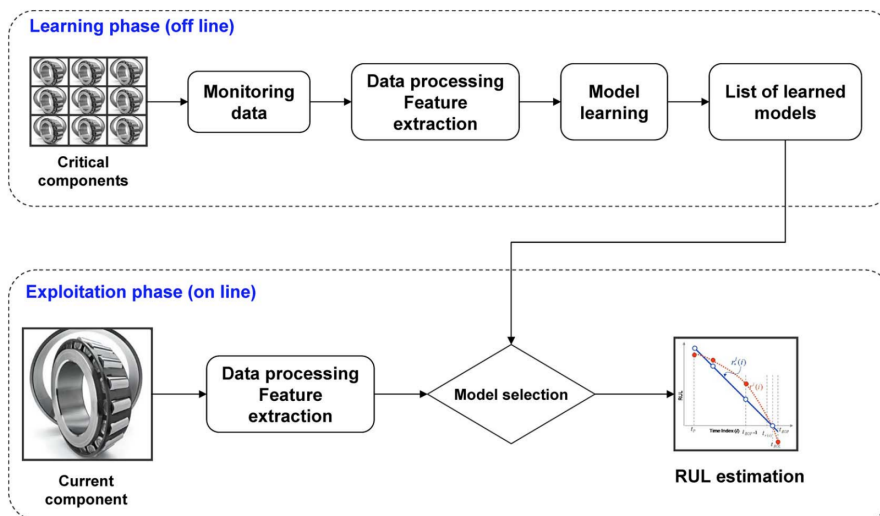


**Figure 3.18:** RUL estimation steps [171].

---

---

# 4 | Digital Twin

## 4.1 General

A digital twin (DT) is a real or near-real time virtual image of an asset maintained throughout its lifecycle. In order to obtain this, the DT uses data, descriptions and algorithms customised to the requirements the system and customer has. The simulation is represented as a three dimensional model easy accessible at all time. Nowadays digitisation is extremely relevant, hence this is believed to become a key technology for smart manufacturing, operation and maintenance [172, 173]. Thus, the digital twin has been getting a lot attention in various industries the last years, with the global research firm, Gartner, ranking it on their top 10 strategic technology trends the last three years [174].

## 4.2 Origin and State-of-the-Art

The term digital twin has its origin in either a report from the National Aeronautics and Space Administration of the USA (NASA) [175] or a professor at the University of Michigan, M. Grieves [176]. Grieves defined a digital twin as a system comprising three components: "*A physical product in real space, virtual product in virtual space and the required interconnection between these two*". NASA produced a report where the future development direction of modelling and simulation was outlined. In this paper the DT was described as being capable of mitigating damage or degradation by recommending changes in mission profile to increase both the life span and the probability of mission success. Although described as a somehow innovative idea, the thinking behind the DT is not new, as computer-aided design has existed for some time. However, there there are several differences. Four of them are stated by Gartner [174].

- The link to the real world, potentially in real time for monitoring and control.
- The application of advanced big data analytics and AI to drive new business opportunities.
- The robustness of the models, with a focus in how they support specific business outcomes.
- The ability to interact with them and evaluate "what if" scenarios.

---

Thus, the difference from a digital twin to model-based system engineering (MBSE) is that the DT extends the concept from engineering and manufacturing to the operation and service phases. The DT can be associated the field of mechatronics which is the meeting point of mechanics, electronics and software design. Although often just called digital twin, the concept can be further divided to the fact that the digital twin is used in operation and service, whilst a digital thread is used in the acquisition phase. This digital thread is the digital connectivity through the life cycle and is circular instead of linear [177]. It creates informed decision making at key leverage points in the development process that have the largest impact on acquisition programs. Its capability is enabled through technical advances in modelling, data storage, analytics, computation and networks. Both the digital twin and digital thread make use of all available virtual models which are interconnected to provide the best possible information. They only differ in position during the life cycle. However, because these concepts are often viewed as parts of the same collective term, this study also refers to them as one digital twin. The DT builds upon simulations, which is an ever changing and improving area of technology. In 2018 Morandotti et al. [178] completed a study on the short term (1-3 years) and mid to long term (3-years) trends for simulations. It was found that data is already used to validate, certify and design products at the beginning of a production. Furthermore, sensors on the actual product are used for real-time control of how the product performs and thus to give feedback to both maintenance and design. Experimental data is also used to train software and and to create a bigger data basis. Nevertheless, it is found that simulations are still in a relatively early development phase, considering their future role in the digital twin. For now, data from real systems is most generally only being collected and compared with simulations in order to improve them more or less manually. To gather data to train and improve the knowledge of a system is further used in the mid to long-term trends. Deep learning, a class of machine learning algorithms and thus an automatic analysis benefits from comprehensive data sets. Combining this technology with a digital twin will open a wide array of possibilities to predict performance by simulation and optimise the process and system. The development of the digital twin could go towards a completely decentralised maintenance, where machine learning detects faults before they occur and automation conducts the maintenance and repair. Alternatively this can be executed by maintenance personnel on land that by the use of remotely automated tools on the turbine.

### 4.3 Concept Architecture

The architecture of the digital twin is an important feature and partly explains why it is well suited for a system like an offshore wind turbine. For every defined purpose the systems has, there will be built a simulation model before they are joint in a holistic model. In case of the mechanical components of an OWT, the suitable choice of simulation model are multi-body simulation. These models can be thought of as building bricks or submodels and enables the user to look at specific measurements to interpret them as well as detecting deviations. Because the desired architecture is thought of from the very beginning, one can step wise build up the DT with the

---

simulation models. To keep the single models up to date as change might occur, a model management system is used for all of them. The management system is also needed to support that submodels with different fidelity can coexist. In addition to the simulation models, further algorithms have to be included for the analysis of both real-time and historical data. Over time the DT will gain collected and stored data. The linkup with the physical world happens when data is used in executable simulation models [179]. Prior to creating the DT, it has to be specified what the overall goal for it is, what kind of values that are of interest and which information can be obtained from the system and its surroundings. Thus, before building the twin it has to be clear what the processes and integration points are for the system it will be modelling. The general process from data gathering to finished product is outlined in the list below.

1. Formulation of an integration plan for the company, mapping the inhouse expertise and what has to be hired or employed.
2. Characterise the stakeholder, partners and other industries or authorities that will have input to the project.
3. Define system and system boundaries.
4. Characterise how the submodels should be build up.
5. Define what the simulation is to show to what extent of detail.
6. Define what the problems is and what the input and output will be.
7. Designate experienced personnel to help build up the respectively submodels.
8. On the basis of the characterised submodels and their challenges, sensor and other measurement units are placed on the system.
9. Upgrade the algorithms in the submodels with real-time data.
10. Use this data to improve earlier assumptions and continuous improve the digital twin.
11. Use information of the digital twin to improve maintenance strategy and new designs.

The digital twin is handed over with the product or even before. During operation it will be the basis for simulation-driven assist systems as well as control and service decisions in combination with smart data approaches [180].

## 4.4 Sensors

Gathering the data is a question of scope. For an effective sensor placement in the drivetrain and the rest of the wind turbine, the use of a vulnerability map like seen in figure 2.3 might be beneficial. Sensors communicate the data to the digital world through integration technology between the physical and the digital world and vice

---

versa. This integration technology includes edge, communication interface and security. The sensors may be placed on different parts of the system throughout different steps of the manufacturing process. These captured measurements let the twin get both operational and environmental data. The measurements from the sensors are streamed to a digital platform. As the US Air Force states [179], comparing actual sensor readings with results gained from models at critical locations allows engineers to both update, calibrate and validate the model. Due to this, unpredicted damage can be included in the model when it occurs and the digital model can help to determine when and where structural damage might occur and thus predict the optimal maintenance intervals. Wireless sensor networks (WSNs), that uses miscellaneous sensors [181] is frequently used to further facilitate condition monitoring. It is noticeable, that sensors have very different lifetimes and there are still seen premature failures in them. As there is an intensive ongoing research on the topic, as sensors play an increasing role in a variety of industries.

## 4.5 Big Data and Analytics

The data from the real world is collected by the digital thread which merges it into one framework. It is aggregated and combined with data from the DT, submodels and design specifications. In the words of the International Business Machines Corporation (IBM): *"Big data is a term applied to data sets whose size or type is beyond the ability of traditional relational databases to capture, manage, and process the data with low-latency. And it has one or more of the following characteristics – high volume, high velocity, or high variety."* [182]. Hence, the utilisation of it gives an improved fault analysis due to a foundation of more information than ever before. There is a lot data to get from a system like an offshore wind turbine or even a drivetrain. Thus, it is important to know what to measure and why to limit the amount of data. It takes a lot capacity to store it and advanced technology as well as skilled technical personnel to understand and use it. The Internet of Things (IoT) is what connects the physical with the digital world. IoT can inform the digital twin with performance insight from the real world. This further improves the system. The step prior this was in some way the already mentioned SCADA [63]. The DT uses analytics or simulation to make use of the incoming information. Items such as engineering drawings and connections to external data feeds may also be concluded in this data. This external data can for example be weather forecasts. The data is analysed through algorithmic simulations and visualisation routines that are used by the digital twin to produce insight. The digital platform performs near-real-time analysis to optimise the operation. While a 3D model is what many picture when thinking of a DT, 1D simulations and 1D models might often be sufficient. The digital side of the digital twin combines the components sensors, data, integration and analytics into a real time digital model. The data can be used to update the system or features of it or send signals back to the real system as well.



---

## 4.6 Software

Because the technology behind a digital twin is a combination of several simulation models, many software types can be used. ANSYS launched its simulation platform, ANSYS 19.1 which contains the Twin Builder feature where one can build its own DT [183]. When looking further into the simulation models, SIMPACK is a software that can be used for the dynamic analysis of any mechanical or mechatronical system [184]. Software such as Calyx [185] or Romax [186] can be used for the bearing stiffness calculation. The Functional Mock-up Interface (FMI) is a standardised interface that is used in computer simulation to develop complex cyber-physical systems. It is the key to model based development of systems because it combined different simulation software. Another possibility is the creation of a software library called Functional Mock-up Unit (FMU) [187]. The FMI standard supports two FMUs, Co-Simulation (CS) and Model Exchange (ME). Both can be used for exchanging models and for simulating multiple models together.

## 4.7 Possibilities

Several companies have started using DTs and the technology is assumed to quickly become more common as digitisation moves forward in all industries. An illustration can be seen in the video-screenshot 4.1, made by GE Renewable Energy to convey their idea of a DT [188].

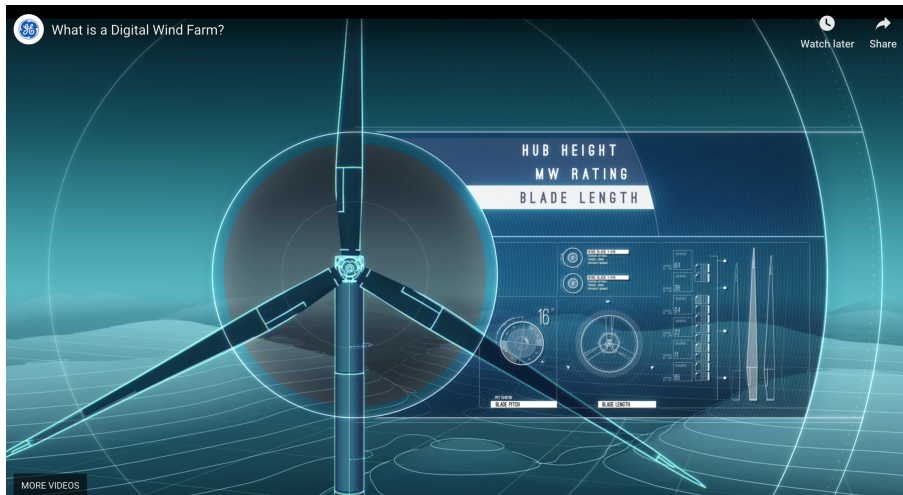


**Figure 4.1:** Digital twin of wind turbine in information video by GE Renewable Energy [188].

The motives for investing time and money in creating a DT are manifold. The simulation gives insight and control over the product from start to end product or in the case of the drivetrain from start to operation, but also during the wind energy production. The digital twin evolves along the real system throughout the whole life cycle and integrates the currently available knowledge about it. The DT is not only used to describe the behaviour but also to derive solutions relevant for the real system, thus it provides functionality for assist systems to optimise operation and

service. Whilst a typical design process often views idealised systems or worst-case scenarios, the digital twin is a real time update on the system with the wanted aspects of it simulated. Figure 4.2 by Schluse et al. shows the different dimensions of the digital twin technology and gives a picture of how comprehensive the vision for it is.

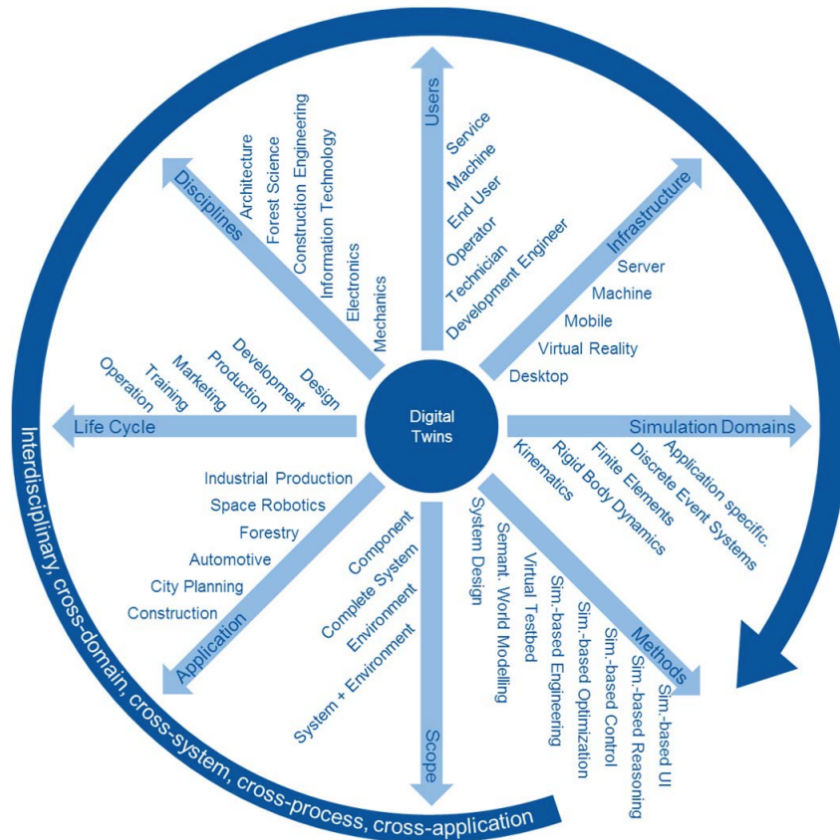


**Figure 4.2:** Different dimensions when using simulation technology throughout the entire life cycle of a system [189].

It is noticeable how the digital twin will cover every aspect of the life cycle, here stated as design, development, production, marketing, training and operation. This will soften the lines between traditional maintenance, IT and all other departments in the offshore wind energy sector. Because the OWT industry is built upon the expertise of several engineering disciplines, mutual understanding and communication will be even more important when everyone is to make use of the same platform. To illustrate this expertise variation, the following three specialisation will have to be able to get information from the same simulation.

- Experts within wind energy to cover aerodynamics, wake effects and power production.
- Civil and mechanical engineers for the various support structures and respective interaction with the sea bottom.
- Electrical engineers to cover the connection to the grid as well as electricity conversion.

---

As mentioned, the digital twin closes the loop from operation and service back to design of new products or updated revisions. A DT includes the relevant data for processing phase-specific simulation tasks. The simulation is built in sub-models and different stakeholders, manufacturers or partners can view parts of it as early as in the production phase. This enables an improved communication between everyone involved. The offshore wind energy industry has many suppliers and stakeholders. Some of these and their possible gain from a DT are listed below.

- **OWT owner:** Control and overview over OWTs operational data. Internal and external communication. Improved and more safe maintenance from land and continuous optimisation of system.
- **Equipment manufacturer:** Simplified communication to show how subsystems perform and validation of quality.
- **Authorities:** Required information and reports can automatically be transferred and checked. This simplifies quality report as well as saving time and minimise man-made errors.
- **Universities and Research:** Updated data and submodels can be shared with universities to study on. Students and scientists can benefit on using "new and real" data and the wind industry on a lot of new work on various issues.

Because of all the different backgrounds contributing to an operating OWT, communication is a key in successful optimisation of the future wind energy designs and solutions. A digital model, imitating the physical system will serve as an efficient visualisation, making the exchange of ideas and opinions easier than over simple numbers and graphs. Consequently, a digital twin will enable a systematic approach for generating value for all involved parts. Furthermore, experts can work together on optimising the system and rework ideas to prevent costly errors. A digital twin could also function as a collaboration platform for exchanging ideas among scientists to try out new concepts in order to make offshore wind energy even more competitive with less environmental friendly energy options. The twin integrates data from several different sources, as analytic and data-driven models, information models, 3D visualisation, models including automation systems and network and continuous data from sensors. It enables information update and exchange [190]. An optimal performance is dependent on all subsystems working optimal, both individually and aggregated. As offshore wind turbines go towards increasingly bigger and more complex solutions, this becomes a comprehensive and complex task. To keep track on how components and parameters interact, a model-driven solution will be beneficial. By creating platforms for digital twins where simulation models, offshore wind turbine documentation and operational data can be shared and analysed the wind energy industry will also have a powerful tool for improving design, production and operation. This kind of information sharing can be seen in an other industry in Norway, where different aquaculture companies share information in a cloud, AquaCloud, in order to get more information to understand the sea lice harming the farming of Atlantic salmon [191]. The digital twin technology would have been extremely expensive and time consuming just some years ago. It has become more feasible due to a development in computational power of big data engines, as

---

well as the comprehensive and flexible storage possibilities. The versatility of the technologies in analytics has also contributed the positive trend.

## 4.8 Challenges

There are several challenges that come along with the digital twin technology. The handling of information security with all the data circulating is an important topic in times where digitisation is as common as it is [192]. Just as challenging is the modelling of all subsystems as the mechanical systems that make up the digital twin. The simulation of a wind turbine as any other structure is just as good as the models it builds upon. Important decisions as what to measure have to be based on knowledge about the system, as too many sensors and data can harden the access to useful conclusions. Because the degradation and failure of bearings has such a strong influence on the downtime and thereof the profitability of the wind turbine, the aim will be to use sensors to update the models that are available and get a realistic view of the component degradation. As seen in chapter 3, previous attempts have shown that the modelling is not where it has to be to simulate the bearings and thus drivetrain of an offshore wind turbine. However, several companies and departments are working on similar models and the mentioned approach is not the only one. Nevertheless, it should be stressed how important the work on good models is in order to get exact results from any simulations.

---

---

# 5 | Case Study

## 5.1 General

A case study was carried out to examine a drivetrain system further. Studies on a small experimental system like this can be used to gather information about an operational drivetrain in an OWT. Using a simple system has many advantages, because it is easier to adjust parameters and examine results than in a complex system. It also made it possible to carry out testing and a case study on a physical system rather than only studying provided data. Investigating the motions and forces in the drivetrain is helpful when considering which loads and movements the bearings are exposed to.

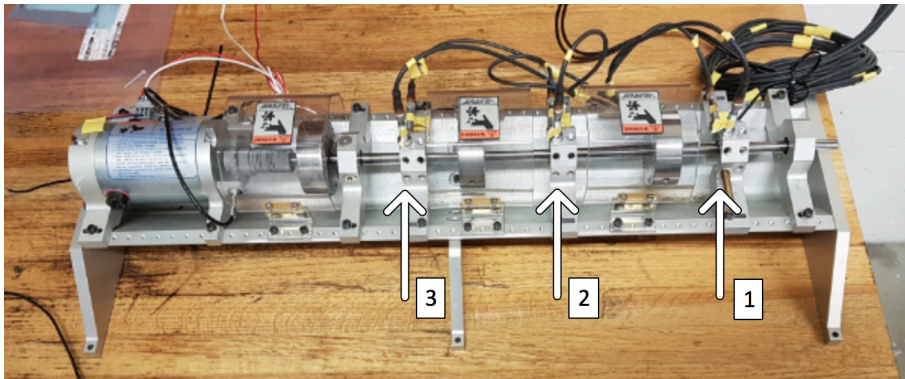


**Figure 5.1:** The test rig with indicated sensor placement and order.

### 5.1.1 Test Rig

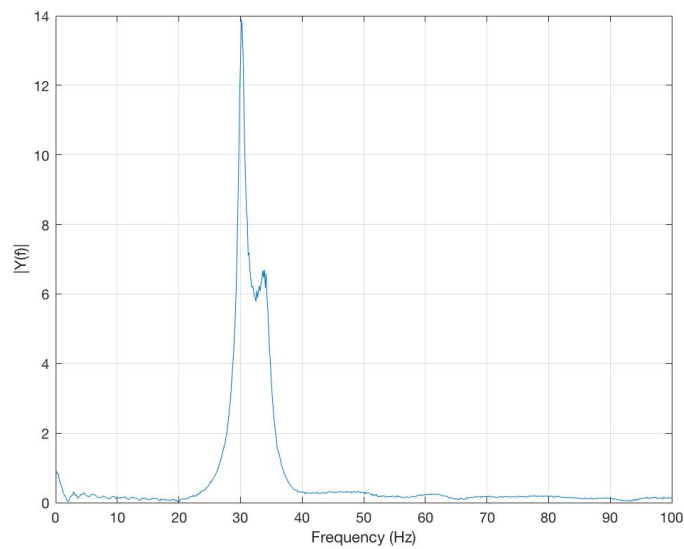
The test rig is located at the NTNU Tyholt campus in Trondheim. As shown in figure 5.1, this is a simple test drivetrain fitted with three rotating disks and three sensor arrangements. These optical sensors measure displacement in both horizontal (X) and vertical (Y) directions. The sensors attached to the system were numbered from right to left, which is adopted to this case study. The total mass of the relevant components for vibration analysis is 16[kg]. The following steps were done in the case study:

1. The system parameters are identified as describes in the Experimental Modal Analysis method
2. FFT analysis fault modes are detected.
3. The mass of unbalance is calculated.

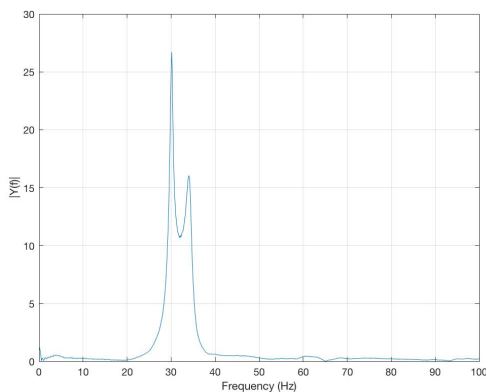
4. The fault mode detection by orbit plot is examined.
5. The initial excitation force is approximated.

### 5.1.2 System Identification

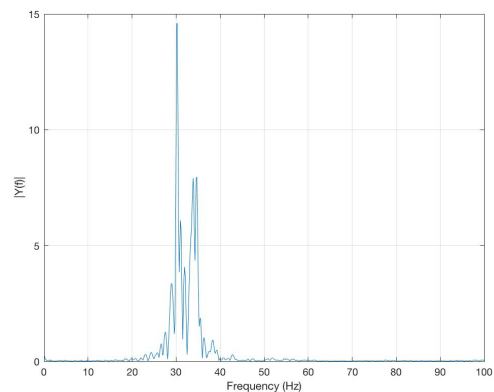
For the system identification, the in chapter 3.3.3 mentioned methods of modal analysis by hammer test were applied. First, the natural frequency was obtained by letting the system reach resonance by slowly increasing the frequency until reaching resonance. At 30[Hz], the system started vibrating vigorously, revealing this to be the critical frequency. In order to control the natural frequency, three hammer test results were examined. The standard when doing test like this is repeating it six times before evaluating the mean of the results. As these tests should only be used for demonstrating purpose, only three were done. Figures 5.2a, 5.2b and 5.2c show three different FFT plots from sensor 3.



(a) Hammer test 1.



(b) Hammer test 2.



(c) Hammer test 3.

**Figure 5.2:** FFT results of amplitude per frequency in sensor 3 by hammer test 1, 2 and 3.

These plots are found magnified in size in appendix A as well. Due to the great similarity between the results from the different sensors, the plots from sensor 1 and 2 are only inserted in the appendix. The peaks in the figures clearly show the natural frequency assumption of 30 [Hz] to be correct. This is the critical speed and would damage the system if operated at over a longer time. The critical speed is commonly given in rpm. Using equation 5.1 for one propeller, the critical speed is found to be 1800 rpm.

$$\begin{aligned} \frac{N}{60} &= 30[\text{Hz}] \\ \implies N &= 1800\text{rpm} \end{aligned} \tag{5.1}$$

A Campbell diagram was used to control the accuracy of the calculated critical speed. It was found that it is correct to correlate a frequency of 30[Hz] to a rotational speed of 1800[rmp].

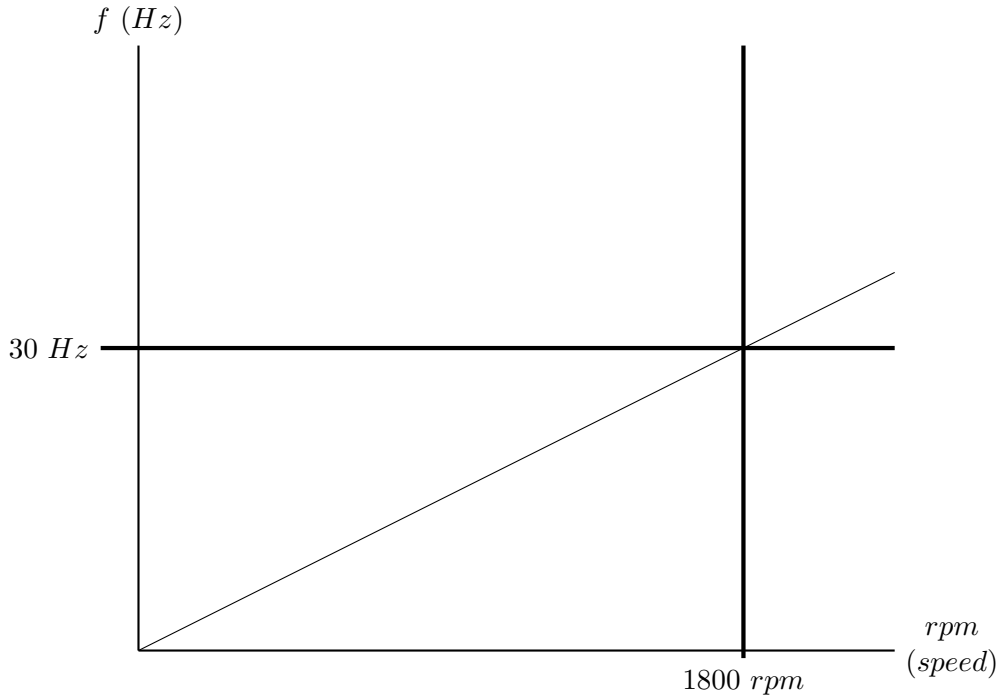
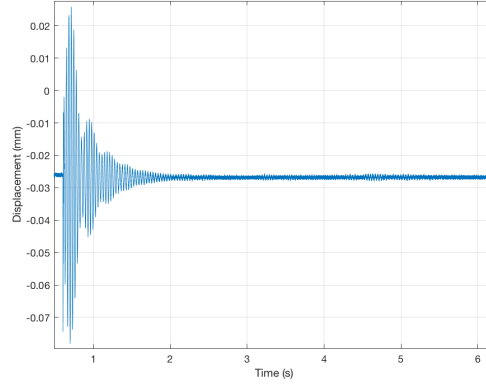


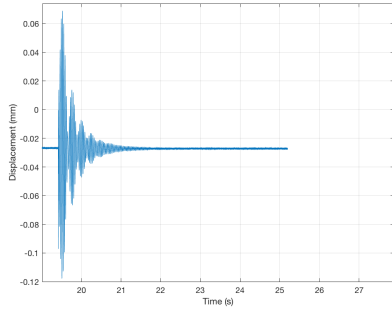
**Figure 5.3:** Campbell diagram.

Furthermore, the damping ratio is calculated. First the logarithmic decrement  $\delta$ , is found by using amplitudes  $x_i$  and  $x_{i+1}$  from the hammer tests. Figures 5.4 shows the displacement over time in sensor 3 for the three test. Again, these and the results for the other sensor can be found in appendix B .

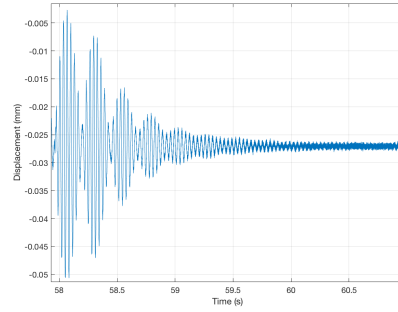




(a) Hammer test 1.



(b) Hammer test 2.



(c) Hammer test 3.

**Figure 5.4:** Displacement for hammer test 1, 2 and 3 sensor 3.

By using  $\omega_n=30$  [Hz] $\cdot 2\pi$  and  $m=16$ [kg], the rest of the parameters can be found as described in the modal analysis. The relevant equations for this are repeated in equation 5.2 and 5.3. The results of the stiffness factor, damping ratio and damping coefficient for sensor 3 are shown in table 5.1. Again, as the sensors show similar answers, only results from one sensor are included.

$$\delta = \ln \frac{x_i}{x_{i+1}}, \quad \zeta = \frac{\delta}{2\pi} \quad (5.2)$$

$$k = \omega_n^2 m, \quad c_c = 2m\zeta\omega_n \quad (5.3)$$

**Table 5.1:** Values for spring coefficient  $k$ ,  $\delta$ , damping ratio  $\zeta$  and damping coefficient  $c_c$  for sensor 3.

Hammer test	k [N/m]	$\delta$	Damping ratio $\zeta$	$c_c$ [Ns/m]
1, sensor 3	568489.213	0.3167	0.0504	304.006
2, sensor 3	568489.213	0.1409	0.0224	135.114
3, sensor 3	568489.213	0.6204	0.0987	595.344

### 5.1.3 Fault Detection

The results from the FFT analysis can also be used to detect fault cases as presented in chapter 3.3.1. The indication of imbalance at 1x is prominent for all sensors in

all three hammer tests. Hence, the drivetrain can be simplified further to a 1DoF mounted rotating machinery with imbalance as seen in figure 3.15. Thus, the mass causing imbalance can be found by equation 5.4. In order to detect possible faults in the drivetrain, harmonic vibrations were induced by forcing the system to vibrate at 24 [Hz]. This frequency was chosen because it is slightly beneath the critical speed. Here it is important not to be too close to the natural frequency of the system to avoid resonance, as well as not using a frequency that would not represent a speed at which the drivetrain would operate.

$$m = \frac{MX}{e} \frac{\sqrt{(1 - (\frac{\omega}{\omega_n})^2)^2 + (2\zeta\frac{\omega}{\omega_n})^2}}{(\frac{\omega}{\omega_n})^2} \quad (5.4)$$

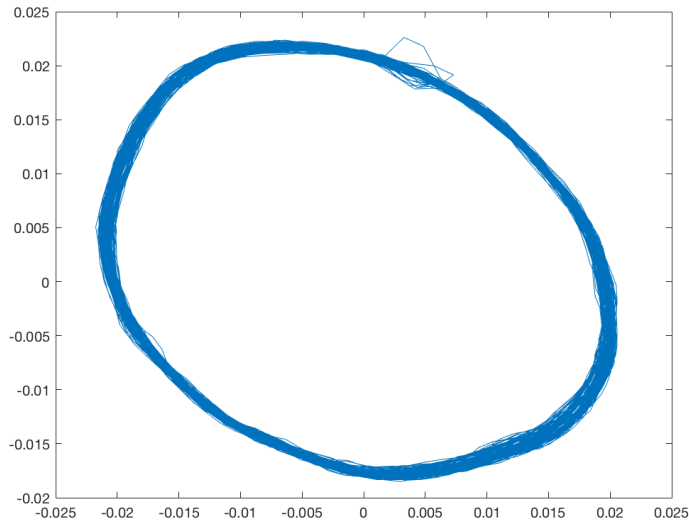
**Table 5.2:** Values for calculation of mass of imbalance.

Parameter	Description	Value	Unit
M	Mass of system	16	[kg]
X	Amplitude of displacement	$0.07081 \cdot 10^{-3}$	[m]
e	Distance from shaft centre to unbalance	$5 \cdot 10^{-3}$	[m]
$\omega$	Forced vibration frequency	24	[Hz]
$\omega_n$	Natural frequency	30	[Hz]
$\zeta$	Damping ratio	0.0571	[-]

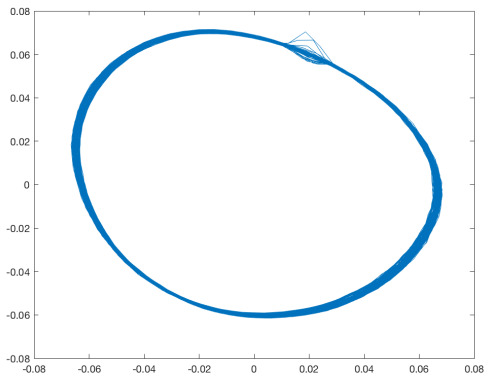
Here the values for damping factor  $\zeta$  and amplitude X are the mean of the three sensors at sensor 3.

$$m = \frac{16[kg]0.07081 \cdot 10^{-3}[m]}{5 \cdot 10^{-3}[m]} \cdot \frac{\sqrt{(1 - (\frac{24}{30})^2)^2 + (2 \cdot 0.0571 \frac{24}{30})^2}}{(\frac{24}{30})^2} = 0.1315[kg] \quad (5.5)$$

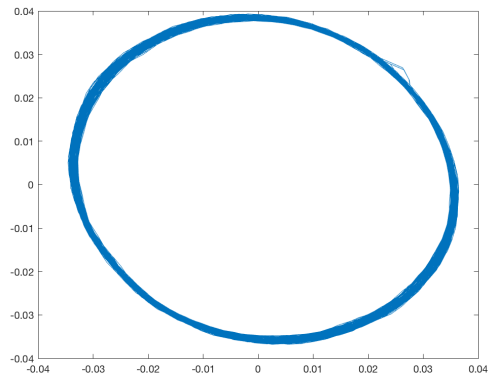
Thus, the mass of imbalance is 0.1315 [kg] grams. As the next step to identify faults, orbit plots were created for the three sensor measurements. The orbit plot is like a heartbeat of a system, hence a good technique to get an overview over the condition of the drivetrain. The orbit represents the path of the shaft centreline with the bearing clearance. Two orthogonal probes are required in order to observe the complete motion of the shaft within. To test how correct they reveal failure modes, a small screw was attached to the mounting of the drivetrain. The shaft would under operation hit this screw slightly. Figure 5.5 has the results of all three sensors at the given frequency.



(a) Sensor 1.



(b) Sensor 2.



(c) Sensor 3.

**Figure 5.5:** Orbit plot at 24 [Hz] at sensor 1, 2 and 3.

Here it would not have been of importance that the circles are centred around zero, because the shaft is not rigid and can therefore move from origo without this representing a fault. The slight elliptic form on the other side suggests that there is a force hindering the the shaft to move in the vertical direction, making it move more horizontal. The peaks in the upper right shows the screw the shaft is hitting. To the contrary, figure 5.6 shows the orbit plots for the three sensor measurements at a frequency below the  $f_n$ , at 12[Hz], as well as above it, 35[Hz]. The movements at 12 [Hz] look very imbalanced and uneven and not like a frequency at which the system should operate. The movements at 35[Hz] are exaggerated elliptic making it challenging to detect any other faults. The results reveal the importance of the choice in frequency in order to obtain descriptive results.

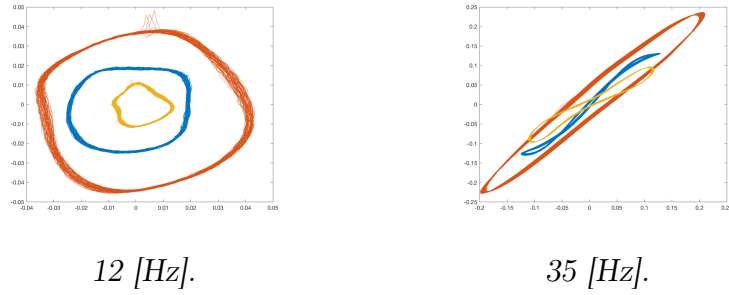


**Figure 5.6:** Orbit plot of three sensors measurements at 12 [Hz] and 35 [Hz].

#### 5.1.4 Fault Severeness

Following, it was of interest to test why techniques like the rms are required when monitoring component as bearings. For this, the test rig was run at 20[Hz] with three different fault cases. This was done by attaching three different small weights on disk 2. The holes where these screw-weights can be attached are shown in figure 5.7. The results for the rms, the mean value and the standard deviation are shown in table 5.3.



**Figure 5.7:** The attachment-placement of weights to produce fault cases.

**Table 5.3:** rms, mean and std of the three fault cases.

	Fault case 1	Fault case 2	Fault case 3
rms·1000 [ $\frac{mm}{s}$ ]	3.0958	5.1597	7.7396
mean [ $\frac{m}{s}$ ]	$-5.1850 \cdot 10^{-7}$	$-8.5874 \cdot 10^{-7}$	$1.2967 \cdot 10^{-6}$
std [ $\frac{m}{s}$ ]	0.0031	0.0052	0.0077

The evaluation of machine vibration by measurements on non-rotating parts from ISO 10816 shows that the bearings at sensors 1 and 2 are in zone B. However, the bearing at sensor 3 is in zone C and thus represents a fault. Normally, small machines should fall into the first categories, making the results even more alarming. Neither the mean nor the standard deviation show any irregularity. This emphasises how important it is to use the correct tools and methods to disclose harmful failure modes in different components.

### 5.1.5 Force calculation

The excitation force calculation is an important step towards improving the modelling of a drivetrain and ultimately OWTs. The displacement found at the different hammer tests can be used to find both velocity and acceleration. Inserting this into the equation of motion gives a calculated initial excitation force. In this example, the mean displacement, velocity and acceleration values from sensor 3 are used. The result is showed in table 5.4. The last test is shown to have the least initial excitation, which is consistent with that the hit was a bit softer than the two previous hits.

**Table 5.4:** Values for spring coefficient  $k$ , damping coefficient  $c_c$  and initial force according to the three hammer tests measured at sensor 3.

Hammer test	$k$ [ $N/m$ ]	Damping coefficient $c_c$ [ $Ns/m$ ]	Force [ $N$ ]
1	568489.213	304.006	0.0249
2	568489.213	135.114	0.0278
3	568489.213	595.344	0.0198

The plot in figure 5.8 shows the characteristic fluctuations in the force. It is noticeable that the plot of the velocity show jumps which can not be found in the acceleration. This is a sign of numerical errors that can come from how the model is set up and that the data is filtered before extracted.

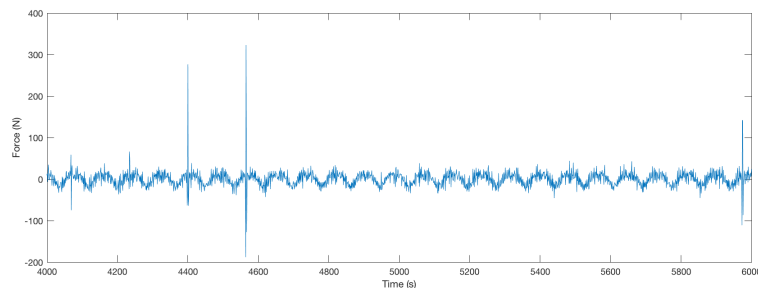


**Figure 5.8:** Plot of the mean force measured at the second sensor at 24[Hz].

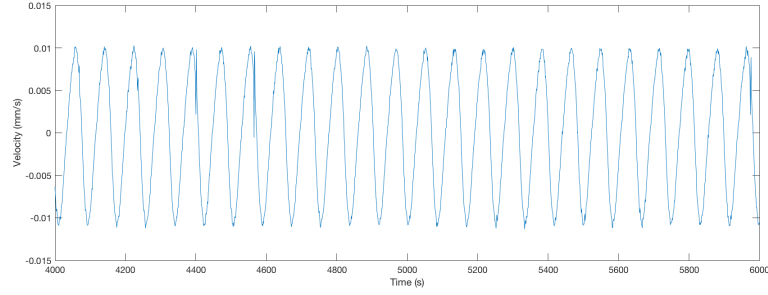


**Figure 5.9:** Plot of the mean velocity measured at the second sensor at 24[Hz].

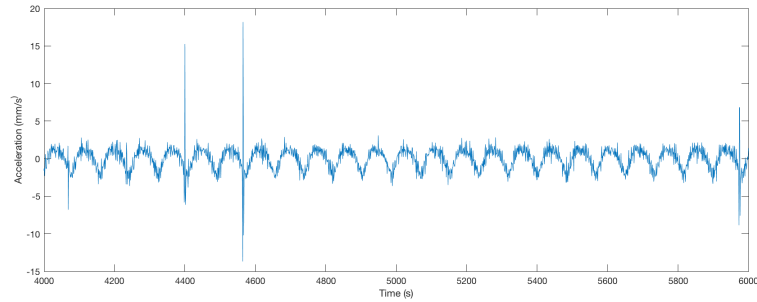


**Figure 5.10:** Plot of the mean acceleration measured at the second sensor at 24[Hz].

Another possibility is to utilise that a drivetrain where the main fault is imbalance can be modelled with  $F = A\sin(\omega t)$ . In this case with the values from the second sensor at at the forced vibration with constant frequency 24[Hz].

$$F(t) = A\sin(\omega t) = m\omega^2\sin(\omega t) \longrightarrow A = \frac{m\omega^2\sin(\omega t)}{\sin(\omega t)} = 2.7[N] \quad (5.6)$$

Although a different answer than found from the previous calculation, the deviation is not unexpected do to simplification in the measurement-modelling.

---

---

## 6 | Discussion

### 6.1 Case Study

The case study showed that it would be advisable to make several tests and discuss the mean value obtained from them rather than examining one by one. This would have given a better representation of the data. However, this was not too important as the tests merely were thought of as a demonstration of how effective the methods reveal failure modes and how significant the choice of failure severeness parameter as the rms is. The results from the test rig showed that sensor 2 measuring the movements in the middle had the highest rms value. This location is farthest away from the bearings and will therefore experience less hold and a higher displacement. It is thus important to notice the location of the bearings in every drivetrain design. The bearing is more prone to error due to excessive vibration and should be monitored carefully. Furthermore, it is expected that the sensor farthest away from where the force/torque is applied will experience a high amplitude because of cumulative effects. The calculation of the mass causing imbalance was done under the assumption of approximately zero horizontal displacement. In this study the horizontal displacements were compared to the vertical displacements were small enough to make this approximation acceptable. Prior to making assumptions like this the movements in the relevant drivetrain should always be controlled as different designs can show different features and results. If a drivetrain shows considerable movements in the X-direction, this has to be included in further studies of its fault detection.

The orbit plots illustrated an interesting problem, being that the shaft seemed to experience more vigorous movements at a quite low speed (12[Hz]) and not only near the critical speed (30[Hz]) or above. This is not as crucial to inspect for wind turbine drivetrains, as these are designed to withstand varying speed due to the high variations in wind speed. However, not all systems are designed for this. Ships that were designed for a certain operational speed that undergo changes in restrictions as to how quickly they can move into a port could experience high wear on the machinery. The imbalance creating the displacement can be minimised as seen in smaller systems as for example the embodiment of drivetrains in cars by Rolls Royce. This shows how important knowledge sharing and -transfer is in this field and where the wind industry could look for answers. The work done on the test rig showed how vibration monitoring advantageous can be used to detect various failures, their placement and severeness. However, there are many factors contributing to uncertainties and work like this should preferably be done with as little human interaction as possible to avoid human errors. It is prominent how



---

simplified the case study is. This can however be beneficial as multi-body simulation on the existing ideas still does not meet the requirements for accuracy. Going back to the most basic components in order to understand them before moving on to trying to combine them to more intricate structures can be a good approach to the downtime challenges which the industry has had over many years.

## 6.2 Bearing Modelling

Since sensors can be attached to the test rig without interfering with its operation, this opens up for online monitoring which consequently can be used in a digital twin. One of the issues seen in this study of drivetrain and bearing modelling, is that the exciting force description is not fully developed yet. It is seen that there is a composed description of imbalance that is much used in the literature. This description could profitably be expanded to include misalignment and other failure modes. This could then be included as a force vector in a multi-body simulation of the drivetrain. Various other numerical techniques to describe the force are found in the literature, such as the inverse Tikhonov method. In order to use and understand more intricate mathematical tools like this, it would be beneficial to collaborate with someone with expertise in mathematics. In the course of this work, a collaboration with members of the department of mathematical sciences was started. Unfortunately, this was not successful as the time was not sufficient to entirely explain the mechanics of the drivetrain bearings in order to formulate an inverse description. Either way, this is an option that should be considered at a later time. It also is noticeable how work on OWT bearings could benefit other systems with issues in their drivetrains, as helicopters. However, it is important not to formulate solutions too general, because descriptions and models benefit from being customised to the actual system they apply.

## 6.3 Model-Based Approach

Because the type and scope of data is significant for further analyses, knowledge about different sensors and their ideal location is important. For this, previous as well as similar studies should be used along with further investigation and testing on OWT drivetrains. Moreover, the creation and application of vulnerability maps is advisable because it gives a picture of where to locate sensors and at which component studies should be intensified. Due to earlier studies not always being consistent with the designation and arrangement of wind turbine subsystems, it is encouraged to be careful when mixing old and new results. Although often applicable, not every method of a wind turbine onshore is beneficial for one operating offshore. As are all studies on the drivetrain not directly transferable. It could be valuable to use a more strict standardisation of for example which components are included in the drivetrain. Model-based approaches with the associated simulations are done in many studies at the time, to test possibilities of a digital twin. This can give valuable insight on the path to a holistic simulation model. Nevertheless, a too expedited start on simulation models before understanding the system well

---

enough to formulate it numerically could be a waste of work. Here it is important to find a golden mean between the interests of how reliable the descriptions should be and how quick DT-prototypes can be tested. The previous mentioned testing of the individual turbine prior to using assumptions is applicable to all theories and methods where it is relevant. This means trying to be as case-specific as possible. As offshore wind turbines and operation of them is constantly under development, it is important to view each turbine as an individual system instead of making hasty generalisations.

## 6.4 Digital Twin

A digital twin represents a revolution in the maintenance of offshore wind turbines if used as describes my the numerous advocates of it. The totality and assembly of it is very important in order to be able to create good models. It allows known failure indicators to be presented in an intuitive matter, as different colour codes for elements like the rms or amplitude found in the FFT from the vibration analysis. The overall goal would be to include all relevant mentioned techniques in one concept that minimises man-made errors and simplifies and elevates the safety and efficiency of the process in design, operation, maintenance and eventually also the decomposing of the structure. This is particularly important for the error-prone drivetrain and its bearings. As these components are hard to reach, the monitoring of them by simulations building on a real time data-feed from sensors will pose a major development in their maintenance. When building simulation models it would be of benefit to stay away from programs that are not completely understood, or present some kind of "black box". The understanding and applicability is crucial when creating work that depends on multiple parameters. This applies especially when aiming towards using the simulation for a digital twin. Small uncertainties in all models will accumulate when including them in a governing model and errors might be challenging to trace back to their sources. Moreover, the digital twin technology should not be confused with a simple simulation. As the concept gains attention, the perception of it can be confused with a simulation with some sensor input, instead of the comprehensive imitation of an asset and its environment it actually is. The hype for the term should not surpass the quality of the simulation. Furthermore, it is important not to rely too much on sensors. As of today, their reliability is very fluctuating. Although the prices are declining as technology develops, caution should be advised in the choice of them. Harsh environmental conditions can affect their lifetime even further. Here it will be helpful to have a model that can predict what most likely would happen based on the information that was provided until the sensor failed. From this, the model could approximate the condition until the sensor works again or has been repaired or replaced. However, the field of sensors is constantly improving and this might not be a problem in some years from now. For wind turbine operators, it will be beneficial to create expert groups, covering the areas as machinery, mathematics, material science and simulation to gather information to start building a twin. The input from all contributors to a well-functioning wind turbine is valuable in this project as its goal also is to serve as a communication tool for an even better operation and maintenance.

---

---

## 7 | Conclusion

Wind energy is an important contributor to the global energy production with a huge potential to take an even larger share of the total. An ever increasing human population which entails a growing demand for cheap and environmental friendly power options makes this requirement even more prominent. However, the wind industry is challenged by premature failures and high downtime. As the production expands offshore in order to increase production, these problems move along with it. Additionally, several problems seem elevated by bigger structures and the extreme conditions at sea. Harsh weather and long distances from land make the maintenance offshore challenging and costly. The faults creating the most downtime are located in the drivetrain. Especially the bearings contribute to difficulties. This thesis has reviewed some of the numerous techniques to detect fault modes and their severeness in the drivetrain, frequently focusing on the bearings. It is observed how abundant such methods are. The sheer quantity in which they exist and how much new work is continuously being published in the field indicates the optimism and the motivation that prevails in the industry. In order to improve the data collection and ensure that results from all different studies are comparable, standardisation of measurements and classifications of subsystems should favourably be used even more consistent than now. As the data and knowledge on offshore wind turbines is not sufficient to draw well substantiated conclusions from yet, the idea has emerged to base the condition monitoring on a model-driven approach. This is not synonymous with turning away from classical fault detection methods, but to combine the knowledge of both fields. The advantages of a model-driven approach have been discussed and the benefits over data-driven approach explained. The development of the concept digital twin in an ever growing number of industries, presents a promising future for the fault detection and condition monitoring of drivetrains in OWTs. The challenging requisite mathematical models that are used for wind turbines make it difficult to create detailed and comprehensive prognosis for the excitation force. Nevertheless, bearings ought to be studied more in order to formulate good numerical descriptions. This can be done by focusing on the most prominent failure modes in the drivetrain with the goal to use this insight in an inverse method. Straight forward techniques should also be explored more closely. The further knowledge acquisition of the degradation and fault root causes for the components is crucial to reduce the downtime. An offshore wind turbine is an expensive and intensive system which depends on having a high availability as well as reliability. To realise this, knowledge about every part through the whole life cycle is required to optimise design, operation and maintenance. A digital twin enables the combination of being a real time simulation for operation monitoring as well as analysis of continuous incoming data. It monitors the life cycle from the very beginning of the planning

---

of the system to the operation time and thus gives constant information as to what could be altered in the design of new wind turbines as well as maintenance actions. A 3D simulation like this will also contribute to the communication between different professionals and stakeholders. Models are always simplifications of the reality. But a simplification is not necessary negative when it comes to studying a system in order to find its weaknesses and strengths. OWTs and even a drivetrain are very complex and one might overlook the important parts because of an information overflow. Hence, the improvement of the twin which is a natural part of the development of the technology in the industry in energy generation is a big step towards a more profitable offshore wind energy production.

## 7.1 Further Work

Further work that can and should be done on this topic is almost inexhaustible. According to what has been mentioned in this study, some main areas of recommendation are listed.

- Further work on the numerical expression of the bearings in the drivetrain. Possibly by working on finding good descriptions for misalignment and other failure modes such as there are for imbalance.
- An individual condition monitoring, that includes factors as sensor location, gearbox configuration and operational speed for each turbine and its components in order to include the uniqueness of each offshore wind turbine.
- A universal platform where work on offshore wind turbine condition monitoring and modelling is shared.
- An individual model for each turbine to handle the variations among them.
- The development of fully understood simulation models that can be used as building blocks for the digital twin.

---

# References

- [1] United Nations. Affordable and clean energy.
- [2] Bundesministerium für wirtschaftliche Zusammenarbeit und Entwicklung. Entwicklung braucht nachhaltige energie.
- [3] United Nations. What are the sustainable development goals.
- [4] Wind Europe. Wind in power 2017.
- [5] Thomas Ackermann et al. *Wind Power in Power Systems*. Wiley, 2012.
- [6] Global Wind Energy Council. Global statistics.
- [7] J.Bøggild (Orsted) A.H. Nymark, M.H. Gottlieb. Europe powered by green energy - how the north seas can lead to change, 2017.
- [8] Rolf Isermann. Model-based fault-detection and diagnosis—status and applications. *Annual Reviews in control*, 29(1):71–85, 2005.
- [9] Erich Hau. *Windkraftanlagen*. Springer Vieweg, Berlin, Heidelberg, 2014.
- [10] Austrian Wind Energy Association. Geschichte der windkraft.
- [11] Martin OL Hansen. *Aerodynamics of wind turbines*. Routledge, 2015.
- [12] K Pope, I Dincer, and GF Naterer. Energy and exergy efficiency comparison of horizontal and vertical axis wind turbines. *Renewable energy*, 35(9):2102–2113, 2010.
- [13] Pixabay. Wind turbine pictures.
- [14] Martin Johannes Kühn. *Dynamics and design optimisation of offshore wind energy conversion systems*. DUWIND, Delft University Wind Energy Research Institute, 2001.
- [15] M Dolores Esteban, J Javier Diez, Jose S López, and Vicente Negro. Why offshore wind energy? *Renewable Energy*, 36(2):444–450, 2011.
- [16] Peter Tavner. Offshore wind turbines: Reliability. *Availability and Maintenance, The Institution of Engineering and Technology, London, UK*, 2012.
- [17] G.M. Joselin Herbert, S. Iniyan, and D. Amutha. A review of technical issues on the development of wind farms. *Renewable and Sustainable Energy Reviews*, 32:619 – 641, 2014.

- 
- [18] DD Imholte, RT Nguyen, A Vedantam, M Brown, A Iyer, BJ Smith, JW Collins, CG Anderson, and B O’Kelley. An assessment of us rare earth availability for supporting us wind energy growth targets. *Energy Policy*, 113:294–305, 2018.
- [19] gewc. Global wind statistics.
- [20] Global Wind Energy Council (GWEA). Global wind report annual market update. technical report.
- [21] Walter Musial and Bonnie Ram. Large-scale offshore wind power in the united states: Assessment of opportunities and barriers. Technical report, National Renewable Energy Lab.(NREL), Golden, CO (United States), 2010.
- [22] Ben Maples, Genevieve Saur, Maureen Hand, R Van de Pietermen, and T Obdam. *Installation, operation, and maintenance strategies to reduce the cost of offshore wind energy*. Citeseer, 2013.
- [23] Teruo Igarashi and Hiroyoshi Hamada. Studies on the vibration and sound of defective rolling bearings: First report: Vibration of ball bearings with one defect. *Bulletin of JSME*, 25(204):994–1001, 1982.
- [24] Amir R. Nejad and Torgeir Moan. On model-based system approach for health monitoring of drivetrains in floating wind turbines. 199:2202–2207, 12 2017.
- [25] Amir Rasekhi Nejad, Yi Guo, Zhen Gao, and Torgeir Moan. Development of a 5 mw reference gearbox for offshore wind turbines. *Wind Energy*, 19(6):1089–1106, 2016.
- [26] Sebastian Pfaffel, Stefan Faulstich, and Kurt Rohrig. Performance and reliability of wind turbines: a review. *Energies*, 10(11):1904, 2017.
- [27] Rebecca Martin, Iraklis Lazakis, Sami Barbouchi, and Lars Johanning. Sensitivity analysis of offshore wind farm operation and maintenance cost and availability. *Renewable Energy*, 85:1226–1236, 2016.
- [28] W. LaCava J.van Dam B.McNiff P.Veers J. Keller S. Butterfield S. Sheng, H. Link and F. Oyague. Wind Turbine Drivetrain Condition Monitoring During GRC Phase 1 and Phase 2 Testing. Technical report, National Renewable Energy Laboratory, 10 2011.
- [29] Ballé Isermann. Trends in the application of model-based fault detection and diagnosis of technical processes. *Control engineering practice*, 5(5):709–719, 1997.
- [30] Shuangwen Sheng. Report on wind turbine subsystem reliability—a survey of various databases. *National renewable energy laboratory-NREL/PR-5000-59111*, 2013.
- [31] Estefania Artigao, Sergio Martín-Martínez, Andrés Honrubia-Escribano, and Emilio Gómez-Lázaro. Wind turbine reliability: A comprehensive review towards effective condition monitoring development. *Applied energy*, 228:1569–1583, 2018.
-

- 
- [32] Amir Rasekhi Nejad, Zhen Gao, and Torgeir Moan. On long-term fatigue damage and reliability analysis of gears under wind loads in offshore wind turbine drivetrains. *International Journal of Fatigue*, 61:116–128, 2014.
- [33] Amir Rasekhi Nejad, Yi Guo, Zhen Gao, and Torgeir Moan. Development of a 5 mw reference gearbox for offshore wind turbines. *Wind Energy*, 19(6):1089–1106, 2016.
- [34] Amir Rasekhi Nejad, Zhen Gao, and Torgeir Moan. Fatigue reliability-based inspection and maintenance planning of gearbox components in wind turbine drivetrains. *Energy Procedia*, 53:248–257, 2014.
- [35] Molka Attia Hili, Tahar Fakhfakh, Lotfi Hammami, and Mohamed Haddar. Shaft misalignment effect on bearings dynamical behavior. *The International Journal of Advanced Manufacturing Technology*, 26(5-6):615–622, 2005.
- [36] SFK USA Inc. Jason Mais. Spectrum analysis.
- [37] Shawn Sheng. Gearbox Reliability Database: Yesterday, Today, and Tomorrow. Technical report, National Renewable Energy Laboratory, 10 2014.
- [38] Walt Musial and Brian McNiff. Wind turbine testing in the nrel dynamometer test bed. Technical report, National Renewable Energy Lab., Golden, CO (US), 2000.
- [39] Erik Oberg, Franklin D Jones, Holbrook L Horton, Henry H Ryffel, and James H Geronimo. *Machinery's handbook*. Industrial Press, Incorporated, 2016.
- [40] James F Manwell, Jon G McGowan, and Anthony L Rogers. *Wind energy explained: theory, design and application*. John Wiley & Sons, 2010.
- [41] J. K. Nisbett R. G. Budynas. *Mechanical Engineering Design*. The McGraw-Hill Companies, 2011.
- [42] L. Renaudin, F. Bonnardot, O. Musy, J.B. Doray, and D. Rémond. Natural roller bearing fault detection by angular measurement of true instantaneous angular speed. *Mechanical Systems and Signal Processing*, 24(7):1998 – 2011, 2010. Special Issue: ISMA 2010.
- [43] A. Greco, S. Sheng, J. Keller, and A. Erdemir. Material wear and fatigue in wind turbine systems. *Wear*, 302, 2013. Wear of Materials 2013.
- [44] T.I. Liu, J.H. Singonahalli, and N.R. Iyer. Detection of roller bearing defects using expert system and fuzzy logic. *Mechanical Systems and Signal Processing*, 10(5):595 – 614, 1996.
- [45] A. Greco J. Keller, B. Gould. Investigation of bearing axial cracking: benchtop and full-scale test results.
- [46] M-H Evans. An updated review: white etching cracks (wecs) and axial cracks in wind turbine gearbox bearings. *Materials Science and Technology*, 32(11):1133–1169, 2016.
-



- 
- [47] J.Keller R. Errichello, S.Sheng and A. Greco. Wind turbine tribology seminar.
- [48] Michael N Kotzalas and Tedric A Harris. Fatigue failure progression in ball bearings. *Journal of tribology*, 123(2):238–242, 2001.
- [49] MR Hoeprich. Rolling element bearing fatigue damage propagation. *Journal of tribology*, 114(2):328–333, 1992.
- [50] RL Errichello. Morphology of micropitting. *Gear technology*, 4:74–81, 2012.
- [51] SFK. Bearing rating life.
- [52] Amir Rasekhi Nejad, Erin E. Bachynski, Zhen Gao, and Torgeir Moan. Fatigue damage comparison of mechanical components in a land-based and a spar floating wind turbine. *Procedia Engineering*, 101:330 – 338, 2015. 3rd International Conference on Material and Component Performance under Variable Amplitude Loading, VAL 2015.
- [53] SFK. Fatigue load limit.
- [54] Toshio Nakagawa. *Maintenance theory of reliability*. Springer Science & Business Media, 2006.
- [55] Fausto Pedro García Márquez, Andrew Mark Tobias, Jesús María Pinar Pérez, and Mayorkinos Papaelias. Condition monitoring of wind turbines: Techniques and methods. *Renewable Energy*, 46:169 – 178, 2012.
- [56] BKN Rao. *Handbook of condition monitoring*. Elsevier, 1996.
- [57] Jack P. Salameh, Sebastien Cauet, Erik Etien, Anas Sakout, and Laurent Rambault. Gearbox condition monitoring in wind turbines: A review. *Mechanical Systems and Signal Processing*, 111:251 – 264, 2018.
- [58] Richard Dupuis. Application of oil debris monitoring for wind turbine gearbox prognostics and health management. In *Annual Conference of the prognostics and health management society*, pages 10–16, 2010.
- [59] Shawn Sheng. Investigation of oil conditioning, real-time monitoring and oil sample analysis for wind turbine gearboxes. In *AWEA Project Performance and Reliability Workshop*, 2011.
- [60] Shuangwen Sheng and Paul Veers. Wind turbine drivetrain condition monitoring-an overview. Technical report, National Renewable Energy Laboratory (NREL), Golden, CO., 2011.
- [61] Wenxian Yang, Peter J Tavner, Christopher J Crabtree, Y Feng, and Y Qiu. Wind turbine condition monitoring: technical and commercial challenges. *Wind Energy*, 17(5):673–693, 2014.
- [62] Nassim Laouti, Nida Sheibat-Othman, and Sami Othman. Support vector machines for fault detection in wind turbines. In *Proceedings of IFAC world congress*, volume 2, pages 7067–707, 2011.

- 
- [63] P. R. Thies A. Koltsidopoulos Papatzimos, T. Dawood. Data insight from an offshore wind turbine gearbox replacement.
- [64] Shen Yin, Steven X Ding, Xiaochen Xie, and Hao Luo. A review on basic data-driven approaches for industrial process monitoring. *IEEE Transactions on Industrial Electronics*, 61(11):6418–6428, 2014.
- [65] Ming-Da Ma, David Shan-Hill Wong, Shi-Shang Jang, and Sheng-Tsaing Tseng. Fault detection based on statistical multivariate analysis and microarray visualization. *IEEE Transactions on Industrial Informatics*, 6(1):18–24, 2010.
- [66] Yuan Yao, Tao Chen, and Furong Gao. Multivariate statistical monitoring of two-dimensional dynamic batch processes utilizing non-gaussian information. *Journal of Process Control*, 20(10):1188–1197, 2010.
- [67] Rongsheng Gong, Samuel H Huang, and Tieming Chen. Robust and efficient rule extraction through data summarization and its application in welding fault diagnosis. *IEEE Transactions on Industrial Informatics*, 4(3):198–206, 2008.
- [68] Evan L Russell, Leo H Chiang, and Richard D Braatz. *Data-driven methods for fault detection and diagnosis in chemical processes*. Springer Science & Business Media, 2012.
- [69] Leo H Chiang, Evan L Russell, and Richard D Braatz. *Fault detection and diagnosis in industrial systems*. Springer Science & Business Media, 2000.
- [70] Yale Zhang and Michael S Dudzic. Online monitoring of steel casting processes using multivariate statistical technologies: From continuous to transitional operations. *Journal of Process Control*, 16(8):819–829, 2006.
- [71] S Joe Qin. Data-driven fault detection and diagnosis for complex industrial processes. *IFAC Proceedings Volumes*, 42(8):1115–1125, 2009.
- [72] S Joe Qin. Survey on data-driven industrial process monitoring and diagnosis. *Annual reviews in control*, 36(2):220–234, 2012.
- [73] Xuewu Dai and Zhiwei Gao. From model, signal to knowledge: A data-driven perspective of fault detection and diagnosis. *IEEE Transactions on Industrial Informatics*, 9(4):2226–2238, 2013.
- [74] SFK. Basic condition monitoring.
- [75] Store norske leksikon. Stroboskop.
- [76] Pierre Tchakoua, René Wamkeue, Mohand Ouhrouche, Fouad Slaoui-Hasnaoui, Tommy Andy Tameghe, and Gabriel Ekemb. Wind turbine condition monitoring: State-of-the-art review, new trends, and future challenges. *Energies*, 7(4):2595–2630, 2014.
- [77] National Instruments. National instruments products for wind turbine condition monitoring.
-

- 
- [78] Jacek Urbanek, Tomasz Barszcz, and Jerome Antoni. Integrated modulation intensity distribution as a practical tool for condition monitoring. *Applied Acoustics*, 77:184–194, 2014.
- [79] Junda Zhu, David He, and Eric Bechhoefer. Survey of lubrication oil condition monitoring, diagnostics, and prognostics techniques and systems. *Journal of chemical science and technology*, 2(3):100–115, 2013.
- [80] Carl S Byington, Nicholos A Mackos, Garrett Argenna, Andrew Palladino, Johan Reimann, and Joel Schmitgal. Application of symbolic regression to electrochemical impedance spectroscopy data for lubricating oil health evaluation. Technical report, ARMY TANK AUTOMOTIVE RESEARCH DEVELOPMENT AND ENGINEERING CENTER WARREN MI, 2012.
- [81] A Agoston, C Ötsch, and Bernhard Jakoby. Viscosity sensors for engine oil condition monitoring—application and interpretation of results. *Sensors and Actuators A: Physical*, 121(2):327–332, 2005.
- [82] Bernhard Jakoby and Michiel J Vellekoop. Physical sensors for water-in-oil emulsions. *Sensors and Actuators A: Physical*, 110(1-3):28–32, 2004.
- [83] James D Halderman and Chase D Mitchell. *Automotive technology*. Pearson, 2014.
- [84] JD Turner and L Austin. Electrical techniques for monitoring the condition of lubrication oil. *Measurement science and technology*, 14(10):1794, 2003.
- [85] Seung-Il Moon, Kyeong-Kap Paek, Yun-Hi Lee, Jai-Kyeong Kim, Soo-Won Kim, and Byeong-Kwon Ju. Multiwall carbon nanotube sensor for monitoring engine oil degradation. *Electrochemical and solid-state letters*, 9(8):H78–H80, 2006.
- [86] Amiyo Basu, Axel Berndorfer, Carlos Buelna, James Campbell, Keith Ismail, Yingjie Lin, Lorenzo Rodriguez, and Simon S Wang. “smart sensing” of oil degradation and oil level measurements in gasoline engines. Technical report, SAE Technical Paper, 2000.
- [87] Simon S Wang and Han-S Lee. The development of in situ electrochemical oil-condition sensors. *Sensors and Actuators B: Chemical*, 17(3):179–185, 1994.
- [88] Surapol Raadnui and Srawut Kleesuwan. Low-cost condition monitoring sensor for used oil analysis. *Wear*, 259(7-12):1502–1506, 2005.
- [89] Shuangwen Sheng. Monitoring of wind turbine gearbox condition through oil and wear debris analysis: a full-scale testing perspective. *Tribology Transactions*, 59(1):149–162, 2016.
- [90] Schaeffler Group. Lubrication of bearings.
- [91] P Sanchez, D Mendizabal, K Gonzalez, CR Zamarreño, M Hernaez, IR Matias, and FJ Arregui. Wind turbines lubricant gearbox degradation detection by means of a lossy mode resonance based optical fiber refractometer. *Microsystem Technologies*, 22(7):1619–1625, 2016.
-

- 
- [92] D Coronado and C Kupferschmidt. Assessment and validation of oil sensor systems for on-line oil condition monitoring of wind turbine gearboxes. *Procedia Technology*, 15:747–754, 2014.
- [93] Junda Zhu, Jae M Yoon, David He, and Eric Bechhoefer. Online particle-contaminated lubrication oil condition monitoring and remaining useful life prediction for wind turbines. *Wind Energy*, 18(6):1131–1149, 2015.
- [94] Junda Zhu, Jae M Yoon, David He, Yongzhi Qu, and Eric Bechhoefer. Lubrication oil condition monitoring and remaining useful life prediction with particle filtering. *International Journal of Prognostics and Health Management*, 4:124–138, 2013.
- [95] Pankaj Gupta and M.K Pradhan. Fault detection analysis in rolling element bearing: A review. *Materials Today: Proceedings*, 4(2, Part A):2085 – 2094, 2017. 5th International Conference of Materials Processing and Characterization (ICMPC 2016).
- [96] N Tandon and A Choudhury. A review of vibration and acoustic measurement methods for the detection of defects in rolling element bearings. *Tribology International*, 32(8):469 – 480, 1999.
- [97] Amiya Ranjan Mohanty. *Machinery condition monitoring: Principles and practices*. CRC Press, 2014.
- [98] Zhaklina Stamboliska, Eugeniusz Rusiński, and Przemyslaw Moczko. Proactive condition monitoring of low-speed machines. In *Proactive Condition Monitoring of Low-Speed Machines*, pages 53–68. Springer, 2015.
- [99] Anthony L Rogers, James F Manwell, and Sally Wright. Wind turbine acoustic noise. *Renewable Energy Research Laboratory, University of Massachusetts at Amherst*, 2006.
- [100] Simon Braun. *Mechanical signature analysis: theory and applications*. Academic Pr, 1986.
- [101] Fausto Pedro García Márquez, Andrew Mark Tobias, Jesús María Pinar Pérez, and Mayorkinos Papaefias. Condition monitoring of wind turbines: Techniques and methods. *Renewable Energy*, 46:169–178, 2012.
- [102] Seyed A Niknam, Tomcy Thomas, J Wesley Hines, and Rapinder Sawhney. Analysis of acoustic emission data for bearings subject to unbalance. *International Journal of Prognostics and Health Management*, 4:80–89, 2013.
- [103] TW Verbruggen. Wind turbine operation & maintenance based on condition monitoring wt- $\omega$ . *Final Report, April*, 2003.
- [104] Xie Ben Wei, Wen Zheng, and Rong Lin. Design of labview-based system of noise measurement on gear box. In *Advanced Materials Research*, volume 328, pages 2167–2171. Trans Tech Publ, 2011.

- 
- [105] Chuan Li, René-Vinicio Sanchez, Grover Zurita, Mariela Cerrada, Diego Cabrera, and Rafael E Vásquez. Gearbox fault diagnosis based on deep random forest fusion of acoustic and vibratory signals. *Mechanical Systems and Signal Processing*, 76:283–293, 2016.
- [106] Yongzhi Qu, Eric Bechhoefer, David He, and Junda Zhu. A new acoustic emission sensor based gear fault detection approach. *International Journal of Prognostics and Health Management*, 4:32–45, 2013.
- [107] Yongzhi Qu, David He, Jae Yoon, Brandon Van Hecke, Eric Bechhoefer, and Junda Zhu. Gearbox tooth cut fault diagnostics using acoustic emission and vibration sensors—a comparative study. *Sensors*, 14(1):1372–1393, 2014.
- [108] Faris Elasha, Matthew Greaves, David Mba, and Duan Fang. A comparative study of the effectiveness of vibration and acoustic emission in diagnosing a defective bearing in a planetary gearbox. *Applied Acoustics*, 115:181–195, 2017.
- [109] Yu Zhang, Wenxiu Lu, and Fulei Chu. Planet gear fault localization for wind turbine gearbox using acoustic emission signals. *Renewable Energy*, 109:449–460, 2017.
- [110] Sorina Costinas, Ioana Diaconescu, and Ioana Fagarasanu. Wind power plant condition monitoring. In *Proceedings of the 3rd WSEAS International Conference on Energy Planning, Energy Saving, Environmental Education (EPESE'09), Canary Islands, Spain*, pages 1–3. Citeseer, 2009.
- [111] Li Zhen, He Zhengjia, Zi Yanyang, and Chen Xuefeng. Bearing condition monitoring based on shock pulse method and improved redundant lifting scheme. *Mathematics and Computers in Simulation*, 79(3):318 – 338, 2008.
- [112] D.E. Butler. The shock-pulse method for the detection of damaged rolling bearings. *Non-Destructive Testing*, 6(2):92 – 95, 1973.
- [113] Dimitrios Koulocheris, Georgios Gyparakis, Andonios Stathis, and Theodore Costopoulos. Vibration signals and condition monitoring for wind turbines. *Engineering*, 5(12):948, 2013.
- [114] P Shakya, AK Darpe, and MS Kulkarni. Vibration-based fault diagnosis in rolling element bearings: ranking of various time, frequency and time-frequency domain data-based damage identification parameters. *International journal of condition monitoring*, 3(2):53–62, 2013.
- [115] Bin Lu, Yaoyu Li, Xin Wu, and Zhongzhou Yang. A review of recent advances in wind turbine condition monitoring and fault diagnosis. In *Power Electronics and Machines in Wind Applications, 2009. PEMWA 2009. IEEE*, pages 1–7. IEEE, 2009.
- [116] David Siegel, Canh Ly, and Jay Lee. Evaluation of vibration based health assessment and diagnostic techniques for helicopter bearing components. In *2011 DSTO International Conference on Health and Usage Monitoring*, 2011.

- 
- [117] Shuangwen Sheng. Wind turbine gearbox condition monitoring round robin study-vibration analysis. Technical report, National Renewable Energy Lab.(NREL), Golden, CO (United States), 2012.
  - [118] Peng Guo and David Infield. Wind turbine tower vibration modeling and monitoring by the nonlinear state estimation technique (nset). *Energies*, 5(12):5279–5293, 2012.
  - [119] Hongyu Yang, Joseph Mathew, and Lin Ma. Vibration feature extraction techniques for fault diagnosis of rotating machinery: a literature survey. 2003.
  - [120] Pratesh Jayaswal and B Agrawal. New trends in wind turbine condition monitoring system. *J Emerg Trends Eng Dev*, 3:133–148, 2011.
  - [121] SA Abdusslam, Mahmud Ahmed, Parno Raharjo, Fengshou Gu, and Andrew Ball. Time encoded signal processing and recognition of incipient bearing faults. Chinese Automation and Computing Society, 2011.
  - [122] Nicholas Waters, Pierre-Philippe Beaujean, and David J Vendittis. Targeting faulty bearings for an ocean turbine dynamometer. *IJPHM Special Issue on Wind Turbine PHM (Color)*, page 139, 2013.
  - [123] Tien-I Liu, Junyi Lee, Palvinder Singh, and George Liu. Using acceleration measurements and neuro-fuzzy systems for monitoring and diagnosis of bearings. In *Sixth International Symposium on Precision Mechanical Measurements*, volume 8916, page 89160B. International Society for Optics and Photonics, 2013.
  - [124] Muhammet Unal, Mustafa Onat, Mustafa Demetgul, and Haluk Kucuk. Fault diagnosis of rolling bearings using a genetic algorithm optimized neural network. *Measurement*, 58:187–196, 2014.
  - [125] Huanhuan Liu and Minghong Han. A fault diagnosis method based on local mean decomposition and multi-scale entropy for roller bearings. *Mechanism and Machine Theory*, 75:67–78, 2014.
  - [126] Yu Guo, Jing Na, Bin Li, and Rong-Fong Fung. Envelope extraction based dimension reduction for independent component analysis in fault diagnosis of rolling element bearing. *Journal of Sound and Vibration*, 333(13):2983–2994, 2014.
  - [127] Giancarlo Genta. *Vibration of structures and machines: practical aspects*. third edition, 1999.
  - [128] G Genta. A fast modal technique for the computation of the campbell diagram of multi-degree-of-freedom rotors. *Journal of sound and vibration*, 155(3):385–402, 1992.
  - [129] Amir Rasekhi Nejad, Yihan Xing, and Torgeir Moan. Gear train internal dynamics in large offshore wind turbines. In *ASME 2012 11th Biennial Conference on Engineering Systems Design and Analysis*, pages 823–831. American Society of Mechanical Engineers, 2012.
-

- 
- [130] N Tandon and A Parey. Condition monitoring of rotary machines. In *Condition monitoring and control for intelligent manufacturing*, pages 109–136. Springer, 2006.
- [131] Y. Amirat, V. Choqueuse, and M. Benbouzid. Wind turbine bearing failure detection using generator stator current homopolar component ensemble empirical mode decomposition. In *IECON 2012 - 38th Annual Conference on IEEE Industrial Electronics Society*, pages 3937–3942, Oct 2012.
- [132] N. Tandon, G.S. Yadava, and K.M. Ramakrishna. A comparison of some condition monitoring techniques for the detection of defect in induction motor ball bearings. *Mechanical Systems and Signal Processing*, 21(1):244 – 256, 2007.
- [133] M. Blodt, P. Granjon, B. Raison, and G. Rostaing. Models for bearing damage detection in induction motors using stator current monitoring. *IEEE Transactions on Industrial Electronics*, 55(4):1813–1822, April 2008.
- [134] Wolfgang Härdle and Léopold Simar. *Applied multivariate statistical analysis*, volume 22007. Springer, 2007.
- [135] EW WEISSTEIN. Correlation coefficient–bivariate normal distribution [online]. mathworld—a wolfram web resource, 2014.
- [136] CC Heyde. Central limit theorem. *Wiley StatsRef: Statistics Reference Online*, 2014.
- [137] Henrik Madsen. *Time series analysis*. Chapman and Hall/CRC, 2007.
- [138] Cornelius Scheffer and Paresh Girdhar. *Practical machinery vibration analysis and predictive maintenance*. Elsevier, 2004.
- [139] P Wriggers and Giorgio Zavarise. Computational contact mechanics. *Encyclopedia of computational mechanics*, 2004.
- [140] Amir R Nejad, Zhen Gao, and Torgeir Moan. Long-term analysis of gear loads in fixed offshore wind turbines considering ultimate operational loadings. *Energy Procedia*, 35:187–197, 2013.
- [141] Saeed Ebrahimi and Peter Eberhard. Aspects of contact problems in computational multibody dynamics. In *Multibody Dynamics*, pages 23–47. Springer, 2007.
- [142] F. Cianetti, A. Cetrini, M. Becchetti, F. Castellani, and C. Braccesi. Dynamic modeling of wind turbines. experimental tuning of a multibody model. *Procedia Structural Integrity*, 8:56 – 66, 2018. {AIAS2017} - 46th Conference on Stress Analysis and Mechanical Engineering Design, 6-9 September 2017, Pisa, Italy.
- [143] Ahmed A Shabana. *Dynamics of multibody systems*. Cambridge university press, 2013.

- 
- [144] Olivier Andre Bauchau. *Flexible multibody dynamics*, volume 176. Springer Science & Business Media, 2010.
- [145] Y Guo, J Keller, S Sheng, P Veers, W LaCava, J Austin, D Houser, AR Nejad, Y Xing, Z Gao, et al. Gearbox reliability collaborative modeling round robin: Gearbox system modeling practice. *NREL TP*, pages 5000–60641, 2014.
- [146] Yi Guo and Robert G Parker. Stiffness matrix calculation of rolling element bearings using a finite element/contact mechanics model. *Mechanism and machine theory*, 51:32–45, 2012.
- [147] Erwin Krämer. *Dynamics of rotors and foundations*. Springer Science & Business Media, 2013.
- [148] David J Ewins. *Modal testing: theory and practice*, volume 15. Research studies press Letchworth, 1984.
- [149] Daniel J Inman. *Vibration with control*. John Wiley & Sons, 2017.
- [150] Brian J Schwarz and Mark H Richardson. Experimental modal analysis. *CSI Reliability week*, 35(1):1–12, 1999.
- [151] Lingmi Zhang and Rune Brincker. An overview of operational modal analysis: major development and issues. In *1st international operational modal analysis conference*, pages 179–190. Aalborg Universitet, 2005.
- [152] P.D. McFadden and J.D. Smith. Model for the vibration produced by a single point defect in a rolling element bearing. *Journal of Sound and Vibration*, 96(1):69 – 82, 1984.
- [153] Maurice L Adams. *Rotating machinery vibration: from analysis to troubleshooting*. CRC Press, 2009.
- [154] A.K. Chopra. *Dynamics of Structures: Theory and Applications to Earthquake Engineering*. Civil Engineering and Engineering Mechanics Series. Prentice Hall, 2012.
- [155] Harald Valland Eilif Pedersen. *Lecture Notes in Mechanical Vibrations, Course TRM4222*. Department of Marine Technology, NTNU, 2014.
- [156] Marc Böswald, Jan Schwochow, Goran Jelcic, and Yves Govers. "new concepts for ground and flight vibration testing of aircraft based on output-only modal analysis". 05 2017.
- [157] Sho Oh and Takeshi Ishihara. Structural parameter identification of a 2.4 mw bottom fixed wind turbine by excitation test using active mass damper. *Wind Energy*, 2018.
- [158] J Sanchez and H Benaroya. Review of force reconstruction techniques. *Journal of Sound and Vibration*, 333(14):2999–3018, 2014.
- [159] Heinz Werner Engl, Martin Hanke, and Andreas Neubauer. *Regularization of inverse problems*, volume 375. Springer Science & Business Media, 1996.



- 
- [160] Mansoor Rezghi and S Mohammad Hosseini. A new variant of l-curve for tikhonov regularization. *Journal of Computational and Applied Mathematics*, 231(2):914–924, 2009.
- [161] Frank Bauer and Mark A Lukas. Comparing parameter choice methods for regularization of ill-posed problems. *Mathematics and Computers in Simulation*, 81(9):1795–1841, 2011.
- [162] Josef Honerkamp and Jürgen Weese. Tikhonovs regularization method for ill-posed problems. *Continuum Mechanics and Thermodynamics*, 2(1):17–30, 1990.
- [163] Misha E Kilmer and Dianne P O’Leary. Choosing regularization parameters in iterative methods for ill-posed problems. *SIAM Journal on matrix analysis and applications*, 22(4):1204–1221, 2001.
- [164] Andreas Kirsch. *An introduction to the mathematical theory of inverse problems*, volume 120. Springer Science & Business Media, 2011.
- [165] Per Christian Hansen. The l-curve and its use in the numerical treatment of inverse problems. 1999.
- [166] Yimin Wei, Pengpeng Xie, and Liping Zhang. Tikhonov regularization and randomized gsvd. *SIAM Journal on Matrix Analysis and Applications*, 37(2):649–675, 2016.
- [167] Teemu Ikonen, Oskari Peltokorpi, and Jouko Karhunen. Inverse ice-induced moment determination on the propeller of an ice-going vessel. *Cold Regions Science and Technology*, 112:1 – 13, 2015.
- [168] Per Christian Hansen. Analysis of discrete ill-posed problems by means of the l-curve. *SIAM review*, 34(4):561–580, 1992.
- [169] Martin Hanke and Per Christian Hansen. Regularization methods for large-scale problems. *Surv. Math. Ind*, 3(4):253–315, 1993.
- [170] Martin Hanke. Limitations of the l-curve method in ill-posed problems. *BIT Numerical Mathematics*, 36(2):287–301, 1996.
- [171] K. Medjaher, D. A. Tobon-Mejia, and N. Zerhouni. Remaining useful life estimation of critical components with application to bearings. *IEEE Transactions on Reliability*, 61(2):292–302, June 2012.
- [172] Reza Golafshan. Investigation on the effects of structural dynamics on rolling bearing fault diagnosis by means of multi-body simulation. *Faculty of Mechanical Engineering, Institute for Machine Elements and System Engineering (iMSE), RWTH Aachen University*, 2018.
- [173] Q. Qi and F. Tao. Digital twin and big data towards smart manufacturing and industry 4.0: 360 degree comparison. *IEEE Access*, 6:3585–3593, 2018.
- [174] Gartner. Gartner top 10 strategic technology trends for 2019.
-

- 
- [175] Edward Glaessgen and David Stargel. The digital twin paradigm for future nasa and us air force vehicles. In *53rd AIAA/ASME/ASCE/AHS/ASC Structures, Structural Dynamics and Materials Conference 20th AIAA/ASME/AHS Adaptive Structures Conference 14th AIAA*, page 1818, 2012.
- [176] Michael Grieves. Digital twin: Manufacturing excellence through virtual factory replication. *White paper*, 2014.
- [177] Jack B Reid. Digital system models. 2016.
- [178] Dario Morandotti and Alessandra Pelosi. Toward digital twin and simulation-driven new product development. 2018.
- [179] Peter Hehenberger and David Bradley. *Mechatronic Futures: Challenges and Solutions for Mechatronic Systems and their Designers*. Springer, 2016.
- [180] Stefan Boschert and Roland Rosen. *Digital Twin—The Simulation Aspect, pages 59–74*. Springer International Publishing, Cham, 2016.
- [181] Siliang Lu, Peng Zhou, Xiaoxian Wang, Yongbin Liu, Fang Liu, and Jiwen Zhao. Condition monitoring and fault diagnosis of motor bearings using undersampled vibration signals from a wireless sensor network. *Journal of Sound and Vibration*, 414:81 – 96, 2018.
- [182] IBM. Big data analytics.
- [183] ANSYS. Ansys 19.1 delivers the first comprehensive solution for simulation-based digital twins.
- [184] SIMPACK. What is simpack.
- [185] Ansol. Calyx.
- [186] Romax Technology. Bearings.
- [187] D. Hauf, S. Süß, A. Strahilov, and J. Franke. Multifunctional use of functional mock-up units for application in production engineering. In *2017 IEEE 15th International Conference on Industrial Informatics (INDIN)*, pages 1090–1095, July 2017.
- [188] GE Renewable Energy. Meet the digital twin.
- [189] Michael Schluse and Juergen Rossmann. From simulation to experimentable digital twins: simulation-based development and operation of complex technical systems. In *Systems Engineering (ISSE), 2016 IEEE International Symposium on*, pages 1–6. IEEE, 2016.
- [190] DNV-GL. Digital twins for blue denmark.
- [191] NCE Seafood. Aquacloud the use of artificial intelligence in sea lice management.
- [192] Strukturlandschaft der Inneren Sicherheit. Die strukturlandschaft der inneren sicherheit der bundesrepublik deutschland. *Cyber-Sicherheit*, 18:69, 2014.

---

# Appendices

---

# A | FFT for all three hammer tests.

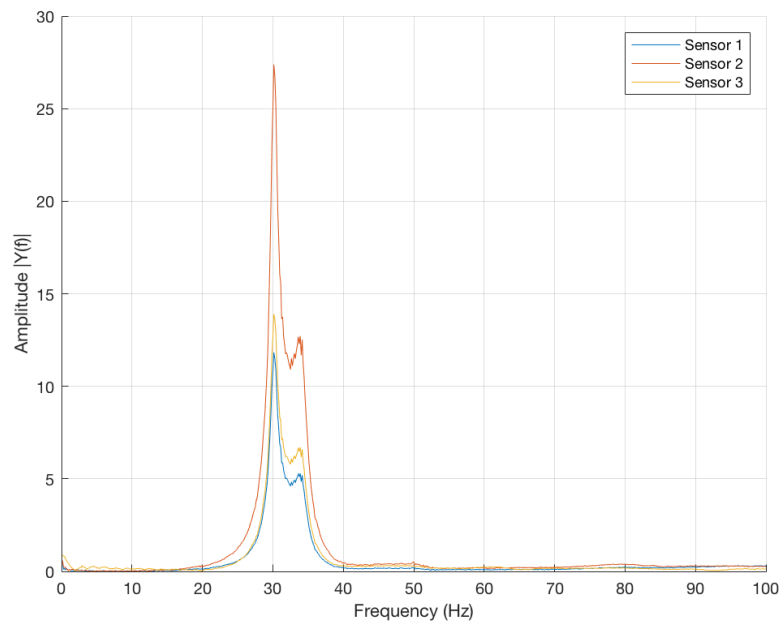


**Figure A.1:** Hammer test 1.

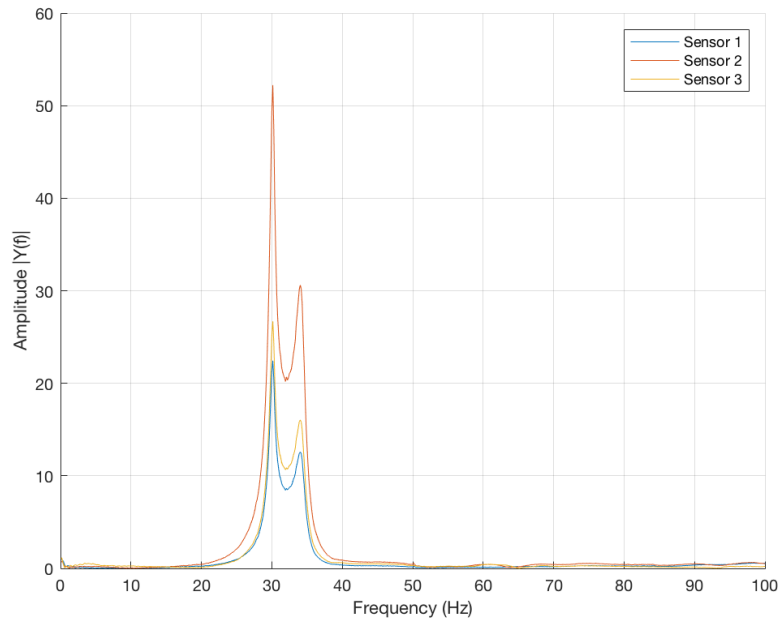


**Figure A.2:** *Hammer test 2.*

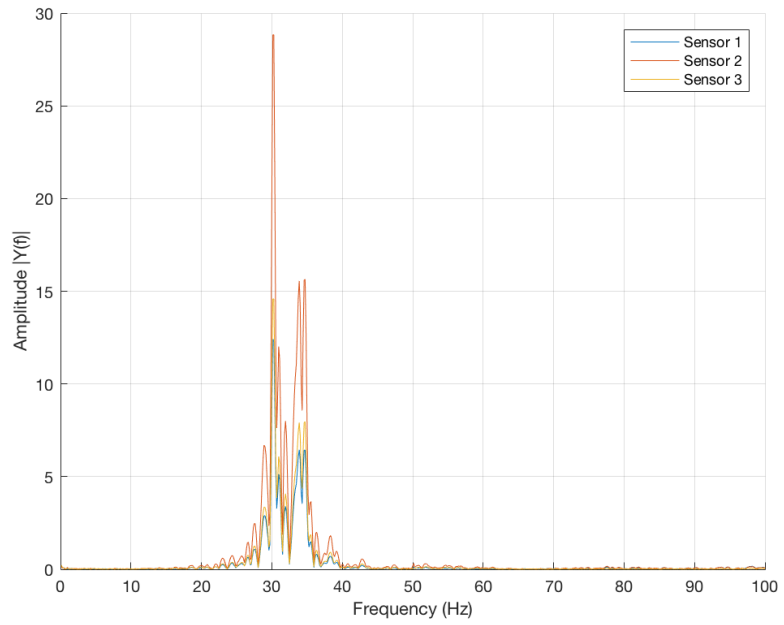


**Figure A.3:** *Hammer test 3.*

---

## B | Displacement for all three hammer tests.

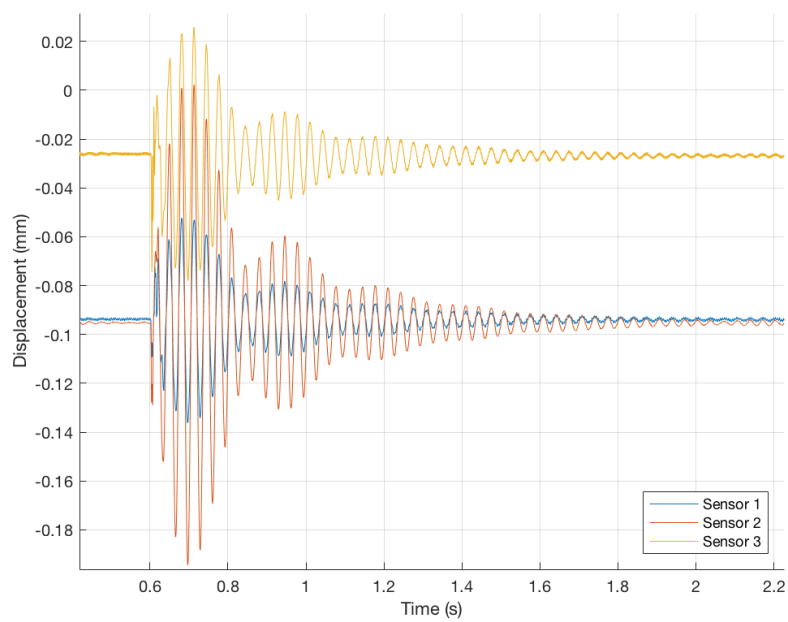


*Figure B.1: Hammer test 1 displacement.*

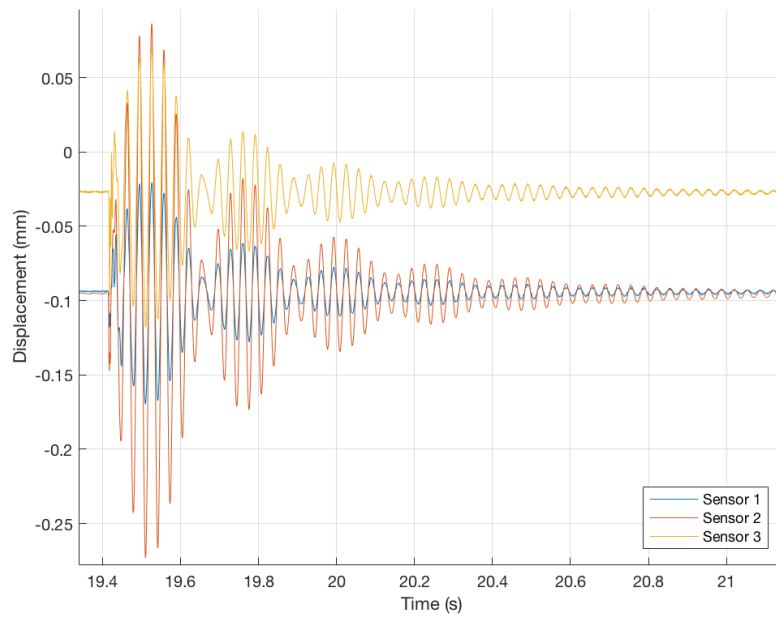


*Figure B.2: Hammer test 2 displacement.*

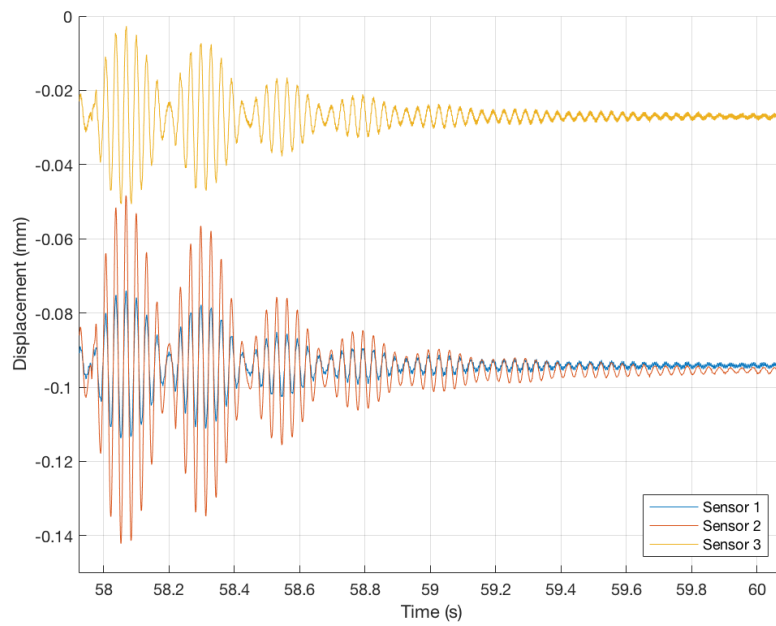


*Figure B.3: Hammer test 3 displacement.*

---

## C | Orbit plot

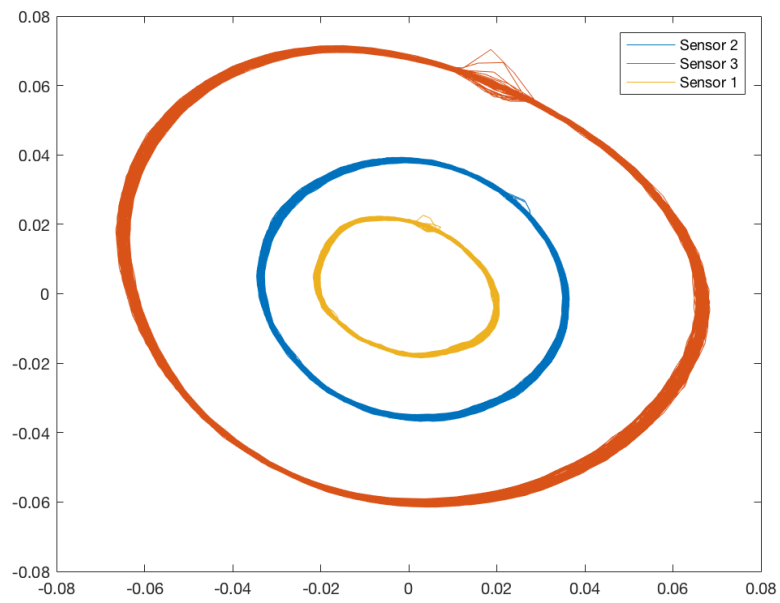


*Figure C.1: Orbit plot at 24[Hz].*